MINISTRY OF HIGHER EDUCATION
AND SCIENTIFIC RESEARCH
University of Baghdad
College of engineering

OPTIMAL CONTROL OF A TURBO-GENERATOR INCLUDING AN EXCITER AND GOVERNOR

A thesis
Submitted to the college of engineering university of Baghdad
in partial fulfillment of the requirements for the degree
of Master of Science in electrical engineering

by
ALAA ABOUD ABDULRASOUL
Bsc. (Elect. Eng.)

Supervised by
DR. MOHAMMED K. AL-ALAWI

December 2008

بِسْمِ اللَّهِ الرَّحْمَنِ الرَّحِيمِ

قَالُوا سُبْحَانَكَ

لَا عِلْمَ لَنَا إِلَّا مَا عَلَّمْتَنَا

إِنَّكَ أَنْتَ الْعَلِيمُ الْحَكِيمُ

صَدَقَ اللَّهُ الْعَظِيمُ

We, the undersigned, certify that we have read this thesis entitled **"Optimal Control of A turbo Generator Including An Exciter And Governor"** and as an examining committee examined the student **"Alaa Aboud Abdulrasoul"** in its contents and that in our opinion, it meets the standard of a thesis for the Degree of **Master of Science In Electrical Engineering**.

Signature:
Name: Prof. Dr. Ali Al-Kiliddar
Date: /   /2009
(Chairman/Univ. of Baghdad)

Signature:
Name: Asist. Prof. Azam A. Ma'arof
Date: 13 / 1 /2009
(Member/Univ. of Baghdad)

Signature:
Name: Dr. Turki K. Hassan
Date: 14 / 1 /2009
(Member/Univ. of Almustansirya)

Signature:
Name: Asist. Prof. Dr. Mohammed K. Hadi Al-Alawi
Date: 14 / 1 /2009
(Supervisor/Univ. of Baghdad)

Approved by the University of Baghdad:

Signature:
Name: Prof. Dr. Ali Al-Kiliddar
Date: /   /2009
Dean of College of Engineering

Acknowledgments

I would like to express my sincere thanks and gratitude to my supervisor, Dr Mohammad K. Hadi, for his encouragement guidance given throughout the period of this research.

Thanks are also to all members of electrical engineering department in college of engineering university of Baghdad for the great help.

I would like to express my gratitude and appreciation to my family for their love, sacrifices and patience during my all years of study. And finally many thanks to my wife Intissar for her support.

ALAA

ABSTRACT

This research deals with the investigation of the load changes influence upon the stability of a turbo-generator. The state equations of the linearized control system must be derived. Then the modern control theory was used with the state equations before an optimization technique is applied. To find the optimal control that minimizing a function (cost function) of both state deviation and control effort.

Firstly the study was made to select a proper model for the synchronous machine infinite bus (SMIB) starting from two axis theorem and the swing equation. Then the model is extended by adding the models of generator-exciter and turbine-governor.

An optimization method which is called the linear optimal control (LOC) is used to improve over all electrical power system stability. This method was checked by using number of test studies applied to enhance the voltage regulator, the turbine governor and a combined control system test models.

The results of testing the (LOC) method show an improvement in overall steady state and transient stability of electrical power system that obtained from increasing the damping of mechanical mode and synchronizing torque which is shown in the test of voltage regulator control system. The degree of stability of a power system can be increased by shifting the poles to the negative side of s-plane. The best quality of the control system obtained from the improvement occurred in overall time domain performance indices. The trial and error in the selection of the (Q and R) weighted matrices of the cost function also can be reduced in this test.

Finally the closed form solution of the Riccati matrix equation can be solved by using a simple MATLAB 7 programming language.

CONTENTS

LIST OF SYMBOLS

A .... state matrix

A_C .... co-state matrix

D ....mechanical damping coefficient

e_{fd} ....Field voltage, volt

$\tilde{E}_t$ ....Complex generator terminal voltage

E_t ....Generator terminal voltage

E_t ....Generator terminal voltage

E_B ....Infinite bus voltage

E_{fd} ....exciter output voltage, volt

f .... Frequency in Hz

H ....Inertia constant in MW.s/ MVA

h ....Hamilton function

I_d ....Current in d-axis winding

I_q ....Current in q-axis winding

I_f .... Current in field winding

I_t ....Generator terminal Current

$\tilde{I}_t$ ....Complex Generator terminal Current

$\tilde{I}_t^*$ .... Complex conjugate Generator terminal Current

J .... Combined moment of inertia of generator and turbine, kg. m^2

j ....Cost function or performance index

K ....Riccati matrix equation

KK ....Close loop feedback gain

K_A ....Regulator gain

K_C ....Rectifier voltage drop

K_E ....Exciter gain

K_D .... Damping of mechanical mode pu torque/ pu speed deviation

K_G .... Reciprocal of regulation or droop

K_S .... Synchronizing torque in pu torque/ rad

K_{ST} .... Total Synchronizing torque (K1Δδ+K2ΔΨ$_{fd}$) in pu torque/ rad

L .... Lagrange function

L_a .... Leakage inductance of armature winding

L_f .... Leakage inductance of field winding

L_l .... leakage inductance

L_{adu} .... per unit mutual inductance

L_{ads} .... Saturated mutual inductance

$L_{ads}^{'}$ .... Saturated transient mutual inductance

M .... Hamiltonian co-state matrix

M_p .... percent over shoot

n .... Speed in rev/ min

p .... Lagrange multiplier

P .... Active power in p.u

P_{amp} .... peak amplitude

P_{ref} .... Reference mechanical power

P_e .... Air gap power

P_f .... Number of field poles pair

Q .... Reactive power in p.u

R_a, R_f .... Armature and field resistance respectively

S .... Laplace operator

S_E .... Saturation function

t .... Time in sec

t_r .... Rise time in sec

t_s .... settling time in sec

T_A .... Regulator time constant

T_C .... Controller internal tima constant

T_E .... Exciter time constant

VIII

T_{CH} ....Chest time constant

T_{RH} ....Reheat time constant

T_{CO} .... Cross over time constant

T_d' .... Short circuit direct axis transient time constant

T_d'' .... Short circuit direct axis sub-transient time constant

T_{do}' .... Open circuit direct axis transient time constant

T_{do}'' ....Open circuit direct axis sub transient time constant

T_q'' .... Short circuit qudrature axis sub-transient time constant

T_{qo}'' ....Open circuit quadrature axis sub transient time constant

T_M ....Mechanical torque in N. M

$\overline{T}_m$ .... Mechanical torque in p.u

T_G... Governor time constant

U_E...Exciter control signal

U_G ....Governor control signal

V_{ref} .... Reference voltage

[X] .... Eigen vector matrix

X_a ....Armature reactance

X_d..Direct axis steady state reactance

X_q..quadrature axis steady state reactance

X_d' ....Direct axis transient reactance

X_d'' .... Direct axis sub transient reactance

X_f ....Field reactance

X_{kd}... Quadrature axis damper reactace

X_{md}... Direct axis mutual reactance

X_{mq}... quadrature axis mutual reactance

X_q' ....Quadrature axis transient reactance

X_q'' .... Quadrature axis subtransient reactance

X_T.. Total system reactance

ω_o ....Rated speed in electrical. Rad/ sec = $2\Pi f_o = 314$ for a 50 Hz system

ω_s .... Angular frequency of stator currents in electrical rad/ sec

ω_r .... Angular frequency of rotor in electrical rad/ sec

$\overline{\omega}_r$ .... Angular frequency of rotor in p.u

ω_n .... Natural undamped frequency rad/ sec

ω_d .... Damping frequency rad/ sec

ΔP_L .... Change of load power

ΔV_L .... Change of load voltage

ΔP_M .... Change in mechanical power

$\Delta \delta$ .... Rotor angle deviation in ele. Rad

$\Delta \omega_r$ .... Speed deviation in p.u $= (\omega_r - \omega_o)/ \omega_o$

δ .... Rotor angle in electrical radians

δ_i .... Internal Rotor angle in electrical radians

Ψ .... flux linkage

Ψ_d .... Direct axis flux linkage

Ψ_q .... Qudrature axis flux linkage

Ψ_{fd} .... Field flux linkage

λ .... Eigen value

ξ .... Damping ratio

LIST OF ABBREVIATIONS

AMPL .... Amplifier

AVR.. Automatic voltage regulator

AGC.. Automatic generation control

BRLS…………………………………………….…..Brushless A.C exciter

CV .... Control value

CH .... Chest

Ex...Exciter

GV .... Gate value

Gov. .... Governor

HP ....High pressure

IP ....Intermediate pressure

LP ....Low pressure

LFC..Load frequency control

LQG.. Linear quadratic Gaussian

LOC. .... Linear optimal control

MVA.. Mega volt ampere

MVAR .... Mega volt ampere reactive

MW...Mega watt active power

N.N. .... Neural network

P.u...Per unit

PID..Proportional integral drevative

RH .... Reheater

S. T. ....Steam turbine

S. G...Synchronous generator

SMIB .... Single machine infinite bus

T. L...Transmission line

VR ....Voltage regulator

CHAPTER ONE
INTRODUCTION

The electrical system units such as generators and associated turbines, synchronous condensers, must operate so that to ensure a definite quality of the normal conditions in the system by maintaining within certain limits, the operating variable quantitivaly characterizes this quality. Excitation regulators control the voltage of synchronous machines, speed governors and frequency regulator maintain the frequency within specified limit[1].

1.1 Power System Stability

Extensive research has been conducted to overcome power system stability problems. For analytical studies, researches have classified the power system stability into three categories:

- **Steady state stability**

This corresponds to the stability of the power system around an operating point. If the system is able to maintain synchronism after small changes in operating conditions, it is said that it has steady state stability.

- **Transient stability**

Transient stability refers to the ability of the power system to regain stability after a sudden and severe disturbance.

- **Dynamic stability**

Dynamic stability is the stability of the power system under small and sudden disturbance. These types of disturbances can lead to long term sustained oscillations.

A small signal perturbation model around an equilibrium point can be considered for dynamic stability studies and the system can be described by non linear differential equations. However for stability studies and control design, the power system must be described by linear differential equations.

A power system stability is ultimately concerned with the quality of electricity supply, it is one of the main research topics in power system studies[2].

There are three means of improving power system stability:

- **Generator excitation control.**

- **Turbine output power control.**

- **System operating condition and configuration control.**

This means that the control system consists of a number of nested control loops that control different quantities in the system, resulting in a number of decupled control loops operating in different time scales[2].

Modern power systems are highly complex and non linear and their operating conditions can vary significantly over a wide range. Power system stability can be defined as that property of a power system that enables it to remain in state of operating equilibrium under normal operating conditions and to regain an acceptable state of equilibrium after being subjected to a disturbance[2].

The ability of a power system to maintain stability depends to large extent on the controls available on the system to damp the electromechanical oscillations. Hence the study and design of controls are very important. Thus a properly designed and operated power system should therefore meet the following fundamental requirements:

1. The system must be able to meet the continuously changing load demand.

2. The system should supply must meet certain minimum standard requirement with regard to the following factors:

- **Constancy of frequency.**

- **Constancy of voltage.**

- **Level of reliability[2].**

1.2 Instability of power system

In evaluation of stability the concern in the behavior of the power system when subjected to a transient disturbance the disturbance may be small or large.

Small disturbances in the form of load changes take place continually, and the system adjusts it self to the changing conditions. The system may be able to operate satisfactorily under these conditions and successfully supply the maximum amount of load.

Instability that may result can be of two forms:

1. **Steady increase in generator rotor angle due to lack of synchronizing torque.**

2. **Rotor oscillations of increasing amplitude due to lack of sufficient damping torque.**

In today's practical power system, the small signal stability problem is usually one of insufficient damping of system oscillations. Small signal analysis using linear techniques provides valuable information about the inherent dynamic characteristics of the power system and assists in its design[2].

In general, the response of a power system to impacts is oscillatory. If the oscillations are damped, so that after sufficient time has elapsed the deviation or the change the state of the system due to the small impact is small (or less than some prescribed finite amount), the system is stable. If on the other hand the oscillations grow in magnitude of a sustained indefinitely, the system is unstable[3].

The time response of a control system consists of two parts: the transient response and the steady state response. By transient response, we mean that which goes from the initial state to the final state. By steady state response, we mean the manner in which the system out put behaves as (t) approaches infinity[4].

1.3 Literature Survey

In the following several researches are summarized in the paragraphs:

In 1971 Hamdy A. M, et.al.[5] used the linear optimal control design. The performance function of the quadratic form was chosen, in that paper three cases were investigated the first with an optimal excitation control (U_E) the second with governor control (U_G) and the third with both excitation and governor control (U_E, U_G). This method was applied for 190 MVA single machine infinite bus system, the results of the optimal controls were shown to be more effective than the conventional control with different cases.

In 1981 B. S. Habibullah[6] considered a fairly accurate synchronous machine model useful for digital computation of transient and dynamic behavior of power systems.

A linear optimal governor controller was designed to stabilize a controllable power system. The controller required neither a state estimator nor an observer for its implementation. That work had successfully tested the stabilizing schemes of various designs by the power group at the University of British Columbia.

In 1989 G. Orelind, et.al.[7] described the development and testing of a digital gain switching governor for hydro generators. Optimal gains were found at different load points by minimizing a quadratic performance criterion prior to controller operation. It was shown that during operation the gain sets were switched in depending on gate position and speed error magnitude. With gain switching operation, the digital governor was shown to have a substantial reduction of noise on the command signal and up to 42% faster response to power requests.

In 1992 Youssef A. Smaili, et.al.[8] investigated the application of H_{∞} optimal control theory to the design of a supplementary excitation and governor control system to improve the stability and performance robustness of an electric power system. That study was based on a single machine infinite bus system. The simulation results showed that the controlled system is robust in face of different types of disturbances that a power system can be subjected to such as changes in voltage or power reference level and three phase short circuit occurred at the infinite bus terminal.

In 1997 H. Bourles, et.al.[9] proposed a robust continuous governor control for small signal and transient stability. The method was applied on a steam turbine with two sections with reheat type. A linear quadratic control was also used to ensure that the steady state objectives are met and that good transient response was obtained.

A comparison between the current and proposed governor controls has been made using Eurostag, a time simulation software for stability studies.

In 1997 Hioaki Nakanish, et.al.[10] proposed a method to design an optimal control system by use of a neural network as a state feed back controller in the regulating problem. Simulation results showed the effectivity of the proposed method.

In 1997 H. yang, et.al.[11] reported a (NN) application that used a generator excitation Control system.

The conventional way to Design an optimal controller for the system was to linearize the system at several selected operating points and implement optimal control at these points. In the paper neural network was trained to give the optimal control Gains over the whole operating range of the excitation system. It was shown that the inherent parallel processing feature made this Design applicable for on-line application.

In 1998 M.L. Kothari, et.al.[12] dealt with the development of small perturbation dynamic model of a single machine-infinite bus system.

A systematic approach based on phase compensation technique for designing optimum power system stabilizers has been presented. Investigations revealed that for designing optimum power system stabilizer, the amortisseurs in the synchronous generator model can be neglected comfortably and hence resulting in considerable simplification in the Design process due to over all reduction in the Dimension of the Dynamic model of the system.

In 2000 Young-Hyun Moon, et.al.[13] presented a new optimal tracking approach to the load frequency control (LFC) problem. Intrinsically has the nature of optimal tracking on the point that generation plant is so special a type of system that the generator automatically supplies its output exactly equal to the load demand. With the use of the optimal tracking approach, the optimal feed back Gains have been calculated for the new LFC scheme adopting the modified PID controller. The optimality of the calculated Gains has been tested for the single machine Infinite bus. It was show that the new LFC scheme with the modified PID controller improved the system damping and reduced system oscillation.

In 2006 Firas Mohammed To'aima[14] an extensive study was made to select a simulation model for the synchronous machine tied to infinite Bus. That work used a linear Quadratic Gaussian (LQG) Controller is used to control the generator and the turbine. The results showed that the use of the LQG controller increased the damping torque that substitutes the need of the power system stabilizer (P_{ss}).

1.4   Aim of Thesis

This thesis demonstrates stability of a synchronous generator connected to an Infinite bus including an exciter and Governor Control.

Controlling the power plants is one of the most important issues in recent works, since it enhances the steady state stability as well as the transient stability; usually this is achieved through controlling the generator terminal voltage by the voltage regulator and the turbine speed by the governor.

Also because one of the Drawbacks of the linear optimal controller design process is that there is no systematic way to determine the weighting matrices Q

and R used in the performance index. These are determined by trial and error process requiring a number of simulation studies[15].

The linear optimal control (LOC) is used with the mathematical model of a synchronous generator including an exciter and governor control[5, 6, 8, 9, 14]. In the present work this controller can be used for testing the power system stability.

A model of a basic power system will be developed to examine the different test modes:

1. Voltage regulator test mode.

2. Turbine Governor Test mode.

3. Combined Governor turbine-Generator exciter test mode.

The results of testing all different test models as in above cases in time domain are compared with and without linear optimal control design (LOC).

The results of testing the (LOC) method show an improvement in overall steady state and transient stability of electrical power system. Also this test can increasing the damping of mechanical mode and synchronizing torque in the test of exciter-regulator control system. This test show an increasing the degree of stability of a power system by shifting the eigen values far from imaginary axis to the left hand side of the s-plane. The figures obtained in time domain shows that the overall time domain performance indices are improved to obtain best quality of the control system. This test can also reduce the trial and error in the selection of the (Q and R) weighted matrices of the cost function.

For the solution of a Riccati matrix equation, a simple MATLAB 7 program was also given in this work (closed form solution). This program can be applied with other applications of a linear optimal control that are depends on solution of a Riccati matrix equation.

1.5 Thesis Outline

This thesis consists of six chapters divided as follows:

Chapter one An Introduction to power system stability and its control; Literature survey on some of the related previous researches and works are included in this chapter with the aim of thesis.

Chapter two, there is a brief description of synchronous Generator Modeling for stability studies.

Chapter three, deals with Turbine Generator without control, which Involves Generator-Exciter modeling and turbine-Governor modeling.

Chapter four, a linear optimal control method for stability enhancement is presented.

Chapter five, explains the results of the designed the linear optimal control for the system with and without control.

Chapter six, reports the final conclusions and future work suggestions for enhancing the stability of the power system.

CHAPTER TWO

SYNCHRONOUS GENERATOR MODELING FOR STABILITY STUDIES

2.1 Introduction

When studying the stability of electrical power system, it is necessary to have mathematical models for all of its elements. The model may be obtained in the form of a set of differential algebraic equations that may be represented in a block diagram and transfer function. The most important elements of a power system from the point of view of dynamic stability and control studies are synchronous machines, and control system used[1].

Synchronous generators from the principal source of electric energy in power system stability problem is largely one of keeping interconnected synchronous machines in synchronism. Therefore, an understanding of their characteristics and accurate modeling of their dynamic performance are of fundamental importance to the study of power system stability[2].

Thus it is very important to develop usable and realistic models of the synchronous machines. Mainly the mechanical properties of the synchronous machines have been modeled using the swing equation, while a very simplistic model of the electrical properties of the synchronous machine has been used. It should be emphasized that the description there aims towards the development of models usable for studying dynamic phenomena in the power system. It is not the purpose of these models to give a detailed and deep understanding of the physical functions of the synchronous machine. Of course it is desirable to have a good insight into the physics of the synchronous machine to be able to derive appropriate models[3].

2.2   Fundamental Concepts of Stability of Dynamic Systems[2]

2.2.1   State Space Representation:

The behavior of a dynamic system, such as a power system, may be described by a set of n first order non linear ordinary differential equations of the following form:

$$\frac{dx_i}{dt} = f_i\,(x_1, x_2, \ldots, x_n, u_1, u_2, \ldots, u_r, t),\, i = 1, 2, \ldots, n$$

Where:

n is the order of the system and r is the no. of inputs. This can be written in the following form by using vector matrix notation;

$$\frac{dx}{dt} = F\,(x, u, t) \quad \ldots\ldots\ldots\ldots\ldots\ldots\ldots\ldots\ldots\ldots\ldots\ldots\ldots\ldots\ldots\ldots\ldots\ldots\ldots(2.1)$$

Where:

$$X = \begin{bmatrix} x_1 \\ . \\ . \\ . \\ x_n \end{bmatrix} \qquad U = \begin{bmatrix} u_1 \\ u_2 \\ . \\ . \\ u_r \end{bmatrix} \qquad F = \begin{bmatrix} f_1 \\ f_2 \\ . \\ . \\ f_n \end{bmatrix}$$

The column vector X is referred to as the state vector, and its entries x_i as state variable. The column vector u is the vector of inputs to the system. These are the external signals that influence the performance of the system. Time is denoted by t and the derivatives of the state variable X with respect to time is denoted by $\frac{dx}{dt}$. If the derivatives of the state variables are not explicit functions of time, the system is said to be autonomous. In this case, equation (2.1) simplifies to

$$\frac{dX}{dt} = F\,(x, u) \quad \ldots\ldots\ldots\ldots\ldots\ldots\ldots\ldots\ldots\ldots\ldots\ldots\ldots\ldots\ldots\ldots\ldots\ldots\ldots(2.2)$$

We are often interested in output variables that can be observed on the system. These may be expressed in terms of the state variables and the input variables in the following form:

$$Y= g (x, u) \dotfill (2.3)$$

Where:

$$Y = \begin{bmatrix} y_1 \\ . \\ . \\ . \\ y_m \end{bmatrix} \qquad g = \begin{bmatrix} g_1 \\ . \\ . \\ . \\ g_m \end{bmatrix}$$

The column vector Y is the vector of outputs and g is a vector of nonlinear functions relating state and input variables to output variables[2].

2.2.2 Linearization

Let x_0 be the initial state vector and u_0 the input vector corresponding to the equilibrium point about which the small signal performance is to be investigated. Since x_0 and u_0 satisfy equation (2.2).

We have:

$$\frac{d x_0}{dt} = f(x_0, u_0) = 0 \dotfill (2.4)$$

Let us perturb the system from the above state, by letting:

$$x = x_0 + \Delta x \qquad u = u_0 + \Delta u$$

Where:

The prefix Δ denotes a small deviation.

The new state must satisfy equation (2.2).

Hence:

$$\frac{d x}{dt} = \frac{dx_0}{dt} + \frac{d\Delta x}{dt} = f[(x_0 + \Delta x),(u_0 + \Delta u)]$$

As the perturbations are assumed to be small, the non linear function f(x,u) can be expressed in terms of Taylors series expansion. With terms involving second and higher order powers of Δx and Δu neglected, we may write:

$$\dot{x}_i = \dot{x}_{i_0} + \Delta \dot{x}_i = f_i\left[(x_0 + \Delta x),(u_0 + \Delta u)\right] = f_i(x_0, u_0) + \frac{\partial f_i}{\partial x_1}\Delta x_1 + ... +$$
.........................(2.5)
$$\frac{\partial f_i}{\partial x_n}\Delta x_n + \frac{\partial f_i}{\partial u_1}\Delta u_1 + ... + \frac{\partial f_i}{\partial u_r}\Delta u_r$$

Since

$$\dot{x}_{i0} = f_i(x_0, u_0) \text{ we obtain}$$
$$\Delta \dot{x}_i = \frac{\partial f_i}{\partial x_1}\Delta x_1 + ... + \frac{\partial f_i}{\partial x_n}\Delta x_n + \frac{\partial f_i}{\partial u_1}\Delta u_1 + ... + \frac{\partial f_i}{\partial u_r}\Delta u_r$$
....(2.6)

With:

i = 1, 2, …, n in a like manner, from equation (2.3), we have:

$$\Delta y_j = \frac{\partial g_i}{\partial x_1}\Delta x_1 + ... + \frac{\partial g_i}{\partial x_n}\Delta x_n + \frac{\partial g_i}{\partial u_1}\Delta u_1 + ... + \frac{\partial g_i}{\partial u_r}\Delta u_r$$
....(2.7)

With:

j = 1, 2, …, m therefore, the linearized forms of equations (2.2) & (2.3) are:

$$\frac{d\Delta x}{dt} = A\Delta x + B\Delta u$$ ....(2.8)

$$\Delta y = C\Delta x + D\Delta u$$ ....(2.9)

Where:

$$A = \begin{bmatrix} \frac{\partial f_1}{\partial x_1} & \cdot & \cdot & \cdot & \frac{\partial f_1}{\partial x_n} \\ \cdot & \cdot & \cdot & \cdot & \cdot \\ \cdot & \cdot & \cdot & \cdot & \cdot \\ \frac{\partial \dot{f}_n}{\partial x_1} & \cdot & \cdot & \cdot & \frac{\partial \dot{f}_n}{\partial x_n} \end{bmatrix} \qquad B = \begin{bmatrix} \frac{\partial f_1}{\partial u_1} & \cdot & \cdot & \cdot & \frac{\partial f_1}{\partial u_r} \\ \cdot & \cdot & \cdot & \cdot & \cdot \\ \cdot & \cdot & \cdot & \cdot & \cdot \\ \frac{\partial \dot{f}_n}{\partial u_1} & \cdot & \cdot & \cdot & \frac{\partial \dot{f}_n}{\partial u_r} \end{bmatrix}$$

$$C = \begin{bmatrix} \frac{\partial g_1}{\partial x_1} & \cdot & \cdot & \frac{\partial g_1}{\partial x_n} \\ \cdot & \cdot & \cdot & \cdot \\ \frac{\partial \dot{g}_m}{\partial x_1} & \cdot & \cdot & \frac{\partial \dot{g}_m}{\partial x_n} \end{bmatrix} \qquad D = \begin{bmatrix} \frac{\partial g_1}{\partial u_1} & \cdot & \cdot & \frac{\partial g}{\partial u_r} \\ \cdot & \cdot & \cdot & \cdot \\ \frac{\partial \dot{g}_m}{\partial u_1} & \cdot & \cdot & \frac{\partial \dot{g}_m}{\partial u_r} \end{bmatrix}$$

The above partial derivatives are evaluated at the equilibrium point about which the small perturbation is being analyzed.

In equation (2.8) and (2.9):

Δx: is the state vector of dimension n
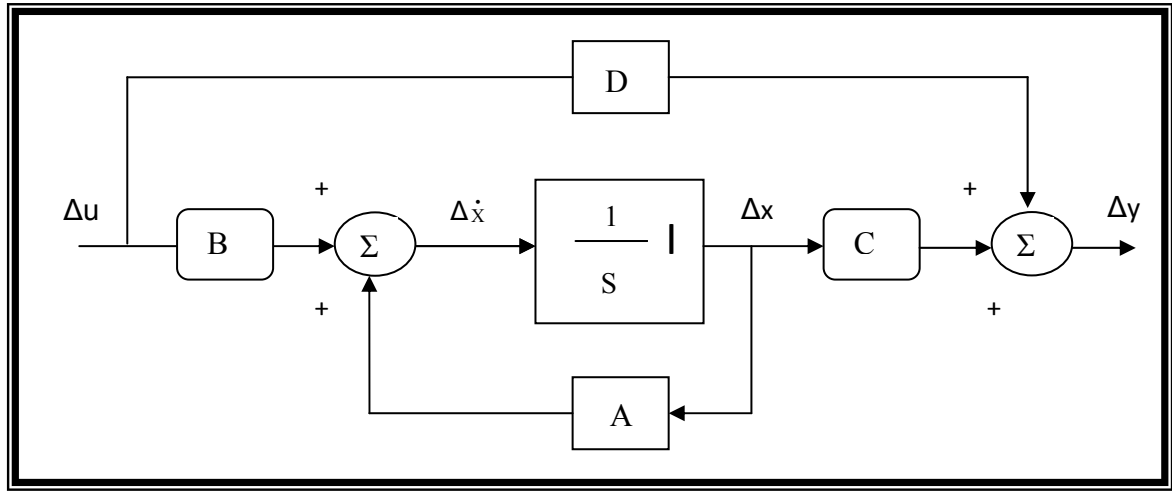
Δy: is the o/p vector of dimension m

Δu: is the i/p vector of dimension r

A: is the state or plant matrix of size n×n

B: is the control or i/p matrix of size n×r

C: is the o/p matrix of size m×n

D: is the (feedforward) matrix which defines the proportion of i/p which appears directly in the o/p, size m×r

Figure (2.1) shows the block diagram of the state space representation[2].

Figure (2.1): Block Diagram of The State – Space Representation[2]

2.3 Machine Parameters

There have been several methods used to determine the parameters of a synchronous machine. All of these methods base their analysis on acquiring the operational Inductance obtaining some time constants from the inductance data and then using this to determine the parameters of the machine[16].

The machine data from manufacturers are usually in the form of reactance's, time constants and resistances; most are derived from measurements taken from the stator winding. The sub transient period refers to the first few cycles of the short circuit when the stator current decay is very rapid, attributable mainly to the changes in the currents of the damper windings. The rate of the current decay in the transient period is slower and is attributed mainly to changes in the currents of the rotor field windings[17].

Following a disturbance, currents are induced in the machine rotor circuits. For a short circuit, some of these induced rotor currents decay more rapidly than others. Machine parameters that influence rapidly decaying components are called the sub transient parameters, while those influencing the slowly decaying components are called the transient parameters and these influencing sustained components are the synchronous parameters.

The synchronous machine characteristics of interest are the effective Inductances (or reactance's) as seen from the terminals of the machine and associated with the fundamental frequency currents during sustained, transient and subtransient conditions. In addition to these inductances, the corresponding time constant which determines the rate of decay of currents and voltages from the standard parameters used in specifying synchronous machine electrical characteristics[2].

2.3.1 The Two Axis Theorem

The electrical characteristic equations describing a three phase synchronous machine are commonly defined by a two dimensional reference frame. This involves the use of parks transformation[18] to convert currents and flux linkages in to two fictitious windings located apart. A typical synchronous machine consists of three stator windings mounted on the stator and one field winding mounted on the rotor. These axes are fixed with respect to the rotor (d – axis) and the other lies along the magnetic neutral axis (q – axis). Which model the short – circuited paths of the damper windings. Electrical quantities can then be

expressed in terms of d and q – axis parameters. Figure (2.2) presents the diagram of d – q axis in the machine[19].
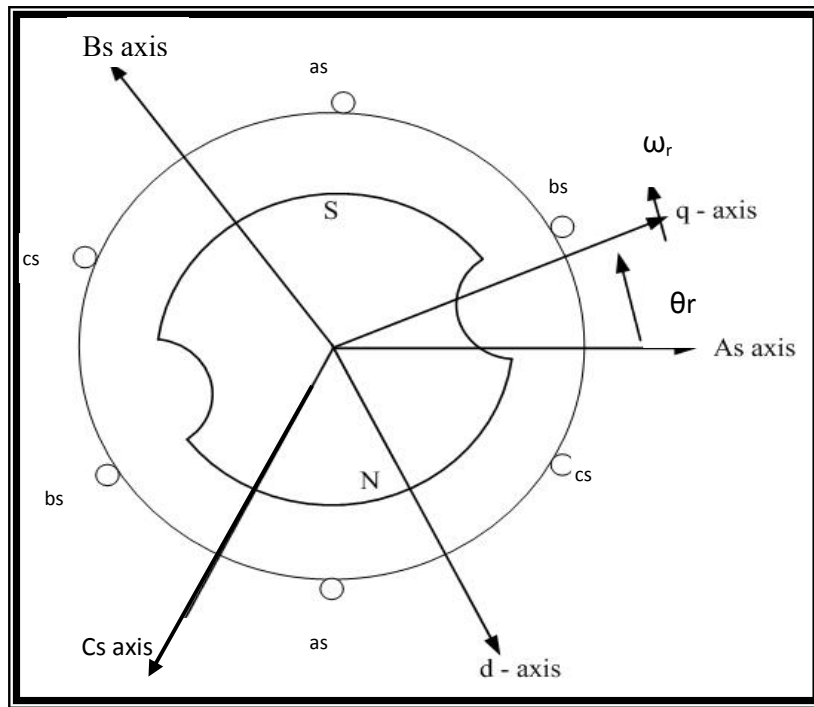
Figure (2.2): Illustration of The Positions of d –q Axis on A Two Pole Machine[20]

2.3.2   Direct and quadrature axis

The direct axis reactance during transient is not the same as that in the steady state. The value of X_d to be used during transients is called the direct axis transient reactance $X_d^{'}$ [16].

$$X_d^{'} = X_a + \frac{X_{md} X_f}{X_{md} + X_f}$$ ....(2.10)

Where:

X_a: leakage reactance of armature winding

X_{md}: mutual reactance between the field and d – axis winding

X_f: leakage reactance of the field winding

The next figure (2.3) shows the direct axis equivalent circuit.
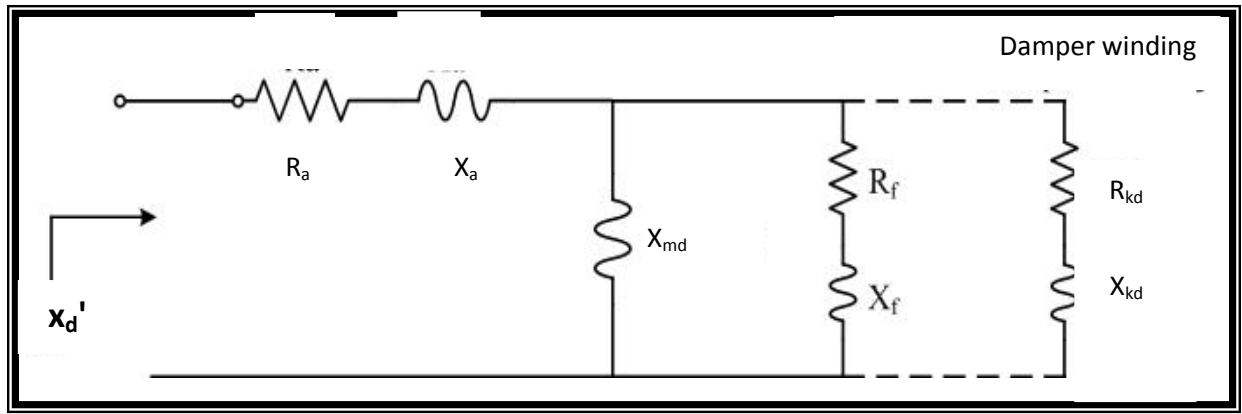
Figure (2.3): Direct axis equivalent circuit[16]

Since during transients the flux linkage with the field winding change, they will also change with any closed circuit on the rotor[16]

The leakage reactance of damper winding is negligible in the steady state but during subtransient and transient state, it will be significant as it affects the time constants in those periods. The equation for direct axis subtransient reactance X_d'' is[16]:

$$X_d'' = X_a + \frac{X_{md} X_f X_{kd}}{X_{md} X_f + X_{md} X_{kd} + X_f X_{kd}} \quad \dots\dots\dots\dots\dots(2.11)$$

The quadrature axis equivalent circuit as shown in Figure (2.4) is similar to the direct axis equivalent circuit but it has no field winding[21]
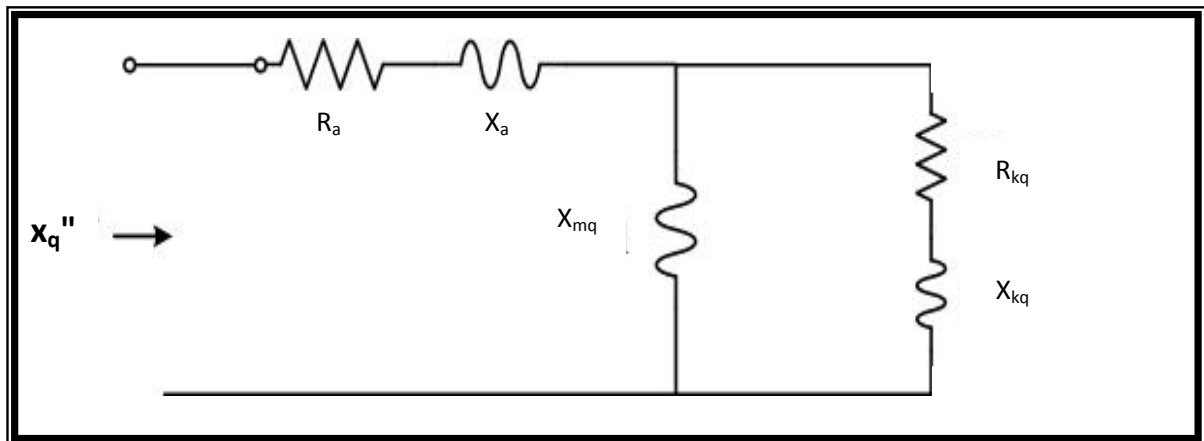
Figure (2.4): Quadrature Axis Equivalent Circuit[16].

$$X_q'' = X_a + \frac{X_{mq} X_{kq}}{X_{mq} + X_{kq}} \quad \text{...(2.12)}$$

Consequently, various time constants can be obtained as follows[21].

$$T_d' = \frac{1}{\omega_0 R_f}(X_f + \frac{X_{md} X_a}{X_{md} + X_a}) \quad \text{..(2.13)}$$

$$T_{d_0}' = \frac{1}{\omega_0 R_f}(X_{md} + X_f) \quad \text{..(2.14)}$$

$$T_{d0}'' = \frac{1}{\omega_0 R_{kd}}(X_{kd} + \frac{X_{md} X_f}{X_{md} + X_f}) \quad \text{...(2.15)}$$

$$T_d'' = \frac{1}{\omega_0 R_{kd}}(X_{kd} + \frac{X_{md} X_f X_a}{X_{md} X_f + X_{md} X_a + X_a X_f}) \text{...................................(2.16)}$$

$$T_{q_0}'' = \frac{1}{\omega_0 R_{kq}}(X_{kq} + X_{mq}) \quad \text{..(2.17)}$$

$$T_q'' = \frac{1}{\omega_0 R_{kq}}(X_{kq} + \frac{X_{mq} X_a}{X_{mq} + X_a}) \quad \text{.. (2.18)}$$

2.4 Small – Signal Stability[2]

Small signal stability is the ability of the power system to maintain synchronism when subjected to small disturbances. A disturbance is considered to be small if the equations that describe the resulting response of the system may be linearized for the purpose of analysis with electric power systems. The change in electrical torque of synchronous machine following a perturbation can be resolved in to two components

$$\Delta Te = Ks\,\Delta\delta + K_D\,\Delta\omega \text{...(2.19)}$$

Where:

Ks $\Delta\delta$ is the component of torque change in phase with the rotor angle perturbation $\Delta\delta$ and is referred to as the synchronizing torque component; Ks is the synchronizing torque coefficient.

$K_D\,\Delta\omega$ is the component of torque in phase with the speed deviation $\Delta\omega$ and is referred to as the damping torque component; K_D is the damping torque coefficient.

System stability depends on the existence of both components of torque for each of the synchronous machines.

Instability that may result can be of two forms:

1. Steady increase in generator rotor angle due to lack of synchronizing torque.

2. Rotor oscillations of increasing amplitude due to lack of sufficient damping torque. In practical power systems, the small signal stability problem is usually one of insufficient damping of system oscillations. Small signal analysis using linear techniques provides valuable information about the inherent dynamic characteristic of the power system and assists in its design[2].

2.5 Inertia Constant and Swing Equation[2]

The equations of central importance in power system stability analysis are the rotational inertia equations describing the effect of unbalance between the electromagnetic torque and the mechanical torque of the individual machines.

When there is no balance between the torques acting on the rotor, the net torque causing acceleration (or deceleration) is:

$$T_a = T_m - T_e$$ ....(2.20)

Where:

T_a: accelerating torque in N.M

T_m: mechanical torque in N.M

T_e: electromagnetic torque in N.M

In the above equation, T_m and T_e are positive for generator and negative for motor. The combined inertia of the generator and prime mover is accelerated by the unbalance in the applied torques. Hence the equation of motion is:

$$J\frac{d\omega_m}{dt} = T_a = T_m - T_e$$ ....(2.21)

Where:

J: combined moment of inertia of generator and turbine, Kg.m^2.

ω_m: angular velocity of the rotor, mech rad/ sec.

t: time in sec.

The above equation can be normalized in terms of per unit inertia constant H, defined as the kinetic energy in watt – seconds at rated speed divided by the V.A base. Using ω_{om} to denote rated angular velocity in mechanical radians per second, the inertia constant is:

$$H = \frac{1}{2} \frac{J\omega_{om}^2}{VA_{base}}$$ ....(2.22)

The moment of inertia J in terms of H is:

$$J = \frac{2H}{\omega_{0m}^2} VA_{base}$$ ....(2.23)

Substituting the above in equation (2.21) gives:

$$\frac{2H}{\omega_{om}^2} VA_{base} \frac{d\omega_m}{dt} = T_m - T_e$$ ....(2.24)

Rearranging yields:

$$2H \frac{d}{dt}\left(\frac{\omega_m}{\omega_{0m}}\right) = \frac{T_m - T_e}{VA_{base} / \omega_{0m}}$$ ....(2.25)

Noting that $T_{base} = VA_{base}/\omega_{om}$, the equation of motion in per unit form is:

$$2H \frac{d\bar{\omega}_r}{dt} = \bar{T}_m - \bar{T}_e$$ ....(2.26)

In the above equation:

$$\bar{\omega}_r = \frac{\omega_m}{\omega_{0m}} = \frac{\omega_r/P_f}{\omega_0/P_f} = \frac{\omega_r}{\omega_0}$$ ....(2.27)

Where:

ω_r is angular velocity of the rotor in electrical rad/s, ω_o is the rated value, and P_f is the number of field pole pairs. If δ is the angular position in electrical

radians with respect to synchronously rotating reference and δ_0 is its value at t= 0.

$$\delta = \omega_r t - \omega_0 t + \delta_0 \quad \dotfill (2.28)$$

Taking the time derivative, then:

$$\frac{d\delta}{dt} = \omega_r - \omega_0 = \Delta\omega_r \quad \dotfill (2.29)$$

$$\frac{d\delta^2}{dt^2} = \frac{d\omega_r}{dt} = \frac{d(\Delta\omega_r)}{dt} = \omega_0 \frac{d\overline{\omega}_r}{dt} = \omega_o \frac{d(\Delta\overline{\omega}r)}{dt} \quad \dotfill (2.30)$$

Substituting for $\frac{d}{dt}\overline{\omega}_r$ given by the above equation in (2.26), then:

$$\frac{2H}{\omega_0} \frac{d\delta^2}{dt^2} = \overline{T}_m - \overline{T}_e \quad \dotfill (2.31)$$

It is often desirable to include a component of damping torque, not accounted for in the calculation of T_e separately. This is accomplished by adding a term proportional to speed deviation in the above equation as follows:

$$\frac{2H}{\omega_0} \frac{d\delta^2}{dt^2} = \overline{T}_m - \overline{T}_e - K_D \Delta\overline{\omega}_r \quad \dotfill (2.32)$$

From equation (2.29)

$$\Delta\overline{\omega}_r = \frac{\Delta\omega_r}{\omega_0} = \frac{1}{\omega_0} \frac{d\delta}{dt} \quad \dotfill (2.33)$$

Equation (2.32) represents the equation of motion of synchronous machine. And it is commonly referred as (swing equation) because it represents swings in rotor angle δ during disturbances.

The swing equation (2.32) can be expressed as two first order differential equations:

$$\frac{d(\Delta\overline{\omega}_r)}{dt} = \frac{1}{2H}\left(\overline{T}_m - \overline{T}_e - K_D \Delta\overline{\omega}_r\right) \quad \dotfill (2.34)$$

$$\frac{d\delta}{dt} = \omega_0 \Delta\overline{\omega}_r + \delta_o \quad ....(2.35)$$

In the above equation, time t is in seconds rotor angle δ is in electrical radians, and ω_0 is equal to $2\pi f$[2].

The block diagram from representation of equation (2.34), (2.35) is shown in Figure (2.5).
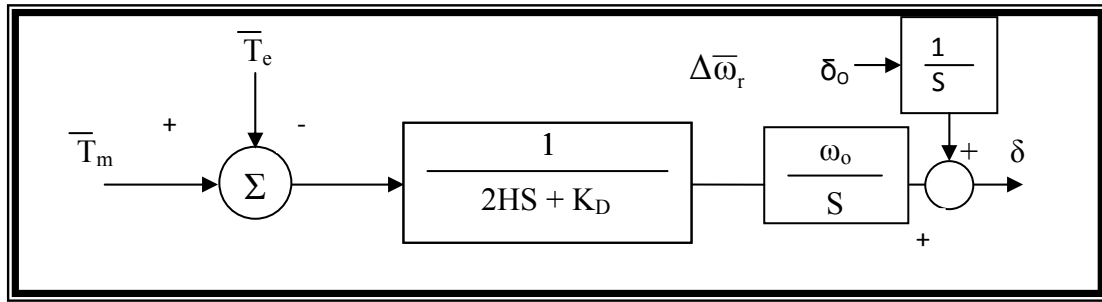
Figure (2.5): Block Diagram Representation of Swing Equation[2]

2.6 Generator Represented by the Classical Model [2]

With the generator represented by the classical model and all resistances neglected, the system representation is shown in Figure (2.6) below.
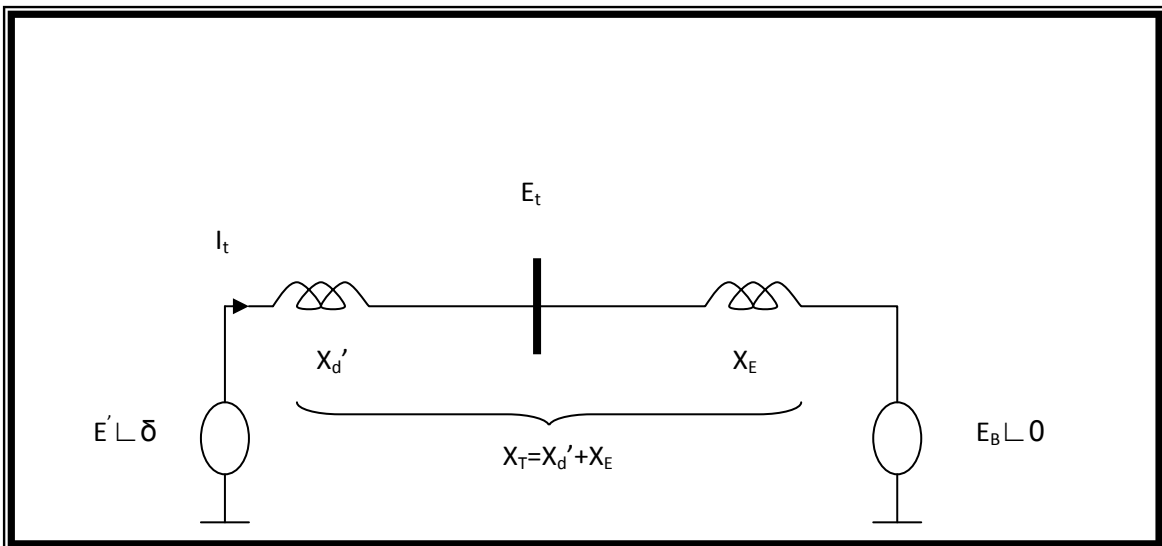
Figure (2.6) Synchronous machine connected to infinite bus bar[2]

Here E' is the voltage behind X_d', its magnitude is assumed to remain constant at the pre disturbance value. Let δ be the angle by which E' leads the infinite bus voltage E_B. As the rotor oscillates during a disturbance, δ changes[2].

With E' as reference pharos,

$$\tilde{I}_t = \frac{E'\angle o - E_B \angle -\delta}{jx_T} = \frac{E' - E_B\left(\cos\delta - j\sin\delta\right)}{jx_T} \quad \dots\dots\dots\dots\dots\dots\dots\dots(2.36)$$

The complex power behind X_d' is given by:

$$S' = p + jQ' = \tilde{E}'\,\tilde{I}_t^* = \frac{E'E_B\sin\delta}{X_T} + j\frac{E'\left(E' - E_B\cos\delta\right)}{X_T} \quad \dots\dots\dots\dots\dots(2.37)$$

With the stator resistance neglected, the air gap power (p_e) is equal to the terminal power (p_e). In per unit, the air gap torque is equal to the air gap power. Hence:

$$T_e = P_e = \frac{E'E_B}{X_T}\sin\delta \quad \dots\dots\dots\dots\dots\dots\dots\dots\dots\dots\dots\dots\dots\dots(2.38)$$

By linearizing about an initial operating condition represented by $\delta = \delta_0$ yields

$$\Delta T_e = \frac{\partial T_e}{\partial \delta}\Delta\delta = \frac{E'E_B}{X_T}\cos\delta_o\left(\Delta\delta\right) \quad \dots\dots\dots\dots\dots\dots\dots\dots\dots\dots\dots(2.39)$$

Where:

$$K_s = \frac{\partial T_e}{\partial \delta} = \frac{E'E_B}{X_T}\cos\delta_o$$

The equations of motion in per unit are:

$$\frac{d}{dt}\Delta\omega_r = \frac{1}{2H}\left(T_m - T_e - K_D\,\Delta\omega_r\right) \quad \dots\dots\dots\dots\dots\dots\dots\dots\dots(2.40)$$

$$\frac{d}{dt}\delta = \omega_0\,\Delta\omega_r + \delta_o \quad \dots\dots\dots\dots\dots\dots\dots\dots\dots\dots\dots\dots\dots\dots\dots(2.41)$$

Where:

$\Delta\omega_r$ is the per unit speed deviation, δ is the rotor angle in electrical radians, ω_0 is the base rotor electrical speed in radians per seconds.

Liniarizing equation (2.40) and substituting for ΔT_e given by equation (2.39) we obtain:

$$\frac{d}{dt}\Delta\omega_r = \frac{1}{2H}\left[\Delta T_m - K_s\Delta\delta - K_D\,\Delta\omega_r\right] \text{.....................................(2.42)}$$

Where:

Ks: synchronizing torque coefficient in pu Torque/ rad.

K_D: damping torque coefficient in pu Torque/ per unit speed deviation.

H: inertia constant in MW. S/ MVA.

$\Delta\omega_r$: speed deviation in p.u= $(\omega_r - \omega_0)/\omega_0$.

$\Delta\delta$: rotor angle deviation in ele. Rad.

ω_0: rated speed in ele. Rad/ s and equal to 2Π fo.

By linearizing equation (2.41)

$$\frac{d}{dt}\Delta\delta = \omega_0\,\Delta\omega_r \text{...(2.43)}$$

Writing equations (2.42) and (2.43) in the matrix form (2.8)

We obtain:

$$\frac{d}{dt}\begin{bmatrix}\Delta\omega_r \\ \Delta\delta\end{bmatrix} = \begin{bmatrix}-\dfrac{K_D}{2H} & -\dfrac{K_S}{2H} \\ \omega_0 & 0\end{bmatrix}\begin{bmatrix}\Delta\omega_r \\ \Delta\delta\end{bmatrix} + \begin{bmatrix}\dfrac{1}{2H} \\ 0\end{bmatrix}\Delta T_m \text{.......................(2.44)}$$

The elements of the state matrix A are seen to be dependent on the system parameter K_D, H, K_S, and the initial operating conditions represented by the values of E' and δ_0.

The block diagram approach that was first used by Heffron and Phillipsand later by demello and Concordia[22] represented in Figure (2.6) can be used to describe the small signal performance.
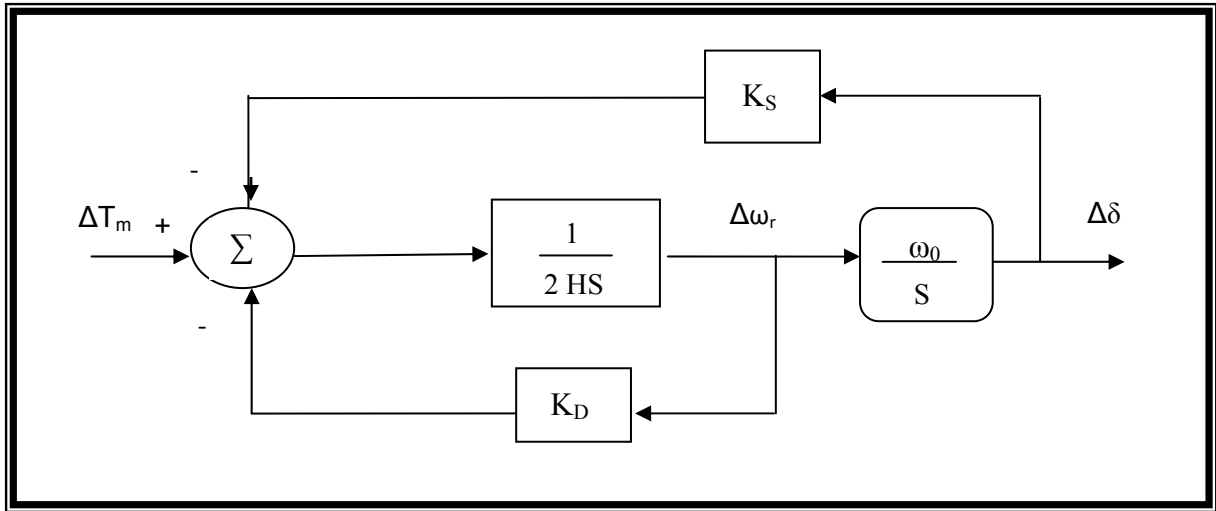
***Figure (2.7): Block Diagram of a Single-Machine Infinite Bus System
With Classical Generator Model[2]***

2.7 Effect of Synchronous Machine Field Flux Variation[2]

The system performance will be considered now including the effect of field flux variations. The amortisseur effects will be neglected and the field voltage will be assumed constant (manual excitation control).

As in the case of the classical generator model, the acceleration equations (2.40) and (2.41) that are derived. the rotor angle δ (in elect. Rad) by which $q -$ axis leads the reference E_B. as shown in Figure (2.8), the rotor angle δ is the sum of the internal angle δ_i and the angle by which E_t leads E_B. A convenient mean will be needed for identifying the rotor position with respect to an appropriate reference and keeping track of it as the rotor oscillates[2].
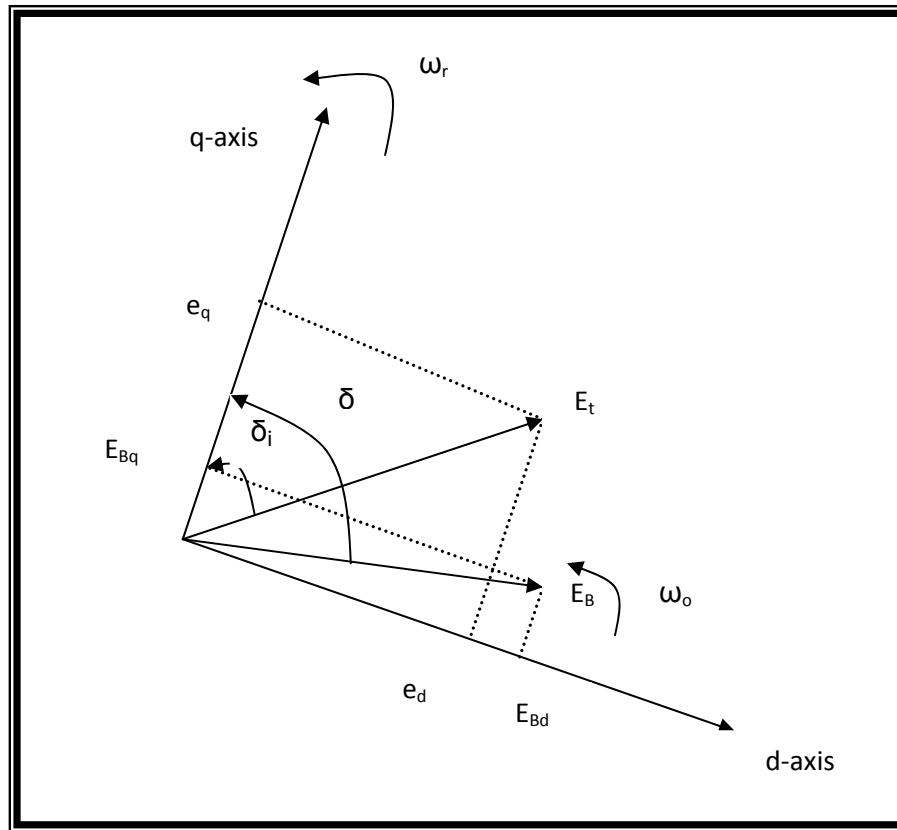
Figure(2.8)d-q axis vector diagram [2]

The q-axis offers this convenience when the dynamics of rotor circuits are represented in the machine model. The choice of E_B as the reference of measuring rotor angle is convenient from the view point of solution of network equations.

The field circuit dynamic equation is:

$$\frac{d}{dt}\psi_{fd} = \omega_0\left(e_{fd} - R_{fd} * i_{fd}\right) = \frac{\omega_o * R_{fd}}{L_{adu}} E_{fd} - \omega_o R_{fd} i_{fd} \quad\text{.......................(2.45)}$$

Where

E_{fd} :is the exciter output voltage ($E_{fd} = \frac{L_{adu}}{R_{fd}} e_{fd}$)

e_{fd} :field voltage.

The equations (2.40), (2.41) and (2.45) describe of the synchronous machine with $\Delta\omega_r$, δ and ψ_{fd} as the state variables.

From the equivalent circuit that are shown in figure (2.9) below:
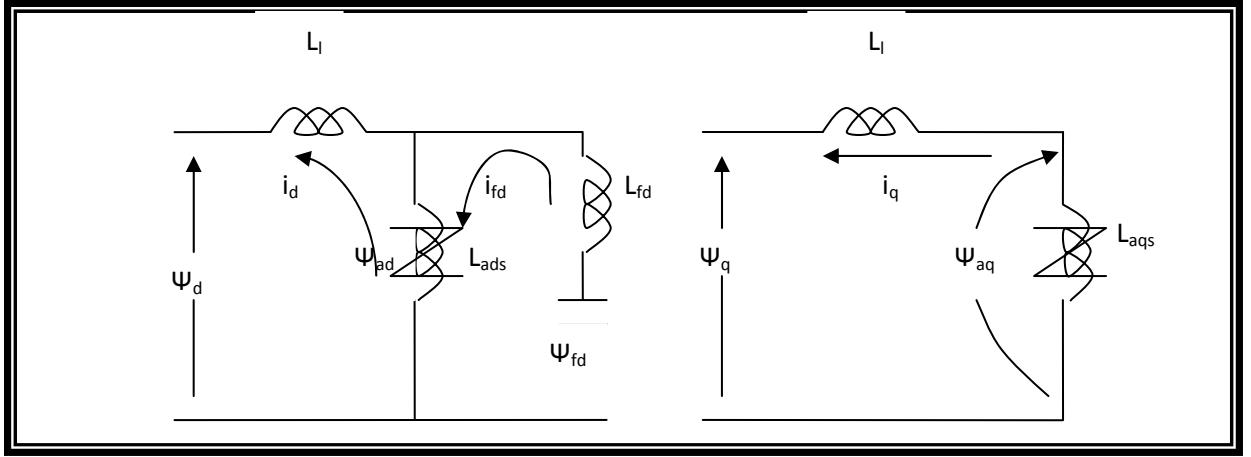
Figure (2.9) S.M equivalent circuit relating flux linkage in d-q axis[2]

The stator and rotor flux linkages are given by:

$$\psi_d = -L_l i_d + L_{ads}\left(-i_d + i_{fd}\right) = -L_l i_d + \psi_{ad} \quad\text{............................(2.46)}$$

$$\psi_q = -L_l i_q + L_{aqs}\left(-i_q\right) = -L_l i_q + \psi_{aq} \quad\text{....................................(2.47)}$$

$$\psi_{fd} = L_{ads}\left(-i_d + i_{fd}\right) + L_{fd}i_{fd} = \psi_{ad} + L_{fd}i_{fd} \quad\text{....................................(2.48)}$$

In the above equations ψ_{aq} & ψ_{ad} are the air gap mutual flux linkage, L_{ads} and L_{aqs} are the saturated values of the mutual inductance.

From (2.48) the field current may be expressed as:

$$i_{fd} = \frac{\psi_{fd} - \psi_{ad}}{L_{fd}} \quad\text{...(2.49)}$$

The d-axis mutual flux linkage can be written in term of ψ_{fd} and i_d as follows:

$$\psi_{ad} = L_{ads}'\left(-i_d + \frac{\psi_{fd}}{L_{fd}}\right) \quad\text{...(2.50)}$$

Where:

$$L_{ads}' = \left(\frac{1}{\dfrac{1}{L_{ads}} + \dfrac{1}{L_{fd}}}\right)$$

Since there are no rotor circuits considered in the q-axis the mutual flux linkage is given by

$$\psi_{aq} = -L_{aqs}i_q \quad \text{...(2.51)}$$

The air gap torque is

$$T_e = \psi_{ad}i_q - \psi_{aq}i_d \quad \text{...(2.52)}$$

With $p\psi$ terms and speed variations neglected the stator voltage equations are:

$$e_d = -R_a i_d - \Psi_q = -R_a i_d + \left(L_l i_q - \psi_{aq}\right) \text{.....................................(2.53)}$$

$$e_q = -R_a i_q + \psi_d = -R_a i_q - \left(L_l i_d - \psi_{ad}\right) \text{.....................................(2.54)}$$

"the assumption of per unit ω_r=1 (i.e. $\omega_r = \omega_o$ rad/sec) in the stator voltage equations dose not contribute to computational simplicity in itself. The primary reason of making this assumption is that it counterbalances the effect of neglecting $P\Psi_d$, $P\Psi_q$ "[2].

Since there is only one machine the machine as well as the network equations can be expressed in terms of one reference frame i.e, the d-q reference frame of the machine referring to figure (2.8),the machine terminal and infinite bus voltages in terms of the d-q components are:

$$\tilde{E}_t = e_d + je_q \quad \text{...(2.55)}$$

$$\tilde{E}_B = E_{Bd} + jE_{Bq} \quad \text{..(2.56)}$$

The network equation for the system of figure (2.6) resolved to d-q axis is:

$$e_d = R_E i_d - x_E i_q + E_{Bd} \quad \text{...(2.57)}$$

$$e_q = R_E i_q - x_E i_d + E_{Bq} \quad \text{...(2.58)}$$

Where:

$$\tilde{E}_t = \tilde{E}_B + \left(R_E + jX_E\right)\tilde{I}_t \text{ .and } \left(e_d + je_q\right) = \left(E_{Bd} + jE_{Bq}\right) + \left(R_E + jX_E\right)\left(i_d + ji_q\right)$$

$$E_{Bd} = E_B Sin\delta \dots\dots\dots\dots\dots\dots\dots\dots\dots\dots(2.59)$$

$$E_{Bq} = E_B Cos\delta \dots\dots\dots\dots\dots\dots\dots\dots\dots\dots(2.60)$$

Using (2.53) and (2.54) to eliminate e_d, e_q in equation (2.57) and (2.58) and using expressions for $\Psi_{ad,}$ Ψ_{aq} given by (2.50) and (2.51) to obtain i_d & i_q in terms of state variable Ψ_{fd}

$$i_d = \frac{X_{Tq}\left[\psi_{fd}\left(\dfrac{L_{ads}}{L_{ads}+L_{fd}}\right) - E_B Cos\delta\right] - R_T E_B Sin\delta}{D} \dots\dots\dots\dots\dots(2.61)$$

$$i_q = \frac{R_T\left[\psi_{fd}\left(\dfrac{L_{ads}}{L_{ads}+L_{fd}}\right) - E_B Cos\delta\right] + X_{Td} E_B Sin\delta}{D} \dots\dots\dots\dots\dots(2.62)$$

Where:

$$R_T = R_a + R_E \qquad , \qquad X_{Tq} = X_E + \left(L_{aqs} + L_l\right) = X_E + X_{qs} \qquad ,$$

$$X_{Td} = XE + \left(L_{ads}' + L_l\right) = X_E + X_{ds}' \qquad , \qquad D = R_T^2 + X_{Tq}X_{Td}.$$

Equations (2.61), (2.62), (2.49), (2.50) and (2.51) can be used to eliminate i_{fd} & T_e from (2.40), (2.41) and (2.45), these equations are non linear and have to be linearized for small signal analysis.

$$\Delta i_d = m_1 \Delta\delta + m_2 \Delta\psi_{fd} \dots\dots\dots\dots\dots\dots\dots\dots(2.63)$$

$$\Delta i_q = n_1 \Delta\delta + n_2 \Delta\psi_{fd} \dots\dots\dots\dots\dots\dots\dots\dots(2.64)$$

Where:

$$m_1 = \frac{E_B\left(X_{Tq}Sin\delta_o - R_T Cos\delta_o\right)}{D} \quad , \quad n_1 = \frac{E_B\left(R_T Sin\delta_o + X_{Td}Cos\delta_o\right)}{D}$$

$$m_2 = \frac{X_{Tq}}{D}\frac{L_{ads}}{L_{ads}+L_{fd}} \qquad\qquad , n_2 = \frac{R_T}{D}\frac{L_{ads}}{L_{ads}+L_{fd}}$$

By linearizing (2.49), (2.50) and (2.51) and substituting in term of Δi_d, Δi_q we get:

$$\Delta\psi_{ad} = \left(\frac{1}{L_{fd}} - m_2\right) L_{ads}{}' \Delta\psi_{fd} - m_1 L_{ads}{}' \Delta\delta \qquad\qquad ....(2.65)$$

$$\Delta\psi_{aq} = -n_2 L_{aqs}\Delta\psi_{fd} - n_1 L_{aqs}\Delta\delta \qquad\qquad ....(2.66)$$

$$\Delta i_{fd} = \frac{1}{L_{fd}}\left(1 - \frac{L_{ads}{}'}{L_{fd}} + m_2 L_{ads}{}'\right)\Delta\psi_{fd} + \frac{1}{L_{fd}}m_1 L_{ads}{}'\Delta\delta \qquad ....(2.67)$$

$$\Delta T_e = \psi_{ado}\Delta iq + i_{qo}\Delta\psi_{ad} - \psi_{aqo}\Delta i_d - i_{do}\Delta\psi_{aq} \qquad ....(2.68)$$

By substituting Δi_d, Δi_q, $\Delta\psi_{ad}$ and $\Delta\psi_{aq}$ in ΔT_e to obtain:

$$\Delta T_e = K_1\Delta\delta + K_2\Delta\psi_{fd} \qquad\qquad ....(2.69)$$

Also by linearzing (2.40), (2.41) and (2.45) and substitute the expressions for Δi_{fd} and ΔT_e given by (2.67) & (2.69) we obtain the system equations in the desired final form:

$$\frac{d}{dt}\begin{bmatrix}\Delta\omega_r\\ \Delta\delta\\ \Delta\psi_{fd}\end{bmatrix} = \begin{bmatrix}a_{11} & a_{12} & a_{13}\\ a_{21} & 0 & 0\\ 0 & a_{32} & a33\end{bmatrix}\begin{bmatrix}\Delta\omega_r\\ \Delta\delta\\ \Delta\psi_{fd}\end{bmatrix} + \begin{bmatrix}b_{11} & 0\\ 0 & 0\\ 0 & b_{32}\end{bmatrix}*\begin{bmatrix}\Delta T_m\\ \Delta E_{fd}\end{bmatrix} \qquad ....(2.70)$$

Where:

$$a_{11} = -\frac{KD}{2H}, \quad a_{12} = -\frac{K_1}{2H}, \quad a_{13} = -\frac{K_2}{2H}, \quad a_{21} = 2\pi f_o$$

$$a_{32} = -\frac{\omega_o R_{fd}}{L_{fd}} m_1 L_{ads}' \quad, \quad a_{33} = -\frac{\omega_o R_{fd}}{L_{fd}} \left[1 - \frac{L_{ads}'}{L_{fd}} + m_2 L_{ads}' \right]$$

$$b_{11} = \frac{1}{2H} \quad, \quad b_{32} = \frac{\omega_o R_{fd}}{L_{adu}}$$

Figure (2.10) shows the block diagram representation of the machine with constant E_{fd}. In this representation, the dynamic characteristic of the system are expressed in terms of the so called K-constants.

The basis for the block diagram and the expressions for the associated constants are developed below.

$$K_1 = \frac{\Delta T_e}{\Delta \delta} \bigg|_{\Delta \psi_{fd} = const.} \quad \text{...(2.71)}$$

$$K_2 = \frac{\Delta T_e}{\Delta \psi_{fd}} \bigg|_{\Delta \delta = const.} \quad \text{..(2.72)}$$

The component of torque given by $K_1 \Delta \delta$ in phase with $\Delta \delta$ and hence represents synchronizing torque component. The component of torque resulting from variations in field flux linkage is given by $K_2 \Delta \psi_{fd}$.

The variation of $\Delta \psi_{fd}$ is determined by the field circuit dynamic equation

$$\frac{d}{dt} \Delta \psi_{fd} = a_{32} \Delta \delta + a_{33} \Delta \psi_{fd} + b_{32} \Delta E_{fd} \quad \text{..(2.73)}$$

By grouping terms involving $\Delta \psi_{fd}$ and rearranging, we get:

$$\Delta \psi_{fd} = \frac{K_3}{1 + ST_3} [\Delta E_{fd} - K_4 \Delta \delta] \quad \text{...(2.74)}$$

Where:

K_3: is an impedance factor that takes into account the loading effect of the external impedance.

K_4: the demagnetizing effect of a change in the rotor angle (effect of armature reaction).
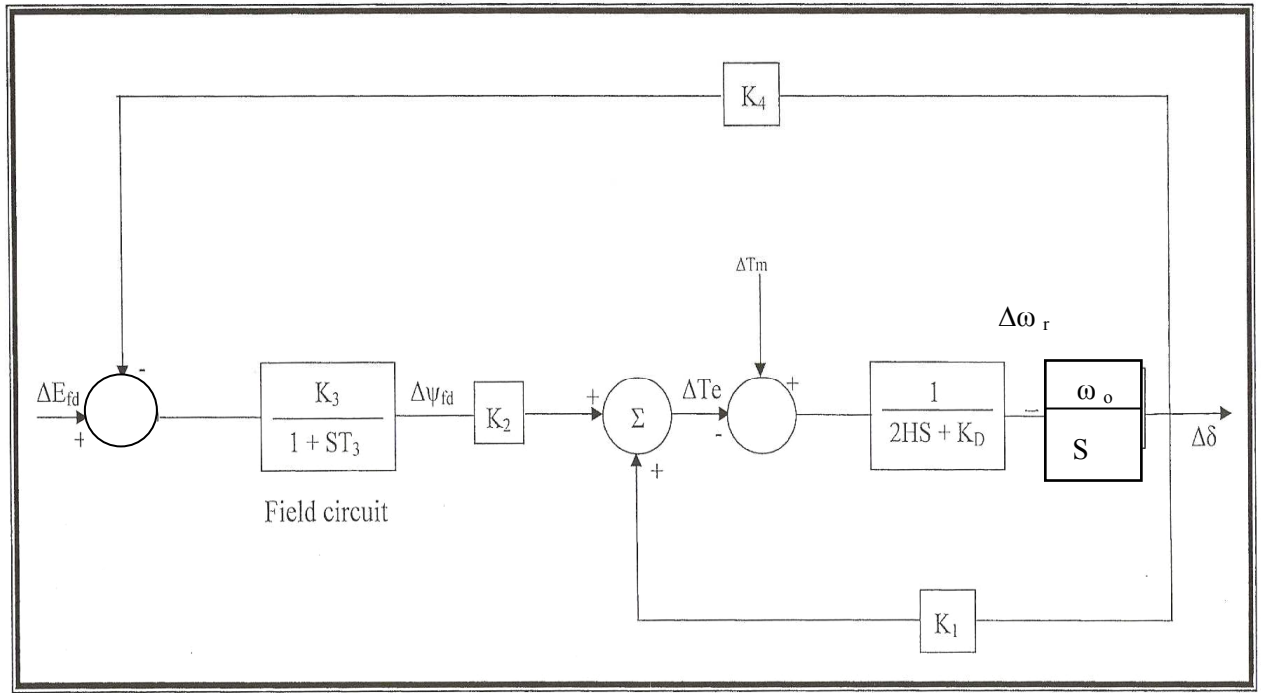
Figure (2.10) block diagram representation of the field flux with constant E_{fd}[2]

The state space model can be derived from figure (2.10), and the model can be shown in equation (2.75) below:

$$\frac{d}{dt}\begin{bmatrix} \Delta\omega_r \\ \Delta\delta \\ \Delta\psi_{fd} \end{bmatrix} = \begin{bmatrix} -\dfrac{K_D}{2H} & -\dfrac{K_1}{2H} & -\dfrac{K_2}{2H} \\ \omega_0 & 0 & 0 \\ 0 & -\dfrac{K_3 K_4}{T_3} & -\dfrac{1}{T_3} \end{bmatrix} \begin{bmatrix} \Delta\omega_r \\ \Delta\delta \\ \Delta\psi_{fd} \end{bmatrix} + \begin{bmatrix} \dfrac{1}{2H} & 0 \\ 0 & 0 \\ 0 & \dfrac{K_3}{T_3} \end{bmatrix} * \begin{bmatrix} \Delta T_m \\ \Delta E_{fd} \end{bmatrix} \quad \text{..................(2.75)}$$

And the numerical model for a SMIB with effect of field flux variation (third order model) is shown bellow:

$$\frac{d}{dt}\begin{bmatrix} \Delta\omega_r \\ \Delta\delta \\ \Delta\psi_{fd} \end{bmatrix} = \begin{bmatrix} -0.3846 & -0.1408 & -0.1681 \\ 314 & 0 & 0 \\ 0 & -0.1506 & -0.4302 \end{bmatrix} \begin{bmatrix} \Delta\omega_r \\ \Delta\delta \\ \Delta\psi_{fd} \end{bmatrix} + \begin{bmatrix} 0.1923 & 0 \\ 0 & 0 \\ 0 & 0.1174 \end{bmatrix} * \begin{bmatrix} \Delta T_m \\ \Delta E_{fd} \end{bmatrix}$$

CHAPTER THREE

SYNCHRONOUS GENERATOR MODEL INCLUDING AN EXCITER AND TURBINE - GOVERNOR

3.1 Introduction

The function of an electrical power system is to convert energy from one of the naturally available forms to the electrical form and to transport it to the points of consumption. Energy is seldom consumed in the electrical form but is rather converted to other forms such as heat, light, and mechanical energy. The advantages of the electrical form of energy is that it can be transported and controlled with relative case and with a high degree of efficiency and reliability[2].

Two principal control systems directly affect a synchronous generator: the Governor, and exciter control. This simplified view is expressed diagrammatically in Figure (3.1) which serves to orient our thinking from the problems of representation of the machine to the problems of control.
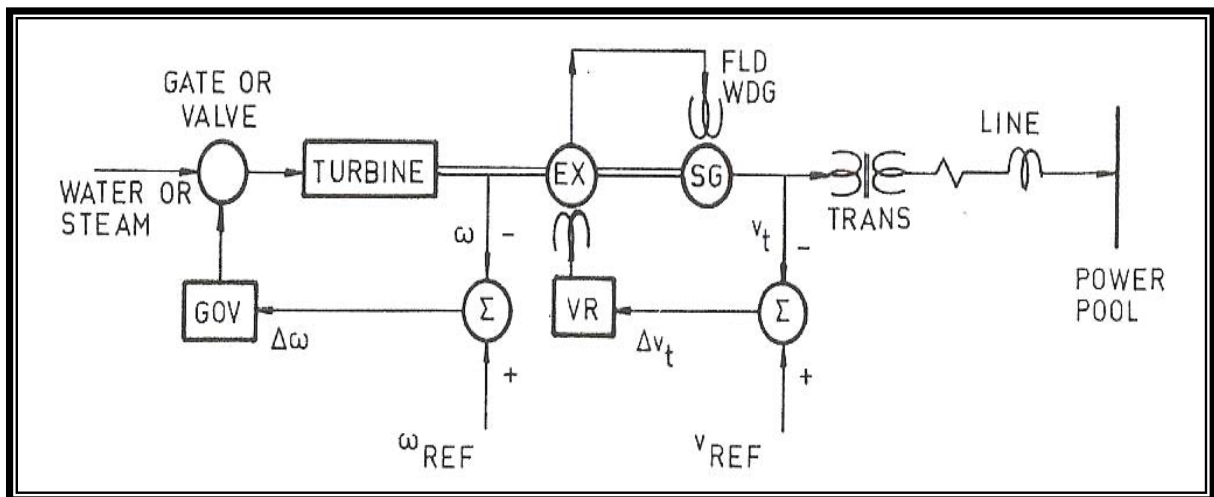
Figure (3.1): basic component of an electric power plant[18]

Referring to Figure (3.1) let us examine briefly the function of each control element. Assume that the generating unit is lossless. This is not a bad assumption when total losses of turbine and generator are compared to total output. Under this assumption all power received as steam must leave the generator terminals as electric power. Thus the unit pictured in Figure (3.1) is nothing more than an energy conversion device that changes heat energy of steam into electrical energy at the machine terminals. The amount of steam power admitted to the turbine is controlled by the governor. The excitation system controls the generated EMF of the generator and therefore controls not only the output voltage but the power factor and current magnitude as well[3].

3.2   Excitation System

The basic function of an excitation system is to provide direct current to the synchronous machine field winding. In addition, the excitation system performs control and protective functions essential to the satisfactory performance of the power system by controlling the field current. The control functions include the control of voltage and reactive power flow, and enhancement of system stability. The protective functions ensure that the capability limits of the synchronous machine, excitation system, and other equipment are not exceeded[2].

3.2.1   Types of Excitation Systems[2]

Excitation system have taken many forms and they may be classified into the following three broad categories based on the excitation power source used[23,24]:-

1. D. C excitation system.

2. A. C excitation system.

3. Static excitation system.

3.2.1.1   Ac Excitation System

These excitation systems used an A. C alternator and either stationary or rotating rectifiers to produce the D. C field requirements. Loading effects on such exciters are significant, and the use of generator field current as an input to the models allows these effects to be represented accurately[24]. For AC excitation systems the exciter consists of a smaller synchronous machine that feeds the exciter winding through a rectifier. The output voltage of the exciter is in this case influenced by the loading. To represent these effects, the exciter current is used as an input signal in the model. In figure (3.2), an example of a model of AC exciter system is shown (IEEE type AC1). The structure of the model is basically the same as for dc excitation system. Some functions have been added. The rectifier of the exciter prevents (for most exciters) the exciter current from being negative. The feedback with the constant K_D represents the reduction of the flux caused by rising field current if. That constant depends on the synchronous and transient reactance's of the exciter. The voltage drop inside the rectifier is described by the constant Kc, and its characteristic is described by F_{EX}, which is a function of the load current. AC and DC excitation systems are sometimes called rotating exciter, since they contain rotating machine. That distinguishing them from static excitation system[25].
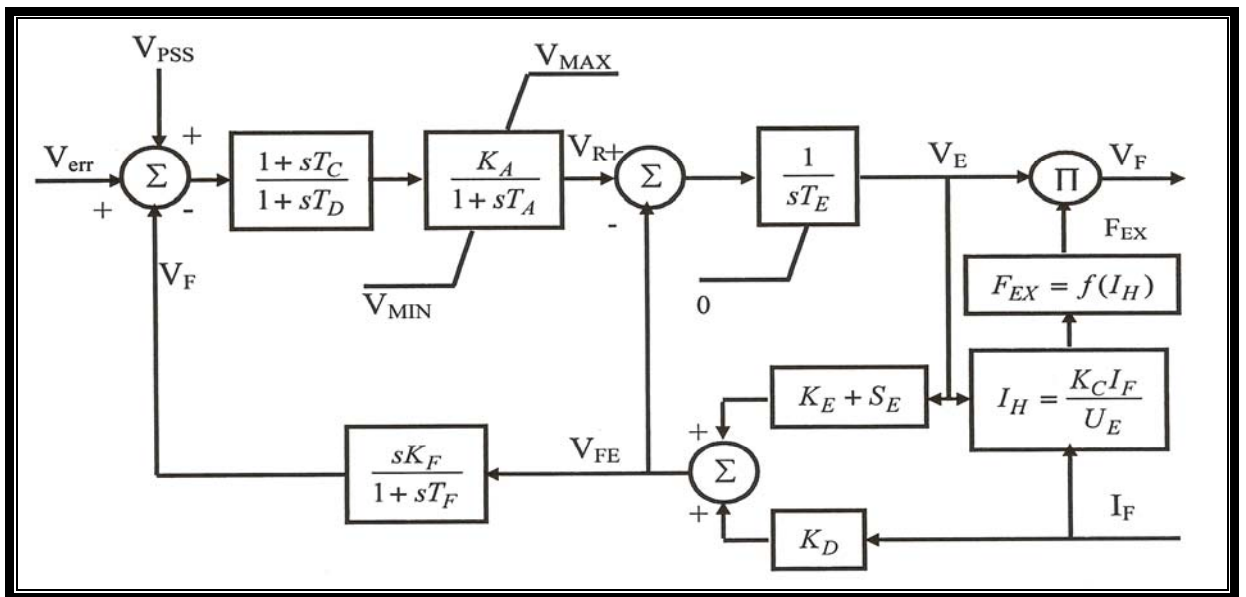
Figure (3.2) Model of an AC exciter system (IEEE Type AC1)[25]

## 3.2.2 Modeling of Excitation System in Power System

The most important component other than the synchronous machine in the power system is the excitation system. The most basic form of expressing the exciter model is in figure (3.3) which can be represented by a gain K_E and a single time constant T_E as shown in equation below:-

$$\frac{E_{fd}}{V_R} = \frac{1}{K_E + ST_E} \quad \dots\dots\dots\dots\dots\dots\dots\dots\dots\dots\dots\dots\dots\dots\dots\dots\dots\dots\dots\dots\dots\dots\dots\dots\dots\dots\dots(3.1)$$

Where:

V_R = the o/p voltage of the regulator

E_{fd} = field voltage
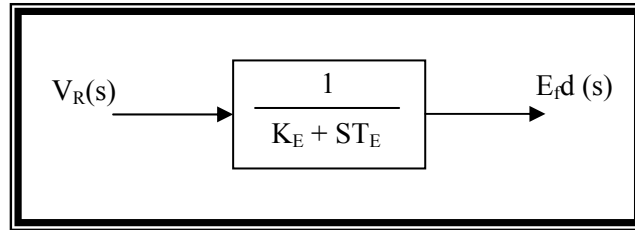
Figure (3.3): Block Diagram of an Exciter Model[2]

There are many different type of excitation system available. Some of which uses a. c power source through solid state rectifiers such as SCR[26]. As result, the output voltage of the exciter becomes a nonlinear function of the field voltage due to the saturation effects which occur in the magnetic circuit. Consequently, there is no straight forward relationship between the field voltage and the terminal voltage of the exciter. However, the modern exciter can be estimated as a linearized model, taking into account major time constant and ignoring the saturation and other non linearities. The excitation system amplifier may be a rotating amplifier, a magnetic amplifier or modern electronic amplifier. In any case, a linearized characteristic of the amplifier is assumed. The amplifier is represented similarly by a gain K_A and a time constant T_A. The transfer function of the amplifier is:-

$$\frac{V_R(s)}{V_{err}(s)} = \frac{K_A}{1+ST_A} \quad \dots\dots\dots\dots\dots\dots\dots\dots\dots\dots\dots\dots\dots\dots\dots\dots\dots\dots\dots\dots\dots\dots\dots\dots\dots\dots(3.2)$$

Where:

V_{err} (s) = (reference voltage V_{ref}) - (output voltage of the sensor V_S). Typically, the time constant of the amplifier is very small and is often neglected.

Figure (3.4): show the block diagram of an amplifier model.

$$V_{err}(s) \quad \boxed{\dfrac{KA}{1 + sT_A}} \quad V_R(s)$$
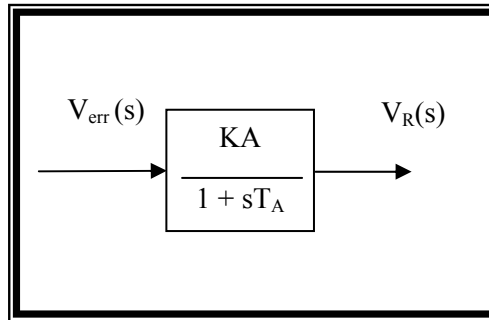
Figure (3.4): Block Diagram of an Amplifier Model[2]

3.2.3 Effect of Excitation System[2]

The state-space model and the block diagram developed in the previous chapter can be extended to include the excitation system. The i/p control signal to the excitation system is normally the generator terminal voltage E_t. In the generator model derived in the previous chapter, E_t is not a state variable. Therefore, E_t has to be expressed in terms of the state variables $\Delta\omega r$, $\Delta\delta$ and $\Delta\psi_{fd}$.

$\widetilde{E}_t$ may be expressed in complex form.

$$\widetilde{E}_t = e_d + je_q \quad\text{...(3.3)}$$

Hence:

$$E_t{}^2 = e_d{}^2 + e_q{}^2 \quad\text{...(3.4)}$$

Applying a small perturbation, then

$$\left(E_{t0} + \Delta E_t\right)^2 = \left(e_{d0} + \Delta e_d\right)^2 + \left(e_{q0} + \Delta e_q\right)^2 \quad\text{...(3.5)}$$

By neglecting second order terms involving perturbed values, the above equation reduces to:

$$E_{t0}\,\Delta E_t = e_{d0}\,\Delta e_d + e_{q0}\,\Delta e_q \dots\dots\dots\dots\dots\dots\dots\dots\dots\dots\dots\dots\dots\dots(3.6)$$

Therefore:

$$\Delta E_t = \frac{e_{d0}}{E_{t0}}\Delta e_d + \frac{e_{q0}}{E_{t0}}\Delta e_q \dots\dots\dots\dots\dots\dots\dots\dots\dots\dots\dots\dots\dots(3.7)$$

In terms of the perturbed values, equations (2.53) and (2.54) obtained in chapter two may be written as

$$\Delta e_d = -R_a\Delta i_d + L_l\Delta i_q - \Delta\psi_{aq} \dots\dots\dots\dots\dots\dots\dots\dots\dots\dots\dots\dots\dots(3.8)$$

$$\Delta e_q = -R_a\Delta i_q + L_l\Delta i_d - \Delta\psi_{ad} \dots\dots\dots\dots\dots\dots\dots\dots\dots\dots\dots\dots\dots(3.9)$$

Then:

$$\Delta E_t = K_5\,\Delta\delta + K_6\,\Delta\Psi_{fd} \dots\dots\dots\dots\dots\dots\dots\dots\dots\dots\dots\dots\dots(3.10)$$

$$K_5 = \frac{e_{do}}{E_{to}}\left[-R_a m_1 + L_l n_1 + L_{aqs}n_1\right] + \frac{e_{qo}}{E_{to}}\left[-R_a n_1 - L_l m_1 - L'_{ads}m_1\right]\dots\dots\dots(3.11)$$

$$K_6 = \frac{e_{do}}{E_{to}}\left[-R_a m_2 + L_l n_2 + L_{aqs}n_2\right] + \frac{e_{qo}}{E_{to}}\left[-R_a n_2 - L_l m_2 + L'_{ads}\left(\frac{1}{L_{fd}} - m_2\right)\right]\dots\dots(3.12)$$

Where:

K_5: is the change in terminal voltage E_t for a small change in rotor angle at constant d-axis fiux linkage.

K_6: is the change in the terminal voltage E_t for a small change in the d-axis flux linkage at constant rotor angle.

As noted before, the constants K_2, K_3, K_4, K_6 are usually positive; however, K_5 may take either positive or negative values. The effect of AVR on damping and synchronizing torque components is therefore primarily influenced by K_5 and K_A[2]. The complete model for the exciter-generator can be given in figure (3.5a) where Gex is the exciter and regulator for AC exciter transfer function.

Figure (3.5a): Block Diagram Representation With Exciter and AVR[2]

$\Delta\omega_r$
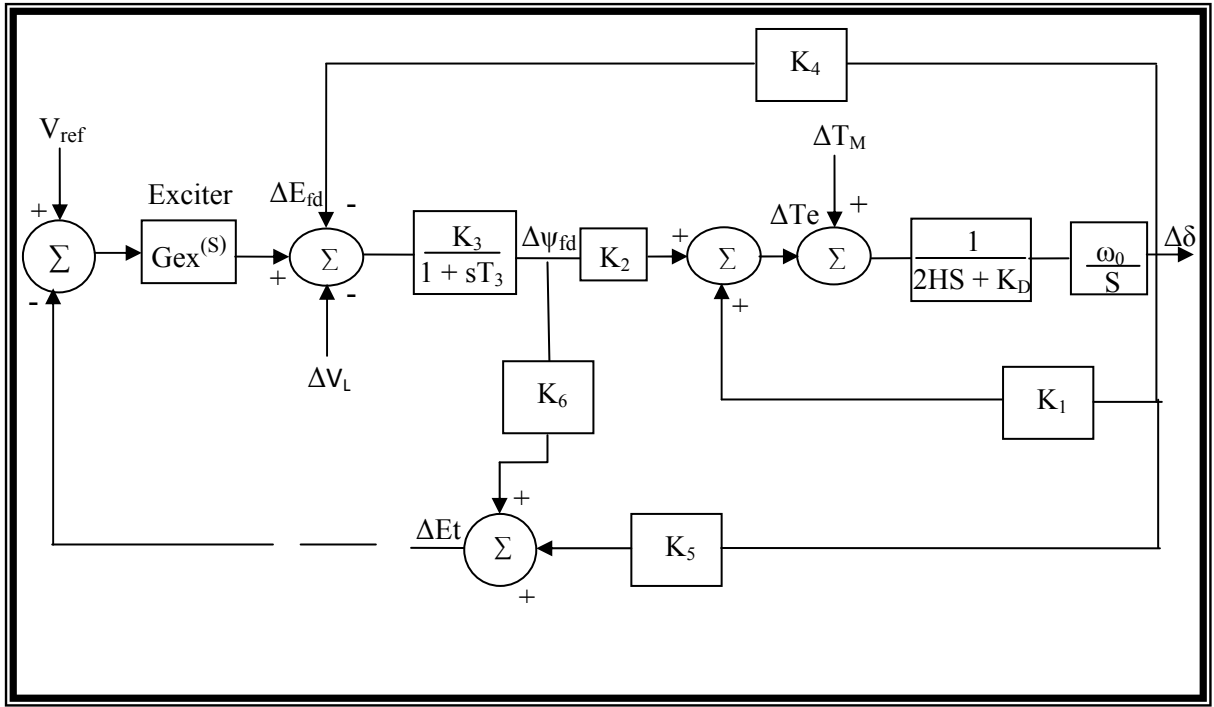
And the state space model equations for this system can be derived from the block diagram shown in Figure (3.5a) as:

$$\frac{d}{dt}\Delta\omega_r = -\frac{KD}{2H}\Delta\omega_r - \frac{K_1}{2H}\Delta\delta - \frac{K_2}{2H}\Delta\Psi_{fd} + \frac{1}{2H}\Delta T_m \quad\text{...(3.13)}$$

$$\frac{d}{dt}\Delta\delta = \omega_0\,\Delta\omega_r \quad\text{...(3.14)}$$

The field flux variation $\Delta\psi_{fd}$ can be calculated:

$$\Delta\Psi_{fd} = \left(\Delta E_{fd} - K_4\,\Delta\delta - \Delta V_l\right)\times\frac{K_3}{1+ST_3} \quad\text{...(3.15)}$$

$$\frac{d}{dt}\Delta\Psi_{fd} = -\frac{K_3 K_4}{T_3}\Delta\delta - \frac{1}{T_3}\Delta\Psi_{fd} + \frac{K_3}{T3}\Delta E_{fd} - \frac{K_3}{T_3}\Delta V_l \quad\text{.............................(3.16)}$$

The field voltage deviation ΔE_{fd} can be calculated:

$$\Delta E_{fd} = \left(V_{ref} - \Delta E_t\right)\frac{K_A}{K_E + ST_E} \quad\text{..(3.17)}$$

Therefore:

$$\frac{d}{dt}\Delta E_{fd} = -\frac{K_A K_5}{T_E}\Delta\delta - \frac{K_6 K_A}{T_E}\Delta\Psi_{fd} - \frac{K_E}{T_E}\Delta E_{fd} + \frac{K_A}{T_E}V_{ref} \quad\text{.....................(3.18)}$$

Then the complete state space equation in matrix form is:

$$\frac{d}{dt}\begin{bmatrix} \Delta\omega_r \\ \Delta\delta \\ \Delta\Psi_{fd} \\ \Delta E_{fd} \end{bmatrix} = \begin{bmatrix} -\dfrac{KD}{2H} & -\dfrac{K_1}{2H} & -\dfrac{K_2}{2H} & 0 \\ W_0 & 0 & 0 & 0 \\ 0 & -\dfrac{K_3 K_5}{T_3} & -\dfrac{1}{T_3} & \dfrac{K_3}{T_3} \\ 0 & -\dfrac{K_A K_5}{T_E} & -\dfrac{K_6 K_A}{T_E} & -\dfrac{K_E}{T_E} \end{bmatrix}\begin{bmatrix} \Delta\omega_r \\ \Delta\delta \\ \Delta\Psi_{fd} \\ \Delta E_{fd} \end{bmatrix} + \begin{bmatrix} \dfrac{1}{2H} & 0 & 0 \\ 0 & 0 & 0 \\ 0 & -\dfrac{K_3}{T_3} & 0 \\ 0 & 0 & \dfrac{K_A}{T_E} \end{bmatrix}\begin{bmatrix} \Delta T_m \\ \Delta V_l \\ V_{ref} \end{bmatrix} \quad (3.19)$$

The numerical model for Westinghouse brushless A.C exciter (BRLS[IEEE,1966[3]]) that are used in this work.

$$\frac{d}{dt}\begin{bmatrix} \Delta\omega_r \\ \Delta\delta \\ \Delta\Psi_{fd} \\ \Delta E_{fd} \end{bmatrix} = \begin{bmatrix} -0.3846 & -0.1408 & -0.1681 & 0 \\ 314 & 0 & 0 & 0 \\ 0 & -0.1506 & -0.4302 & 0.1174 \\ 0 & -68.3006 & -175.6027 & -1.2315 \end{bmatrix}\begin{bmatrix} \Delta\omega_r \\ \Delta\delta \\ \Delta\Psi_{fd} \\ \Delta E_{fd} \end{bmatrix} + \begin{bmatrix} 0 & 0 & 0 \\ 0 & 0 & 0 \\ 0 & -0.117 & 0 \\ 0 & 0 & 492.618 \end{bmatrix}\begin{bmatrix} \Delta T_m \\ \Delta V_L \\ V_{ref} \end{bmatrix}$$

Figure (3.5a) also can be shown in practical power system control the rotating exciter and voltage regulator system as shown below in figure (3.5b).
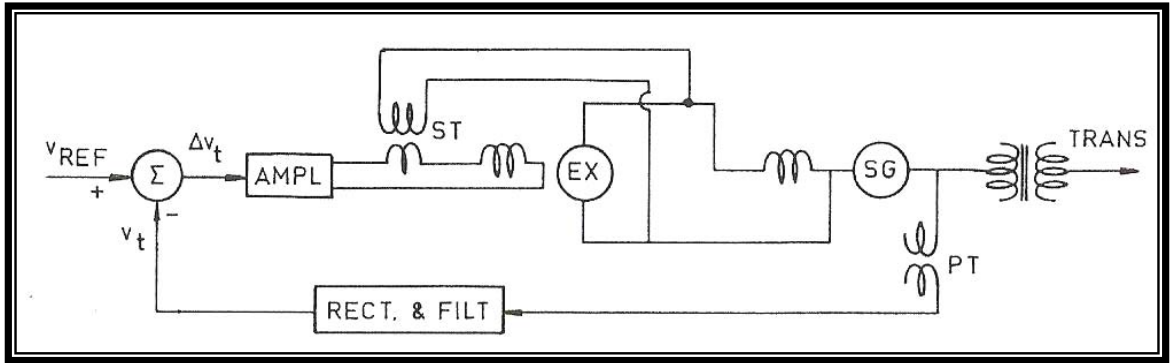

Figure (3.5b): a rotating exciter and voltage regulator system[18]

3.3 Turbine Control

The prime sources of electrical energy supplied by utilities are the kinetic energy of water and the thermal energy derived from fossil fuels and nuclear fission. The turbines convert these sources of energy into mechanical energy that is, in turn converted to electrical energy by the synchronous generators. The turbine governing systems provides a means of controlling power and frequency,

a function commonly referred to as load-frequency control or automatic generation control (AGC). Figure (3.6) portrays the functional relationship between the basic elements associated with power generation and control[2, 27].
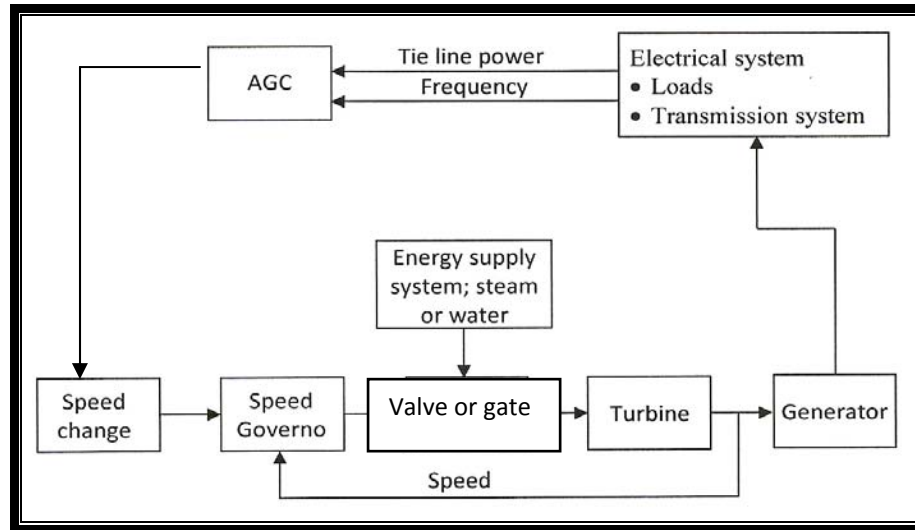
Figure (3.6): Functional Block Diagram of Power Generation and Control System[2]

A steam turbine converts stored energy of high pressure and high temperature steam into rotating energy, which is in turn converted into electrical energy by the generator, the heat source of the boiler supplying the steam may be a nuclear reactor or a furnace fired by fossil fuel (coal, oil ,or gas).

Steam turbines with a variety of configurations have been built depending on unit size and steam conditions. They normally consist of two or more turbine sections or cylinders coupled in series. Each turbine section consists of a set of moving blades attached to rotor and a set of stationary vans. The moving blades are called buckets. The stationary vanes referred to nozzle sections, form nozzles or passages in which steam is accelerated to high velocity. The kinetic energy of this high velocity steam is converted into shaft torque by the buckets.

A turbine with multiple sections maybe either tandem-compound or cross-compound. In a tandem-compound turbine, the sections are all on one shaft, with a single generator. In contrast, a cross-compound turbine consists of two shafts, each connected to a generator and driven by one or more turbine sections;

however, its designed and operated as a single unit with one set of controls. The cross-compounding results in grater capacity and improved efficiency but is more expensive. It is seldom used now; most new units placed in service in recent years have been of the tandem-compound design[2].

Fossil-fuelled units can be of tandem-compound or cross compound design. Typical configurations of a single reheat tandem-compound turbines for fossil-fuelled units are shown in figure (3.7). Tandem-compound units run at 3000 r/ min, cross compound units may have both shafts rated at 3000 r/ min or more commonly, one shaft at 3000 r/ min and the other 1500 r/ min.

Depending on the turbine configuration fossil-fuelled units consist of high pressure (HP), intermediate pressure (IP), and low pressure (LP) turbine sections. They may be of either reheat type or non-reheat type. In a reheat type turbine, the steam upon leaving the HP section returned to the boiler, where its passed through a reheater (RH) before returning to the IP section. Reheating improves efficiency.
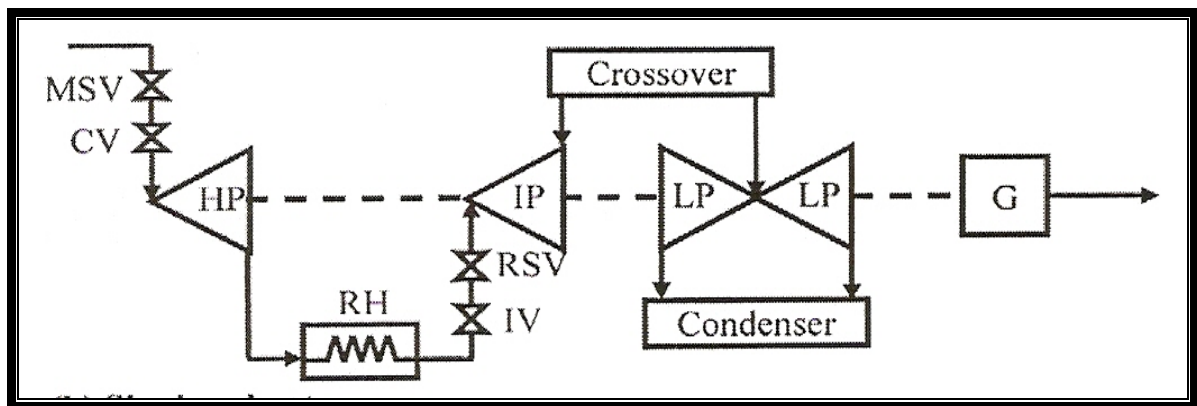
Figure (3.7): Common Configuration of a single reheat Tandem-Compound Steam Turbine of Fossil-Fuelled Units[2]

A general model turbine system can be used to represent various type of turbines: non reheat, tandem-compound (single and double reheat) and cross-compound (single and double reheat) by giving suitable time constants figure (3.8) represents the universal model[28].
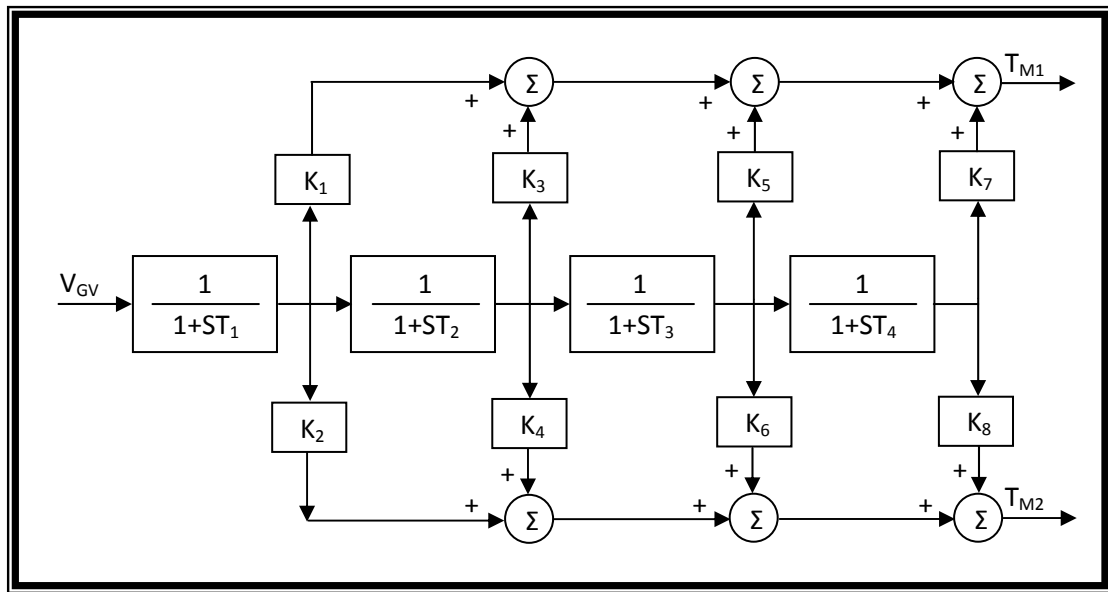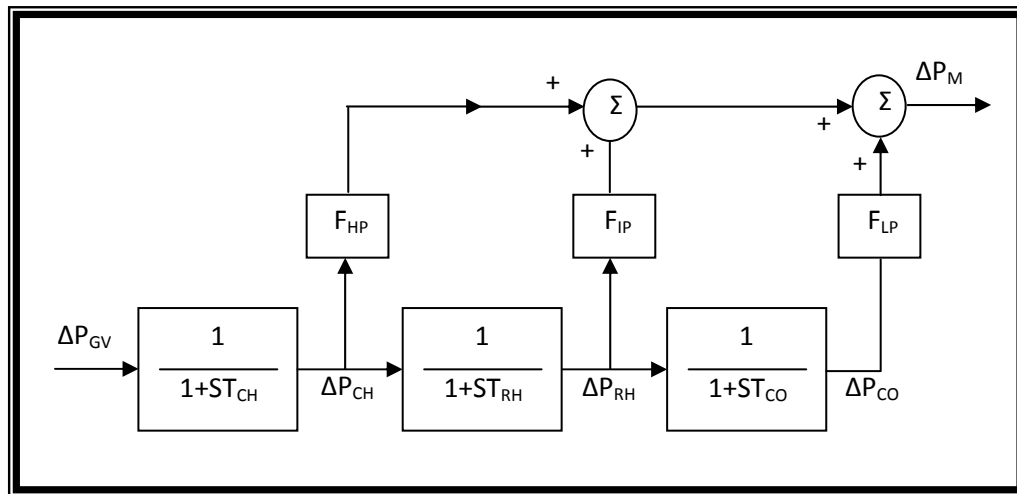
Figure (3.8): General Model for Turbine System[28]

Table (3.1): Parameters Used in General Model for Turbines[28]

System Description	T_1	T_2	T_3	T_4	K_1	K_2	K_3	K_4	K_5	K_6	K_7	K_8
Non-reheat	T_{CH}	0	0	0	1	0	0	0	0	0	0	0
Tandem-compound single-reheat	T_{CH}	T_{RH}	T_{CO}	0	F_{HP}	0	F_{IP}	0	F_{LP}	0	0	0
Tandem-compound double-reheat	T_{CH}	T_{RH1}	T_{RH2}	T_{CO}	F_{VHP}	0	F_{HP}	0	F_{IP}	0	F_{LP}	0
Cross-compound single- reheat	T_{CH}	T_{RH}	T_{CO}	0	F_{HP}	0	0	F_{IP}	$F_{LP/2}$	$F_{LP/2}$	0	0
Cross-compound double- reheat	T_{CH}	T_{RH1}	T_{RH2}	T_{CO}	F_{VHP}	0	0	F_{HP}	$F_{LP/2}$	$F_{LP/2}$	$F_{LP/2}$	$F_{LP/2}$

Where the time constants T_{CH}, T_{RH} and T_{CO} represents delays due to the steam chest and inlet piping, reheaters, and crossover piping respectively. The fractions F_{VHP}, F_{HP}, F_{IP} and F_{LP} represents portions of the total turbine power development in the various cylinders.

43

## 3.3.1 Modeling of a Turbine in Power System

As mentioned earlier different types of turbines have different characteristics. This source of mechanical power can be hydraulic turbine, steam turbine and others. The above types of steam turbine models are discussed in an IEEE transaction report[28].

The model for a single reheat tandem-compound steam turbine is shown in figure (3.9).

Figure (3.9): Single Reheat Tandem-Compound Steam Turbine Model[26]

Where:

ΔP_m: change in mechanical power.

ΔP_{GV}: change in steam valve position.

And the state space representation in the matrix form can derived from the block diagram (3.9) are:

$$\frac{d}{dt}\begin{bmatrix} \Delta P_{CH} \\ \Delta P_{RH} \\ \Delta P_{CO} \end{bmatrix} = \begin{bmatrix} -\dfrac{1}{T_{CH}} & 0 & 0 \\ \dfrac{1}{T_{RH}} & -\dfrac{1}{T_{RH}} & 0 \\ 0 & \dfrac{1}{T_{CO}} & -\dfrac{1}{T_{CO}} \end{bmatrix}\begin{bmatrix} \Delta P_{CH} \\ \Delta P_{RH} \\ \Delta P_{CO} \end{bmatrix} + \begin{bmatrix} \dfrac{1}{T_{CH}} \\ 0 \\ 0 \end{bmatrix}\Delta P_{GV} \quad ....(3.20)$$

3.4 Speed Governing System for Steam Turbine

The prime mover governing system provides a means of controlling real power and frequency. A basic characteristic of a governor is shown in figure (3.10).
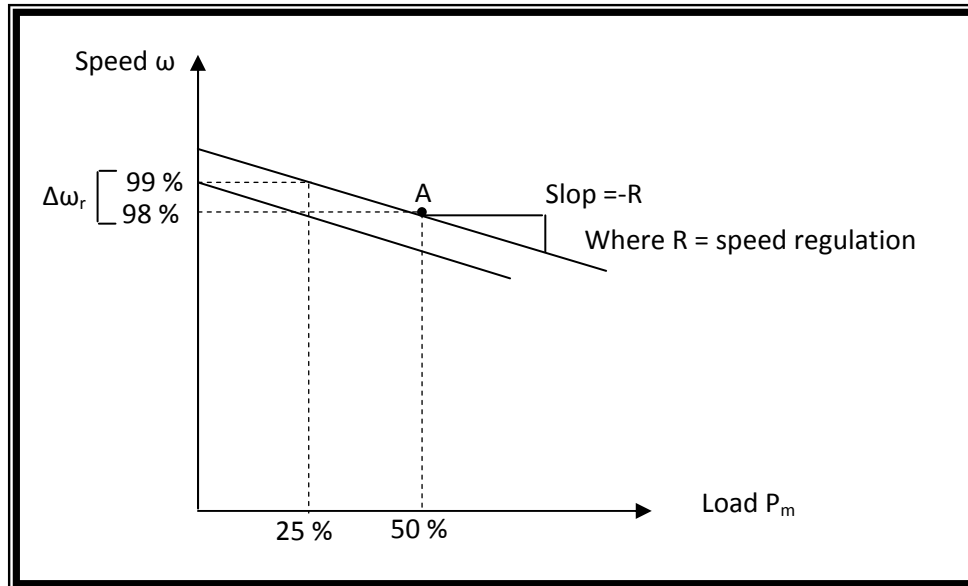
Figure (3.10): Governor Characteristic[2]

From figure (3.10), there is a definite relationship between the turbine speed and the load being carried by the turbine for a given setting. The increase in load will lead to decrease in speed. The example given in figure (3.10) shows that if the initial operating point is at (A) and the load is dropped to 25%, the speed will increase. In order to maintain the speed at A, the governor setting by changing the spring tension in the fly-ball type of governor will be resorted to and the characteristic of the governor will be indicated by the dotted line as shown in figure (3.10)[2].

Figure (3.10) illustrates the ideal characteristic of the governor whereas the actual characteristic departs from the ideal one due to valve openings at different loadings.

Turbine power is in excess of the load power. The speed will ultimately return to its reference value and the steady state turbine power increases by an amount equal to the additional load.

In contrast to the excitation system, the governing system is a relatively slow response system because of the slow reaction of mechanic operation of turbine machine[2].

3.4.1   Mechanical Hydraulic Control

A typical mechanical-hydraulic speed governing system consists of a speed governor, a speed relay, a hydraulic servomotor, and governor-controlled valves which are functionally related as shown in figure (3.11).
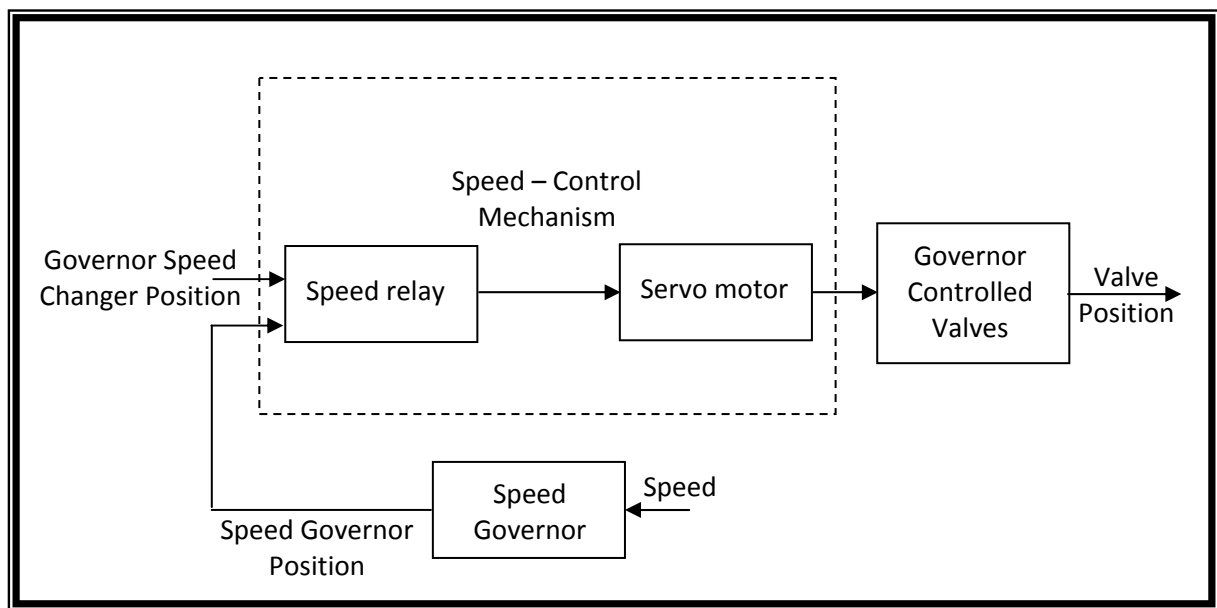
Figure (3.11): block diagram of a Hydraulic Speed-Governing System for Steam Turbines

The block diagram of figure (3.11) shows an approximate mathematical model. The speed governor produces a position which is assumed to be a linear, instantaneous indication of speed and is represented by again K_G which is reciprocal of regulation or droop. The signal P_{ref}, is obtained from the governor speed changer of figure (3.12), and is determined by the automatic generation control system. It represents a composite load and speed reference and is assumed constant over the interval of a stability study[28].

46

The speed relay is represented as an integrator with time constant T_{SR} and direct feedback.
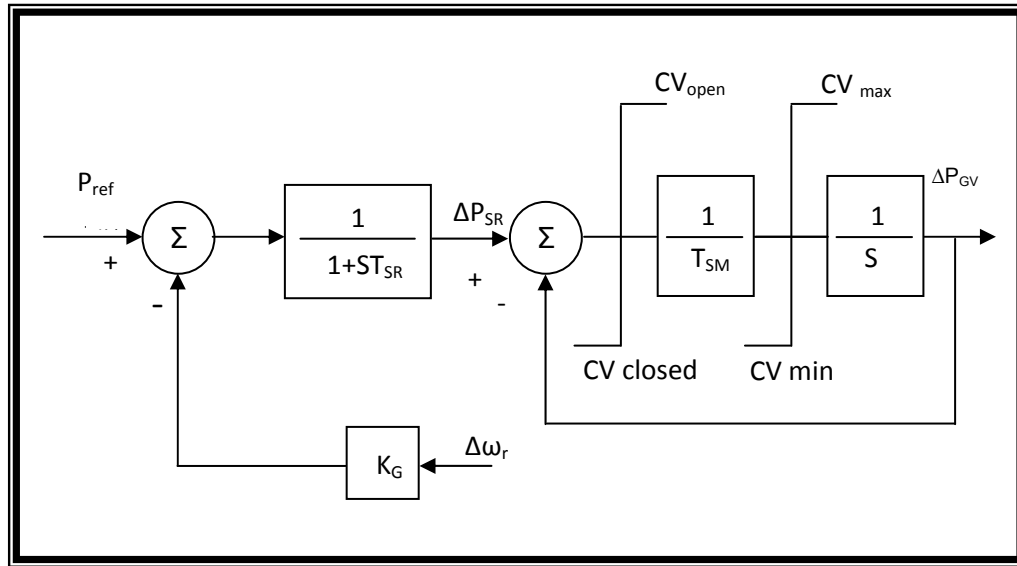
Figure (3.12): block diagram Representation of The Speed-Governing System[28]

The servomotor is represented by an integrator with time constant T_{SM} and direct feedback.

The servomotor moves the valves and is physically large, particularly in large units. Rate limiting of the servomotor may occur for large, rapid speed deviation, and rate limits are shown at the input to the integrator representing the servomotor. Position limits are also indicated and may correspond to wide-open valves or the setting of a load limiter[28].

The state space representation in the matrix form is shown as follows:

$$\frac{d}{dt}\begin{bmatrix} \Delta P_{GV} \\ \Delta P_{SR} \end{bmatrix} = \begin{bmatrix} -\dfrac{1}{T_{SM}} & \dfrac{1}{T_{SM}} \\ 0 & -\dfrac{1}{T_{SR}} \end{bmatrix}\begin{bmatrix} \Delta P_{GV} \\ \Delta P_{SR} \end{bmatrix} + \begin{bmatrix} 0 & 0 \\ \dfrac{1}{T_{SR}} & -\dfrac{K_G}{T_{SR}} \end{bmatrix}\begin{bmatrix} P_{ref} \\ \Delta \omega_r \end{bmatrix} \ \dots\dots\dots\dots\dots\dots\dots(3.21)$$

As in previous the complete turbine governing system model are shown in figure (3.13) below and the state space representation in the matrix form for complete models as follows:

$$\frac{d}{dt}\begin{bmatrix} \Delta\omega_r \\ \Delta P_{SR} \\ \Delta P_{GV} \\ \Delta P_{CH} \\ \Delta P_{RH} \\ \Delta P_{CO} \end{bmatrix} = \begin{bmatrix} -\dfrac{K_D}{2H} & 0 & 0 & \dfrac{F_{HP}}{2H} & \dfrac{F_{IP}}{2H} & \dfrac{F_{LP}}{2H} \\ -\dfrac{K_G}{T_{SR}} & -\dfrac{1}{T_{SR}} & 0 & 0 & 0 & 0 \\ 0 & \dfrac{1}{T_{SM}} & -\dfrac{1}{T_{SM}} & 0 & 0 & 0 \\ 0 & 0 & \dfrac{1}{T_{CH}} & -\dfrac{1}{T_{CH}} & 0 & 0 \\ 0 & 0 & 0 & \dfrac{1}{T_{RH}} & -\dfrac{1}{T_{RH}} & 0 \\ 0 & 0 & 0 & 0 & \dfrac{1}{T_{CO}} & -\dfrac{1}{T_{CO}} \end{bmatrix}\begin{bmatrix} \Delta\omega_r \\ \Delta P_{SR} \\ \Delta P_{GV} \\ \Delta P_{CH} \\ \Delta P_{RH} \\ \Delta P_{CO} \end{bmatrix} + \begin{bmatrix} -\dfrac{1}{2H} & 0 \\ 0 & \dfrac{1}{T_{SR}} \\ 0 & 0 \\ 0 & 0 \\ 0 & 0 \\ 0 & 0 \end{bmatrix}*\begin{bmatrix} \Delta P_L \\ P_{ref} \end{bmatrix}..(3.22)$$

The numerical mathematical model for a single reheat tandem combined governor turbine model that are used in this work are shown below:

$$\frac{d}{dt}\begin{bmatrix} \Delta\omega_r \\ \Delta P_{SR} \\ \Delta P_{GV} \\ \Delta P_{CH} \\ \Delta P_{RH} \\ \Delta P_{CO} \end{bmatrix} = \begin{bmatrix} -0.3846 & 0 & 0 & 0.0577 & 0.0769 & 0.0769 \\ -200 & -10 & 0 & 0 & 0 & 0 \\ 0 & 4.5455 & -4.5455 & 0 & 0 & 0 \\ 0 & 0 & 5 & -5 & 0 & 0 \\ 0 & 0 & 0 & 0.125 & -0.125 & 0 \\ 0 & 0 & 0 & 0 & 4 & -4 \end{bmatrix}\begin{bmatrix} \Delta\omega_r \\ \Delta P_{SR} \\ \Delta P_{GV} \\ \Delta P_{CH} \\ \Delta P_{RH} \\ \Delta P_{CO} \end{bmatrix} + \begin{bmatrix} -0.1932 & 0 \\ 0 & 10 \\ 0 & 0 \\ 0 & 0 \\ 0 & 0 \\ 0 & 0 \end{bmatrix}*\begin{bmatrix} \Delta P_L \\ P_{ref} \end{bmatrix}$$
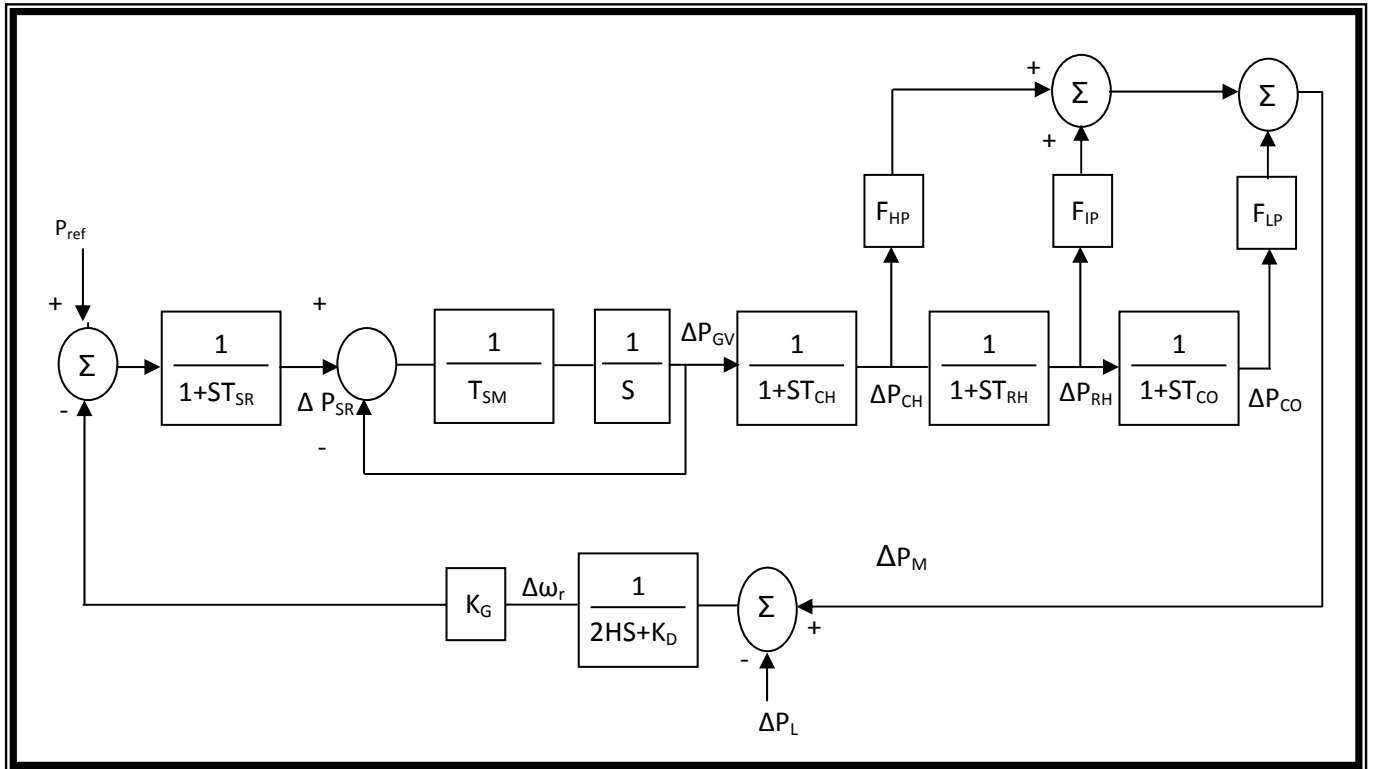

Figure (3.13): block diagram of the Governor Turbine model[28]

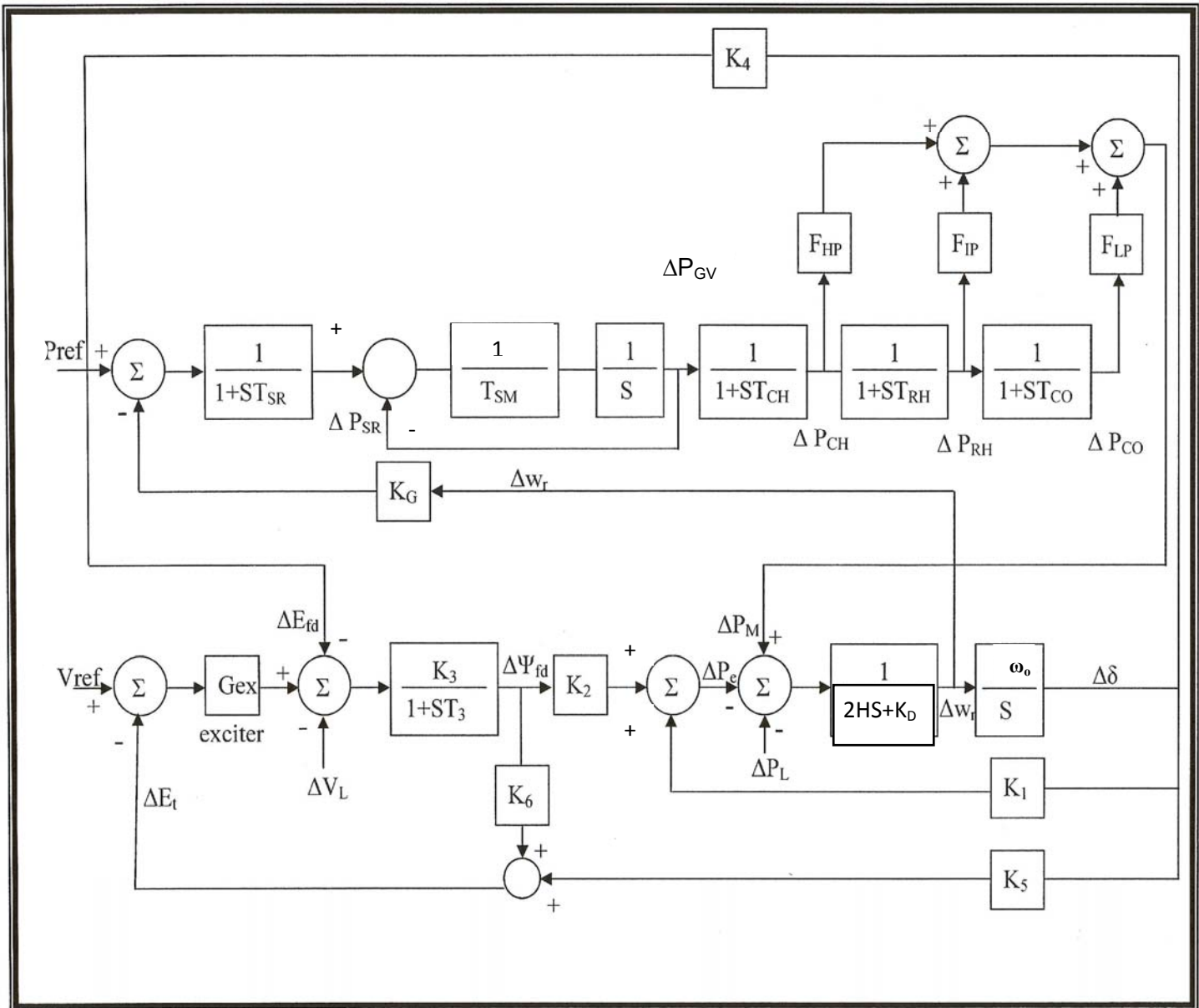# 3.5 Combined Turbine-Generator Modeling[14,16]

The two models which represents the governor-turbine model given in figure (3.13) and the exciter-generator model given in figure (3.5) can be combined to form the turbine-generator model, which can be given in figure (3.14) below[14,16].

Note that ΔV_L and ΔP_L are included to simulate the load change in voltage and power respectively, which effectively represent the change in reactive and real power[16].

And the mathematical model for a (384 MVA 24 KV Turbo. Generator) in a matrix form can be given in equation (3.23) as follows:

$$\frac{d}{dt}\begin{bmatrix}\Delta\omega_r\\\Delta\delta\\\Delta\psi_{fd}\\\Delta E_{fd}\\\Delta P_{SR}\\\Delta P_{GV}\\\Delta P_{CH}\\\Delta P_{RH}\\\Delta P_{CO}\end{bmatrix}=\begin{bmatrix}-\frac{K_D}{2H} & -\frac{K_1}{2H} & -\frac{K_2}{2H} & 0 & 0 & 0 & \frac{F_{HP}}{2H} & \frac{F_{IP}}{2H} & \frac{F_{LP}}{2H}\\ \omega_O & 0 & 0 & 0 & 0 & 0 & 0 & 0 & 0\\ 0 & -\frac{K3K5}{T3} & -\frac{1}{T3} & 0 & 0 & 0 & 0 & 0 & 0\\ 0 & -\frac{KAK5}{TE} & -\frac{KAK6}{TE} & -\frac{KE}{TE} & 0 & 0 & 0 & 0 & 0\\ -\frac{KG}{T_{SR}} & 0 & 0 & 0 & -\frac{1}{T_{SR}} & 0 & 0 & 0 & 0\\ 0 & 0 & 0 & 0 & \frac{1}{T_{SM}} & -\frac{1}{T_{CH}} & 0 & 0 & 0\\ 0 & 0 & 0 & 0 & 0 & \frac{1}{T_{CH}} & -\frac{1}{T_{CH}} & 0 & 0\\ 0 & 0 & 0 & 0 & 0 & 0 & \frac{1}{T_{RH}} & -\frac{1}{T_{RH}} & 0\\ 0 & 0 & 0 & 0 & 0 & 0 & 0 & \frac{1}{T_{CO}} & -\frac{1}{T_{CO}}\end{bmatrix}\begin{bmatrix}\Delta\omega_r\\\Delta\delta\\\Delta\psi_{fd}\\\Delta E_{fd}\\\Delta P_{SR}\\\Delta P_{GV}\\\Delta P_{CH}\\\Delta P_{RH}\\\Delta P_{CO}\end{bmatrix}+\begin{bmatrix}-\frac{1}{2H} & 0 & 0 & 0\\ 0 & 0 & 0 & 0\\ 0 & -\frac{K_3}{T_3} & 0 & 0\\ 0 & 0 & 0 & \frac{K_A}{T_E}\\ 0 & 0 & \frac{1}{T_{SR}} & 0\\ 0 & 0 & 0 & 0\\ 0 & 0 & 0 & 0\\ 0 & 0 & 0 & 0\\ 0 & 0 & 0 & 0\end{bmatrix}\begin{bmatrix}\Delta P_L\\\Delta V_L\\P_{ref}\\V_{ref}\end{bmatrix}\quad...(3.23)$$

$$\frac{d}{dt}\begin{bmatrix}\Delta\omega_r\\\Delta\delta\\\Delta\psi_{fd}\\\Delta E_{fd}\\\Delta P_{SR}\\\Delta P_{GV}\\\Delta P_{CH}\\\Delta P_{RH}\\\Delta P_{CO}\end{bmatrix}=\begin{bmatrix}-0.3846 & -0.1408 & -0.1681 & 0 & 0 & 0 & 0.0577 & 0.0769 & 0.0769\\ 314 & 0 & 0 & 0 & 0 & 0 & 0 & 0 & 0\\ 0 & -0.1506 & -0.4302 & 0.1174 & 0 & 0 & 0 & 0 & 0\\ 0 & 68.3006 & -175.6027 & -1.2315 & 0 & 0 & 0 & 0 & 0\\ -200 & 0 & 0 & 0 & -10 & 0 & 0 & 0 & 0\\ 0 & 0 & 0 & 0 & 4.5455 & -4.5455 & 0 & 0 & 0\\ 0 & 0 & 0 & 0 & 0 & 5 & -5 & 0 & 0\\ 0 & 0 & 0 & 0 & 0 & 0 & 0.125 & -0.125 & 0\\ 0 & 0 & 0 & 0 & 0 & 0 & 0 & 4 & -4\end{bmatrix}\begin{bmatrix}\Delta\omega_r\\\Delta\delta\\\Delta\psi_{fd}\\\Delta E_{fd}\\\Delta P_{SR}\\\Delta P_{GV}\\\Delta P_{CH}\\\Delta P_{RH}\\\Delta P_{CO}\end{bmatrix}+\begin{bmatrix}-0.1923 & 0 & 0 & 0\\ 0 & 0 & 0 & 0\\ 0 & -0.1174 & 0 & 0\\ 0 & 0 & 0 & 492.611\\ 0 & 0 & 10 & 0\\ 0 & 0 & 0 & 0\\ 0 & 0 & 0 & 0\\ 0 & 0 & 0 & 0\\ 0 & 0 & 0 & 0\end{bmatrix}\begin{bmatrix}\Delta P_L\\\Delta V_L\\P_{ref}\\V_{ref}\end{bmatrix}$$

Figure (3. 14): block diagram of the combined turbine-Governor generator model[14,16]

CHAPTER FOUR
A DYNAMIC TEST MODEL FOR POWER SYSTEM STABILITY AND CONTROL STUDIES

4.1   Introduction

The stabilizing technique aforementioned was originally developed by control engineers and is known as linear optimal control. The system to be controlled is described by linear state equations and the control is designed by minimizing a function of both state deviation and control effort[18].

The linear optimal control LOC of electric power system is derived from minimization of the state variable deviations and control effort at the same time. The system state equations, or the state variable equations, must be sought first. A performance index of the system is then chosen, which shall be a function of both the state deviations and the control effort. Finally, the state equations are appended to the performance index by a co-state variable vector to find the (LOC)[18].

4.2   The system state equation[18]

Since modern control theory and computation technique are all developed with the state equations, a proper model should always be chosen and the state equations for a system formulated before an optimization technique is applied to find the optimal control.

After a proper model is chosen, the model for the system without control is first described by a set of nonlinear differential equations written in the form of

$$\dot{X} = f(x) \quad \text{...(4.1)}$$

Where x is the state variable vector.

For the LOC design, the nonlinear state equation of the system without control must be linearized with respect to an initial steady state represented by $\omega_o, \delta_{o, \text{ etc.}}$ including control, the linearized system state equation becomes

$$\Delta \dot{X} = A \Delta X + BU \quad \text{...(4.2)}$$

For a power system with both excitation and governor control, the control vector becomes

$$u = [u_E, u_G]^T \quad \text{...(4.3)}$$

For conciseness, however, equation (4.2) will be written here after simply as:

$$\dot{X} = AX + BU \quad \text{...(4.4)}$$

In (4.4), x is called the state vector, u the control vector, A the system matrix, and B the control matrix. Although A is always a square matrix, B is usually a rectangular matrix and the number of columns of the B matrix depends on how many feedback loops are used for the design.

There are generally two types of linear differential equations with time varying coefficients such as the sine and cosine functions associated with inductances when synchronous machines are described by a-b-c phase coordinates and equations with time-invariant coefficients or constant coefficients such as the inductances when the synchronous machines are described in park's d-q coordinates. Since park's equations are used for most power system dynamic studies, our main concern is with the linear differential equations with constants coefficients.

4.3   The performance index

For the LOC design of an electric power system, a performance index j of the quadratic form is usually chosen[18]:

$$j = \frac{1}{2}\int_0^\infty \left(x^T Q x + u^T R u\right) dt$$ ....(4.5)

Where Q is the weighting matrix of the state variable deviations and R that of the control effort. In most cases, both Q and R are chosen as diagonal matrices[18].

Where the two matrices Q and R are selected by design engineer by trial and error. One should select Q to be positive semi definite and R to be positive definite. This means that the scalar quantity $X^T Q X$ is always positive or zero at each time. And the scalar quantity $U^T R U$ is always positive at each time[29].

4.4   The linear optimal control (LOC)

The LOC is derived from minimization of the performance index as described by (4.5) in conjunction with the state equation (4.4). The major step of the minimization is to append (4.4) and (4.5) to form a Hamiltonian generalized energy function[18].

$$h \overset{\Delta}{=} \frac{1}{2}\left[X^T Q X + U^T R U\right] + P^T \left[A X + B U\right]$$ ....(4.6)

The unknown vector p corresponds to the Lagrange multipliers in classical mechanics and is called the co-state vector in modern control theory[18].

To find LOC, the following condition must be satisfied.

$$\frac{\partial h}{\partial U} = 0$$ ....(4.7)

Carrying out the differentiation, we shall have:

$$RU + B^T p = 0 \quad \text{...(4.8)}$$

And the control law:

$$U = -R^{-1} B^T p \quad \text{...(4.9)}$$

From (4.8) and (4.9) the co-state vector p remains to be found.

4.5   State and co-state equation[18]

In classic mechanics, the Hamiltonian h is generally related to the Lagrangian L as follows:

$$H(p, x, t) = \dot{x}^T p - L(x, \dot{x}, t) \quad \text{...(4.10)}$$

Where h and L are both function of time. By taking the derivative of both sides of equations (4.10)

For L.H.S:-

$$dh = dp^T \frac{\partial h^T}{\partial p} + dx^T \frac{\partial h}{\partial x} + dt \frac{\partial h}{\partial t} \quad \text{...................................(4.11)}$$

For R.H.S:-

$$dh = \left(d\dot{X}^T p + dp^T \dot{x} \right) - \left(dx^T \frac{\partial L}{\partial x} + d\dot{x}^T \frac{\partial L}{\partial \dot{x}} + dt \frac{\partial L}{\partial t} \right) \quad \text{...................(4.12)}$$

Comparing the last terms of both last equations

$$\frac{\partial h}{\partial t} = -\frac{\partial L}{\partial t} \quad \text{..(4.13)}$$

To continue the derivation

$$\frac{\partial L}{\partial x} = \frac{d}{dt} \left(\frac{\partial L}{\partial \dot{x}} \right) \quad \text{...(4.14)}$$

$$p = \frac{\partial L}{\partial \dot{x}} \quad \text{...(4.15)}$$

Resulting in the cancellation of the first and fourth terms of the R.H.S of (4.12) and differentiation of p

$$\dot{p} = \frac{d}{dt}\left(\frac{\partial L}{\partial \dot{x}}\right) = \frac{\partial L}{\partial x} \quad \text{...(4.16)}$$

Comparison of the dx^T terms on the R.H.S of both (4.11) and (4.12) gives

$$\dot{p} = -\frac{\partial h}{\partial x} \quad \text{..(4.17)}$$

Finally direct compression of dp^T terms of both equations results:

$$\dot{x} = \frac{\partial h}{\partial p} \quad \text{...(4.18)}$$

Equations (4.17) and (4.18) constitute the state and co-state equations of the system, let:

$$S \overset{\Delta}{=} BR^{-1}B^T \quad \text{...(4.19)}$$

From (4.8) ,(4.9) and (4.19) , the control term of equation (4.4) becomes:

$$BU \overset{\Delta}{=} -BR^{-1}B^Tp = -Sp \quad \text{...(4.20)}$$

By taking partial differentiation of h of equation (4.6) with respect to x and p respectively one obtains the co-state equation in matrix form as shown below:

$$\begin{bmatrix} \dot{x} \\ \dot{p} \end{bmatrix} = \begin{bmatrix} A & -S \\ -Q & -A^T \end{bmatrix}\begin{bmatrix} x \\ p \end{bmatrix} \quad \text{....................................(4.21)}$$

The last equation is very useful in LOC design.

4.6   Solution of the Riccati matrix equation[18]

To find the LOC, it is necessary to find the solution of the co-state variable vector p. Since we are dealing with the linear state space, the co-state variable vector p can be related to the state variable vector x linearly by:

$$p \; = \; Kx$$ ....(4.22)

Where K is called the Riccati matrix, which is a square matrix. Therefore, the solution of p can be found if K is found.

Consider the general case that K is also a function of time. The time derivative of p of (4.22) becomes:

$$\dot{p} = \dot{K}\,x + K\,\dot{x}$$ ....(4.23)

By substituting of $\dot{x}$ and $\dot{p}$ of (4.21) into (4.23) and replacing p by Kx gives:

$$KA \; + \; A^{T}K \; - \; KSK \; + \; Q \; = \; - \; \dot{K}$$ ....(4.24)

Equation (4.24) is called the Riccati matrix equation.

When synchronous machines of a power system are described in parks d-q coordinates, The coefficients of the system equations are all time-invariant. Therefore, we have time invariant system, and hence:

$$KA \; + \; A^{T}K \; - \; KSK \; + \; Q \; = \; 0, \; k \; = \; const$$ ....(4.25)

4.7   Closed form solution of the Riccati matrix equation[18]

The Riccati matrix K can be calculated from the eigen vectors of the state and co-state system matrix let the matrix (4.21) be

$$M = \begin{bmatrix} A & -S \\ -Q & -A^{T} \end{bmatrix}$$ ....(4.26)

Since for each eigen value a corresponding eigen vector can be found from

$$[M][x_i] = [x_i][\lambda_i], i = 1, 2, \ldots 2 \quad n \quad \ldots\ldots\ldots\ldots\ldots\ldots\ldots(4.27)$$

Where x_i is a column equation may be written in matrix form:

$$[M][X] = [X][\Lambda] \quad \ldots\ldots\ldots\ldots\ldots\ldots\ldots\ldots\ldots\ldots\ldots\ldots\ldots\ldots\ldots\ldots(4.28)$$

Let eigen vector partitioned into four n*n matrices such that

$$[X] = \begin{bmatrix} X_I & X_{III} \\ X_{II} & X_{IV} \end{bmatrix} \quad \ldots\ldots\ldots\ldots\ldots\ldots\ldots\ldots\ldots\ldots\ldots\ldots\ldots\ldots(4.29)$$

By substituting (4.29) in (4.28) we obtain:

$$\begin{bmatrix} A & -S \\ -Q & -A^T \end{bmatrix} \begin{bmatrix} X_I & X_{III} \\ X_{II} & X_{IV} \end{bmatrix} = \begin{bmatrix} X_I & X_{III} \\ X_{II} & X_{IV} \end{bmatrix} \begin{bmatrix} \Lambda_- & \\ & \Lambda_+ \end{bmatrix} \quad \ldots\ldots\ldots\ldots(4.30)$$

Equation (4.30) can be expanded in to four matrix equations. Considering these associated with $[\Lambda_-]$ alone, we shall have

$$AX_I - SX_{II} = X_I\Lambda_- \quad \ldots\ldots\ldots\ldots\ldots\ldots\ldots\ldots\ldots\ldots\ldots\ldots\ldots\ldots\ldots\ldots(4.31)$$

$$-QX_I - A^TX_{II} = X_{II}\Lambda_- \quad \ldots\ldots\ldots\ldots\ldots\ldots\ldots\ldots\ldots\ldots\ldots\ldots\ldots\ldots(4.32)$$

Solving for Λ_- from (4.31) substituting the result in to (4.32) and post multiplying both sides X_I^{-1} gives

$$(X_{II}X_I^{-1})A + A^T(X_{II}X_I^{-1}) - (X_{II}X_I^{-1})S(X_{II}X_I^{-1}) + Q = 0 \quad \ldots(4.33)$$

Since $(X_{II}X_I^{-1})$ satisfies the Riccati matrix equation :

$$K = (X_{II}X_I^{-1}) \quad \ldots\ldots\ldots\ldots\ldots\ldots\ldots\ldots\ldots\ldots\ldots\ldots\ldots\ldots\ldots\ldots(4.34)$$

The linear optimal control LOC now becomes:

$$BU = -Sp = -SKx = -S(X_{II}X_I^{-1})x \quad \ldots\ldots\ldots\ldots\ldots\ldots\ldots\ldots(4.35)$$

In the following procedure, the design of linear optimal control (LOC) by using MATLAB7 program language is given in steps as shown below[18]:

1. Select a proper linear model for the electric power system and obtain the state equations in the form of (4.4).

2. Select the weighting matrices Q & R of the performance index (4.5).

3. Construct the state and co-state system matrix M from (4.26) where S is calculated from (4.19), and compute the eigen value and eigen vector from (4.28).

4. Calculate the Riccati matrix K and the control law BU from (4.34) and (4.35) respectively.

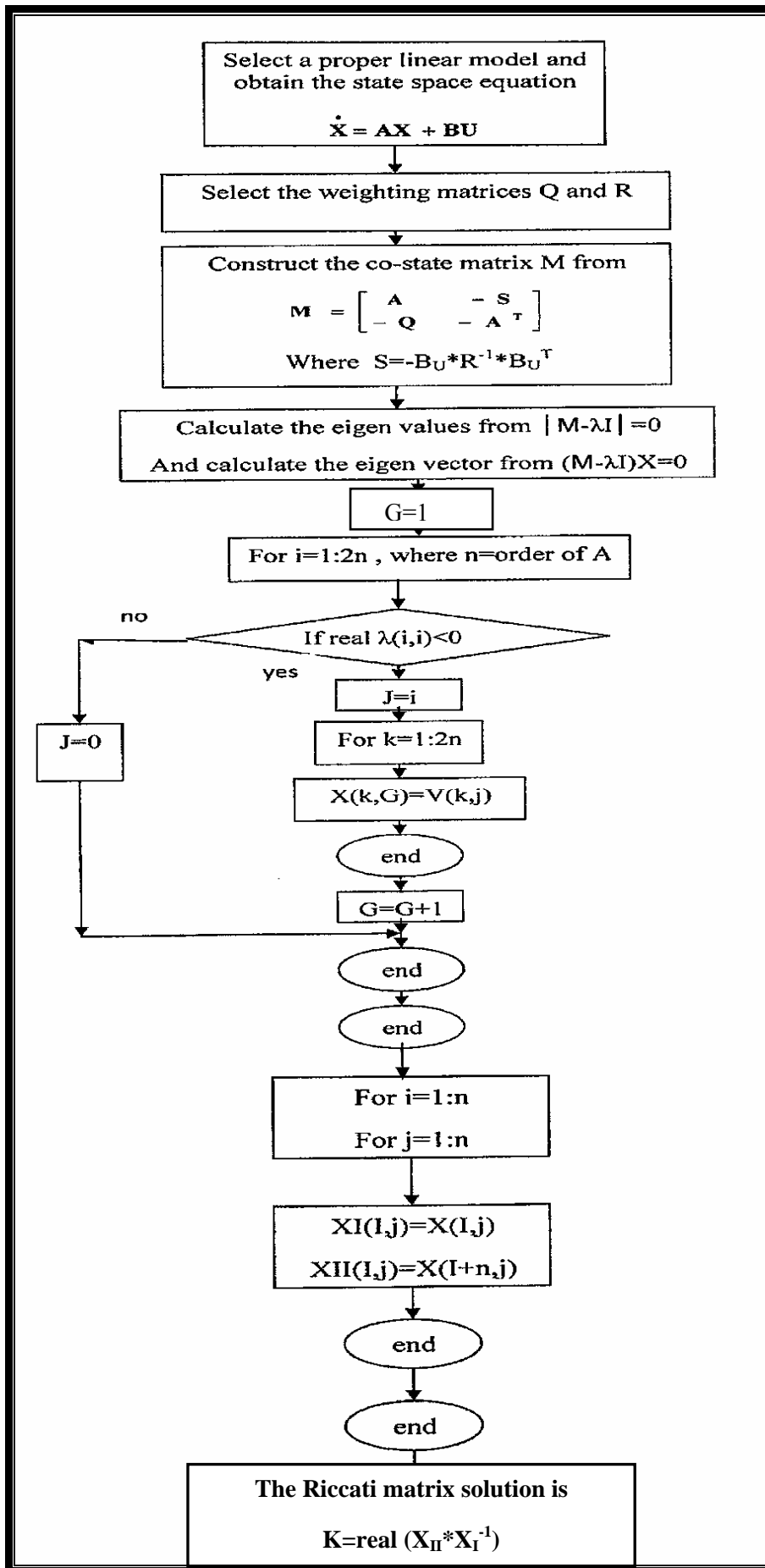5. Find the eigen value of the system with LOC.

A problem was occurred when applied the above procedure for the solution of the Riccati matrix K, the problem was treated with the flow chart (4.1). The aim of the flow chart (4.1) below was to search about the location of the stable eigen values ($-\lambda$) on the diagonal of ($|M-\lambda I|=0$) of order 2n, then rearrange the column eigen vectors of X to obtain (X_I and X_{II}) which are the partitioned egien vectors matrices that are corresponds to a stable eigen values (Λ-) by using MATLAB7 program.

Where:

G: is the accumulator to show the location of stable eigen values $-\lambda$ on the diagonal eigen values of a matrix M of order 2n.

V(k,j):eigen vectors elements of eigen vector matrix X in (k-row and j-column).

Select a proper linear model and obtain the state space equation

$$\dot{X} = AX + BU$$

Select the weighting matrices Q and R

Construct the co-state matrix M from

$$M = \begin{bmatrix} A & -S \\ -Q & -A^T \end{bmatrix}$$

Where $S = -B_U * R^{-1} * B_U^T$

Calculate the eigen values from $|M - \lambda I| = 0$

And calculate the eigen vector from $(M - \lambda I)X = 0$

G=1

For i=1:2n , where n=order of A

If real $\lambda(i,i) < 0$

no

yes

J=i

J=0

For k=1:2n

X(k,G)=V(k,j)

end

G=G+1

end

end

For i=1:n

For j=1:n

XI(I,j)=X(I,j)

XII(I,j)=X(I+n,j)

end

end

The Riccati matrix solution is

$$K = real (X_{II} * X_I^{-1})$$

Flow chart(4.1)closed form solution of the Riccati matrix using MATLAB7 program

59

4.8   A micro machine model and LOC testing[18]

When the principle of LOC was first derived to stabilization of a power system, figure (4.1) schematically shows a dynamic power system model for LOC and stability control tests. A student laboratory dc-motor, synchronous-generator set was adapted to simulate a megawatt hydraulic or steam turbine generator plant with various kinds of stability controls utilizing electronic circuits and power amplifiers. A large turbine generator set was simulated on the micro machine on a per unit basis.

The general layout of the dynamic power system model is schematically shown in figure (4.1).The turbine and governor and valving controls are on the left, the generators and excitation controls are at the center, and the transmission and fault simulation and braking resistance control are on the right.

At the top left of figure (4.1) are the hydraulic power output (HYDRO), which affects the dc motor power input by controlling its armature current, and a governor that has a conventional negative feedback $\Delta\omega$ in addition to an optional phase compensation supplementary governor control U_G. At the bottom left are the steam turbine power output (THRM) and a governor that also has a conventional negative feedback $\Delta\omega$ in addition to an optional fast valving control FV. The dc motor M in the figure, representing the hydraulic or steam turbines, is given a constant field excitation I_f. It has a starting rheostat, and its armature current I_A is controlled by either (HYDRO) or (THRM) to simulate the controlled turbines.

The time constant T'_{do} of the synchronous generator G is adjustable by varying –R effect. The field winding is connected to the exciter and voltage regulator (EX-VR), which has a conventional negative feedback of Δv_t in addition to two optionals: a linear optimal control (EX-CONTR) with various input signals and a forced excitation control FE.

At the top right of figure (4.1) a transmission system is shown. It constitutes three-phase, three section, double-circuit transmission lines connected to an

infinite bus with a voltage v_o. A three phase fault can be simulated on the line including grounding, faulted line opening, fault clearing, and cleared line restoration by relays and circuit breakers.
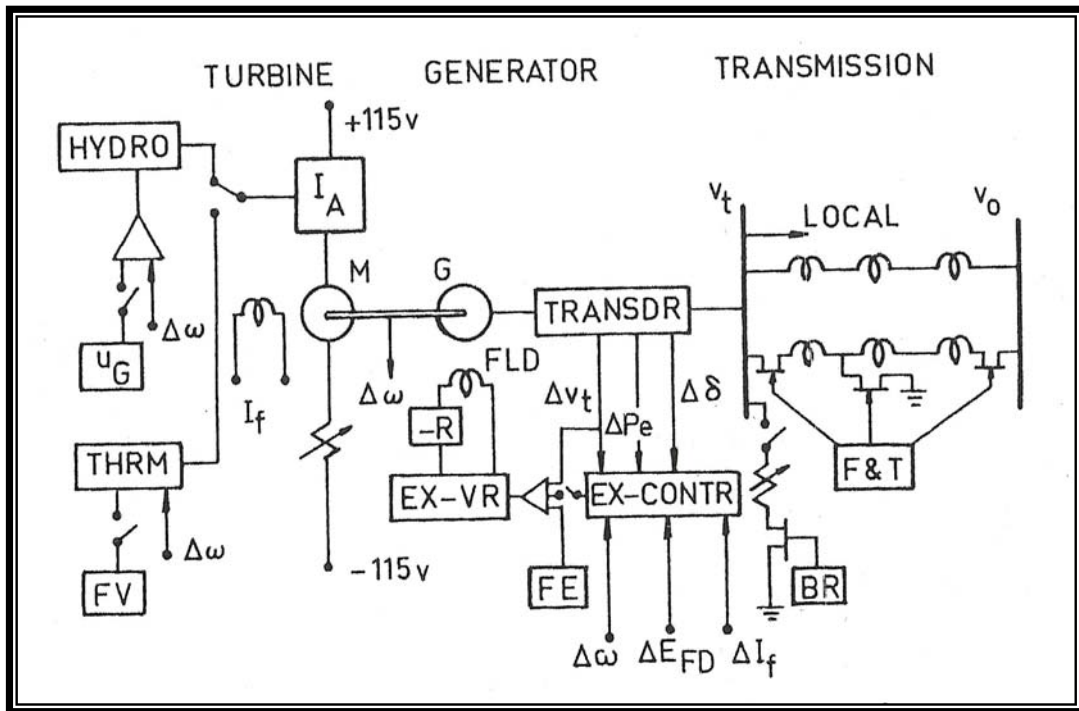

Figure (4.1) a dynamic power system model for control test[18]

Figure (4.2) below shows the test results on the micro machine. The system was unstable due to lack of damping. The same system becomes stabilized in a few seconds with an LOC[18].
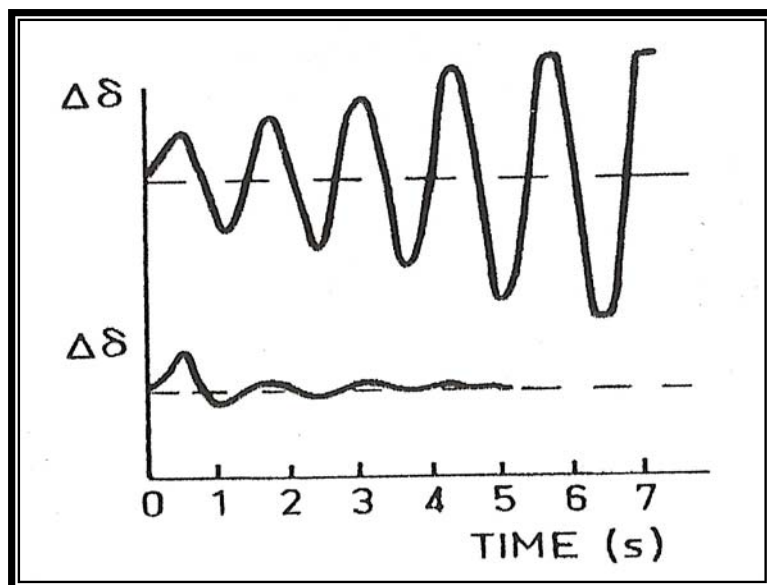

Figure (4.2) micro machine test of LOC[18]

In this work small disturbances ΔV_L and ΔP_L were simulated in previous mathematical models in chapter three. The effects of these disturbances were also taken into account in this work. These small disturbances were continuously acting on a power system acting only on a steady state behavior of a dynamic system.

The design of the linear optimal control was taken into account by calculation of the control law in equation (4.9) that represents the closed loop feedback control gain (KK). This symbol is considered in this work differently from K which is referred to the Riccati matrix equation. The closed loop feedback gain KK is obtained by substituting equation (4.22) into (4.9) then the control law becomes:

$$U = -R^{-1}B^{T}KX \ldots\ldots\ldots\ldots\ldots\ldots\ldots\ldots\ldots\ldots\ldots\ldots\ldots\ldots\ldots\ldots\ldots\ldots(4.36)$$

Let:

$$KK = -R^{-1}B^{T}K \ldots\ldots\ldots\ldots\ldots\ldots\ldots\ldots\ldots\ldots\ldots\ldots\ldots\ldots\ldots\ldots\ldots(4.37)$$

Then the co-state matrix for controlled system can be calculated as:

$$A_C = (A - BKK) \ldots\ldots\ldots\ldots\ldots\ldots\ldots\ldots\ldots\ldots\ldots\ldots\ldots\ldots\ldots\ldots(4.38)$$

In[30] the method of root shifting, may be stated as follows: given a system expressible in state space form by the two standard state and output equations:

$$\dot{X} = AX + BU \ldots\ldots\ldots\ldots\ldots\ldots\ldots\ldots\ldots\ldots\ldots\ldots\ldots\ldots\ldots\ldots\ldots(4.39)$$

$$Y = CX \ldots\ldots\ldots\ldots\ldots\ldots\ldots\ldots\ldots\ldots\ldots\ldots\ldots\ldots\ldots\ldots\ldots\ldots(4.40)$$

If the control loops are introduced, this will modify the actuating signal and consequently the system matrix, the actuating signal U can be given[30]:

$$U = -KKX + V \ldots\ldots\ldots\ldots\ldots\ldots\ldots\ldots\ldots\ldots\ldots\ldots\ldots\ldots\ldots\ldots(4.41)$$

Where KK is a constant matrix representing the feedback gain with dimension governed by dimensions of the matrices B and C, V is an external input reference used to apply step input signal, substituting equation (4.41) in to (4.39) yields[30]:

$$\dot{X} = (A - BKK)X + BV \ \dots\dots\dots\dots\dots\dots\dots\dots\dots\dots\dots\dots\dots\dots\dots\dots..\dots\dots..(4.42)$$

When the effect of input disturbances ΔV_L and ΔP_L were taken in to account equation (4.42) become as follows:

$$\dot{X} = (A - BKK)X \ + BV + d \ \dots\dots\dots..\dots\dots\dots\dots..\dots\dots..(4.43)$$

Where:

d: is small input disturbance represented as ΔV_L , ΔP_L.

In this work LOC linear optimal control technique was tested and applied to a 384 MVA, 24 KV Turbo-Generator using MATLAB7 programming language. This realization and its results are summarized in chapter five.

CHAPTER FIVE

PERFORMANCE OF A DYNAMIC TEST MODEL FOR POWER SYSTEM STABILITY USING (LOC)

5.1 Introduction

In the evaluation of stability the concern is the behavior of the power system when subjected to a disturbance. The disturbance may be small or large. Small disturbances in the form of load changes take place continually, and the system adjusts itself to the changing conditions. The system must be able to operate satisfactorily under these conditions and successfully supply the maximum amount of the load. It must also be capable of surviving numerous disturbances of a severe nature such as short circuit on a transmission line, loss of large generator, or loss of a tie line two sub system[2].

When a disturbance impacts a generator's mechanical and electrical torque balance, the rotor of the machine must either speed up or slow down. The electrical torque will often change more rapidly than the mechanical torque input because it is dependent upon the electrical network variables which can change rapidly. These variables include the power transmission capacity of the network and the state of all other machine rotors in the system. The changes in electrical torque within a generator can be resolved into two components as discussed in chapter two, one in phase with the rotor angle and the other with the rotor speed. These components are often referred to respectively as synchronizing and damping torque. These concepts illustrate two separate aspects of the rotor angle stability problem. A lack of synchronizing torque often leads to rotor angle instability in the first swing of the generator rotor.

Synchronizing torque is restored by fast acting control actions. The problem is referred to as transient stability problem[22].

A power system may be losing its stability due to lack of damping or inadequate synchronizing torque. The sustained low frequency oscillations of a large electrical power system are due to the lack of damping of the system mechanical mode. A synchronous machine may have mechanical damping adequate for the machine itself, but not sufficient for the machine operating in a large electrical power system[18].

Number of model test will be taken into account in this chapter and are listed below as:

- **Generator- Exciter test model.**

- **Turbine- Governor test model.**

- **Combined generator- Exciter and Turbine- Governor test model.**

For controlling electrical power system stability, the linear optimal control LOC method that is widely used in electrical power system control, LOC used in this work for control test. A 384 MVA, 24 KV turbo generator whose details are given in APPENDIX A, are taken as an example to study the effectiveness of LOC method for different test models as listed above acting on power system stability.

The results obtained in this work can be summarized in two parts:-

- **Part one (without LOC):** In this part the results obtained by testing the excitation and turbine Governor control by using MATLAB7 program to show the effectiveness of different controllers that are used in different test models on a stability problem in electrical power system:

- **Performance and results of exciter-voltage regulator (VR) test model control system.**

- **Performance and results of Turbine-Governor test model control system.**

- **Performance and results of combined Turbine-Governor Generator test model control system.**

- **Part Two (with LOC):** In this part the results are obtained by testing the linear optimal control LOC with different test models as in the above using MATLAB7 program to show the effectiveness of the LOC method on a stability problem in electrical power system.

In this work the comparison of the results are obtained in this chapter for the above two parts are based on:

- **Calculations of the eigen value structure method that are used from obtaining the roots of characteristic equation ($|$A-λI$|$ = 0 , $|$A$_C$-λI$|$) = 0) for the system without and with LOC method respectively.**

- **Calculation of system performance indices , damping of mechanical mode and synchronizing torque (K_{ST}, K_D, ω_n, ζ, ω_d) as shown in chapter three and with details in APPENDIX (B,C) in the case of excitation control[2,3,18].**

- **From figures obtained for different test cases using MATLAB7 program the time domain performance indices are evaluated to show the quality of the control system in both steady state and transient stability, with details in APPENDIX D.**

5.2   Results of Part One (without LOC)
5.2.1   Performance and results of Exciter-Voltage regulator (VR) test model

The state space mathematical models that are derived in chapter three, equation (3.19) for voltage regulator control system are programmed using MATLAB7 program. In this control test firstly shown the initial value of K_A in the case of voltage regulator for normal operation system occurring when K_A=40

to give terminal voltage equal to E_t=0.998 p.u . Then different disturbances acting on a power system as small input disturbances will be assumed to be ΔV_L=(0, 5, 10, 15) %, K_A=40, where V_{ref} is an input control signal and E_t is an output signal as shown in figure (3.5a) and the output equation is shown in equation (5.1) below.

Where:

$$E_t = \begin{bmatrix} 0 & K_5 & K_6 & 0 \end{bmatrix} \begin{bmatrix} \Delta\omega_r \\ \Delta\delta \\ \Delta\Psi_{fd} \\ \Delta E_{fd} \end{bmatrix} \dots\dots\dots\dots\dots\dots\dots\dots\dots\dots\dots\dots\dots\dots\dots(5.1)$$

Table (5.1a), (5.1b) shows the system eigen values, and system performance indices for applied step input response to the system state equation, and figures (5.1a), show the time domain performance for $K_A = 40$, ΔV_L=(0, 5, 10, 15) %, for different cases in the same graph.

Table (5.1a): System eigen Values for VR test model

Case	ΔV_L	System eigen values for VR control system			
		λ1	λ2	λ3	λ4
1,2,3,4	0,5,10,15	-0.2833+6.6307i	-0.2833-6.6307i	-0.2492 + 0.7848i	-0.2492 - 0.7848i

Table (5.1b): System Performance Indices for VR test model

Case	ΔV_L	Damping of mechanical mode and Synchronizing torque					Time domain performance indices				
		K_{ST}	K_D	ω_n	ζ	ω_d	t_r	t_s	$P_{.amp}$	%M_P	E_t
1.	0	0.0111	0.6538	0.8204	0.0766	0.818	1.59	13.6	1.37	37.1	0.998
2.	5	0.0111	0.6538	0.8204	0.0766	0.818	1.59	13.7	1.35	37.2	0.987
3.	10	0.0111	0.6538	0.8204	0.0766	0.818	1.59	13.7	1.34	37.2	0.975
4.	15	0.0111	0.6538	0.8204	0.0766	0.818	1.58	13.8	1.32	37.2	0.964
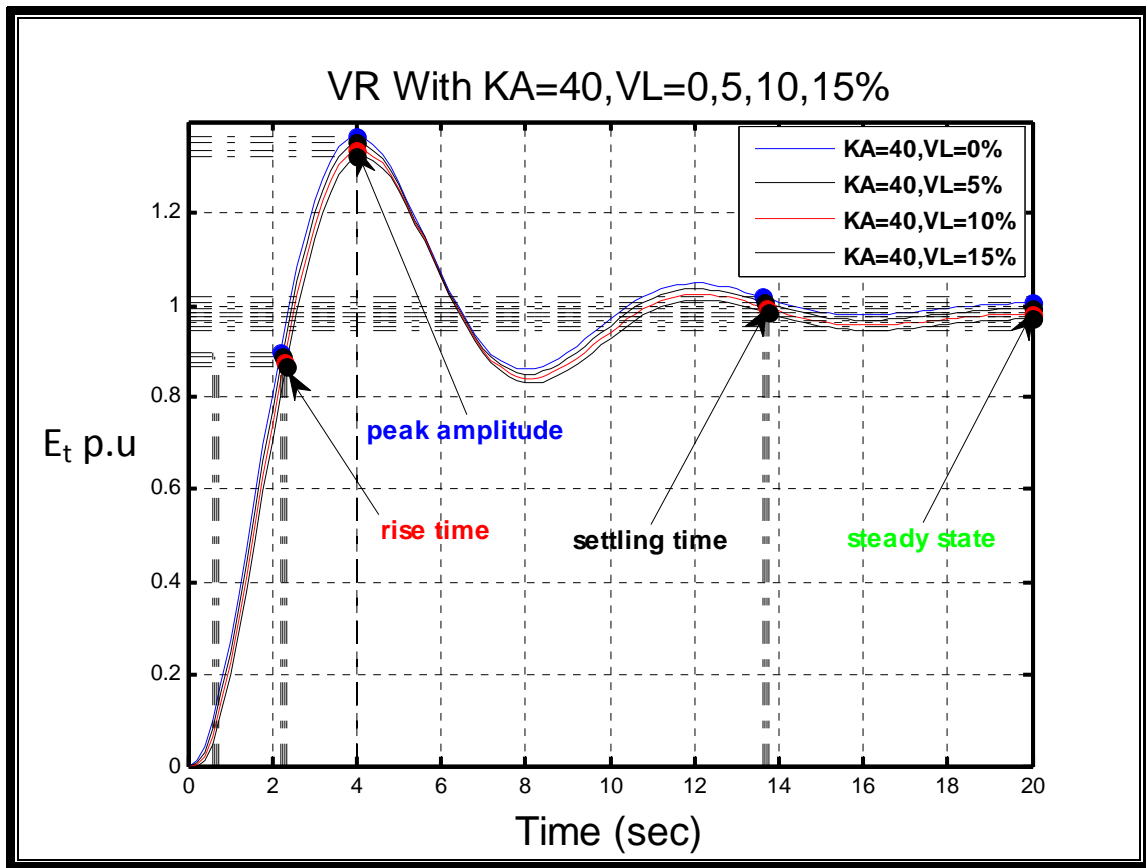
Figure (5.1a): Time Domain Performance for VR test model,
*$K_A = 40, \Delta V_L = (0, 5, 10, 15)\%$*

The above test shows the steady state terminal output voltage reduced from 0.998 to 0.868 p.u then K_A must be actuated to reject the effect of small input disturbance. Then the second test K_A change from 40 to 400 to show the effectiveness of excitation control on stability of a power system. K_A's are considered to be K_A=40, 100, 150, 200, 400 with ΔV_L=15% as a sample tested values. Table (5.1c), (5.1d) show the system eigen values, and system performance indices respectively, and results in figure (5.1b), show the time domain performance for (K_A = 40, 150, 400) , (ΔV_L=15%) selected cases.

Table (5.1c): System eigen Values for VR test model

Case	KA	System eigen values for VR control system			
		λ1	λ2	λ3	λ4
1.	40	-0.2833+6.6307i	-0.2833-6.6307i	-0.2492 + 0.7848i	-0.2492 - 0.7848i
2.	100	-0.2849 + 6.6076i	-0.2849 - 6.6076i	-0.2476 + 1.2452i	-0.2476 - 1.2452i
3.	150	-0.2863 + 6.5874i	-0.2863 - 6.5874i	-0.2461 + 1.5298i	-0.2461 - 1.5298i
4.	200	-0.2878 + 6.5663i	-0.2878 - 6.5663i	-0.2446 + 1.7721i	-0.2446 - 1.7721i
5.	400	-0.2949 + 6.4718i	-0.2949 - 6.4718i	-0.2375 + 2.5427i	-0.2375 - 2.5427i

Table (5.1d): System Performance Indices for VR test model

Case	K_A	Damping of mechanical mode and Synchronizing torque					Time domain performance indices				
		K_{ST}	K_D	ω_n	ζ	ω_d	t_r	t_s	$P_{.amp}$	$\%M_P$	E_t
1.	40	0.0111	0.6538	0.8204	0.0766	0.818	1.58	13.8	1.32	37.2	0.964
2.	100	0.0265	0.5982	1.2662	0.0454	1.2649	0.921	15.7	1.52	54	0.985
3.	150	0.0399	0.5508	1.5514	0.0341	1.5505	0.699	15	1.63	62.4	1
4.	200	0.0530	0.5379	1.7897	0.0289	1.789	0.588	16.2	1.7	67.6	1.01
5.	400	0.1081	0.4746	2.5544	0.0179	2.554	0.416	16.3	1.85	80	1.04
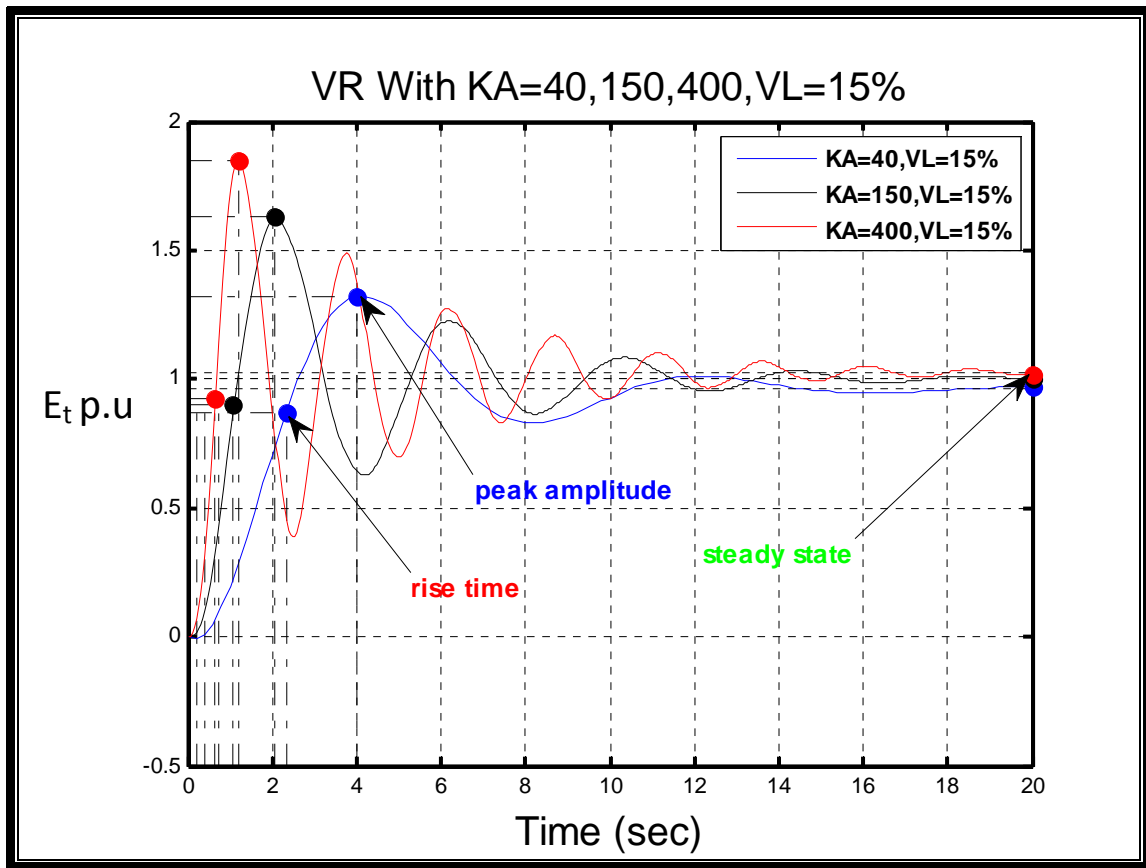
Figure (5.1b): Time Domain Performance for VR test model,
$K_A = 40,150,400, \Delta V_L = 15\%$

Table (5.1c) and (5.1d) show that increasing in K_A can affect both steady state and transient stability of a power system. This effectiveness is shown in tables and figures above. The increase in K_A can improve over all steady state and transient stability but in other word this increasing causes decrease in the damping of mechanical mode torque coefficient and this may lead to losing stability due to insufficient damping torque. This case can also be discussed from the eigen values obtained from above cases, with K_A increase we see that the two roots $\lambda 3, \lambda 4$ are pushed toward the right hand side of s-plane and becomes closer to the imaginary axis of s-plain. Also it is shown that the synchronizing torque increased from 0.0111 to 0.1081, that increase is not acceptable because it may lead to rotor angle instability due to lack of insufficient synchronizing torque.

5.2.2   Performance and results of Turbine-Gov. test model

The same steps that are used in previous test are also applied in the case of turbine-Gov. model whose state space mathematical model are derived in chapter three, Equation (3.22) is also programmed using MATLAB7 program language. In this case P_{ref} is an input control signal and P_m , $\Delta\omega_r$ are taken to be output signals and are shown in equation (5.2) and (5.3) below.

Where:

$$P_m = \begin{bmatrix} 0 & 0 & 0 & F_{HP} & F_{IP} & F_{LP} \end{bmatrix} \begin{bmatrix} \Delta\omega_r \\ \Delta P_{SR} \\ \Delta P_{GV} \\ \Delta P_{CH} \\ \Delta P_{RH} \\ \Delta P_{CO} \end{bmatrix} \quad \text{...(5.2)}$$

$$\Delta\omega_r = \begin{bmatrix} 1 & 0 & 0 & 0 & 0 & 0 \end{bmatrix} \begin{bmatrix} \Delta\omega_r \\ \Delta P_{SR} \\ \Delta P_{GV} \\ \Delta P_{CH} \\ \Delta P_{RH} \\ \Delta P_{CO} \end{bmatrix} \quad \text{...(5.3)}$$

Firstly the control test take into account the change in the input disturbance ΔP_L (0, 5, 10, 15)% as an input disturbance , when governor control gain $K_G = 5$ is taken to be initial value for normal operation when $P_m=1$, $\Delta\omega_r=0$. Tables (5.2a), (5.2b) show the system eigen values, time domain performance indices, and figures (5.2a) show the time domain performance in the case ($K_G = 5$, $\Delta P_L=0, 5, 10, 15\%$).

Table (5.2a) System eigen values Turbine-Gov. test model

Case	ΔP_L	System eign values for Turbine-Gov. control system					
		$\lambda 1$	$\lambda 2$	$\lambda 3$	$\lambda 4$	$\lambda 5$	$\lambda 6$
1,2,3,4	0,5,10,15	-99.9993	-0.1964 + 0.3116i	-0.1964 - 0.3116i	-5.8925	-3.6930 + 0.1721i	-3.6930 - 0.1721i

Table (5.2b) System performance indices for Turbine-Gov. test model

case	ΔP_L	(Pm) Time domain performance					($\Delta\omega_r$) Time domain performance				
		t_r	t_s	$P_{.amp}$	%M_P	P_m	t_r	t_s	$P_{.amp}$	%M_P	$\Delta\omega_r$
1.	0	2.35	19.5	1.24	24.3	1	0.104	18.8	-0.24	∞	0
2.	5	2.29	19.5	1.18	24.6	0.95	0.335	18.8	-0.22	318	0.01
3.	10	2.22	19.4	1.12	24.9	0.9	0.647	18.7	-0.201	152	0.02
4.	15	2.14	19.4	1.06	25.3	0.85	0.95	18.6	-0.182	97.5	0.03
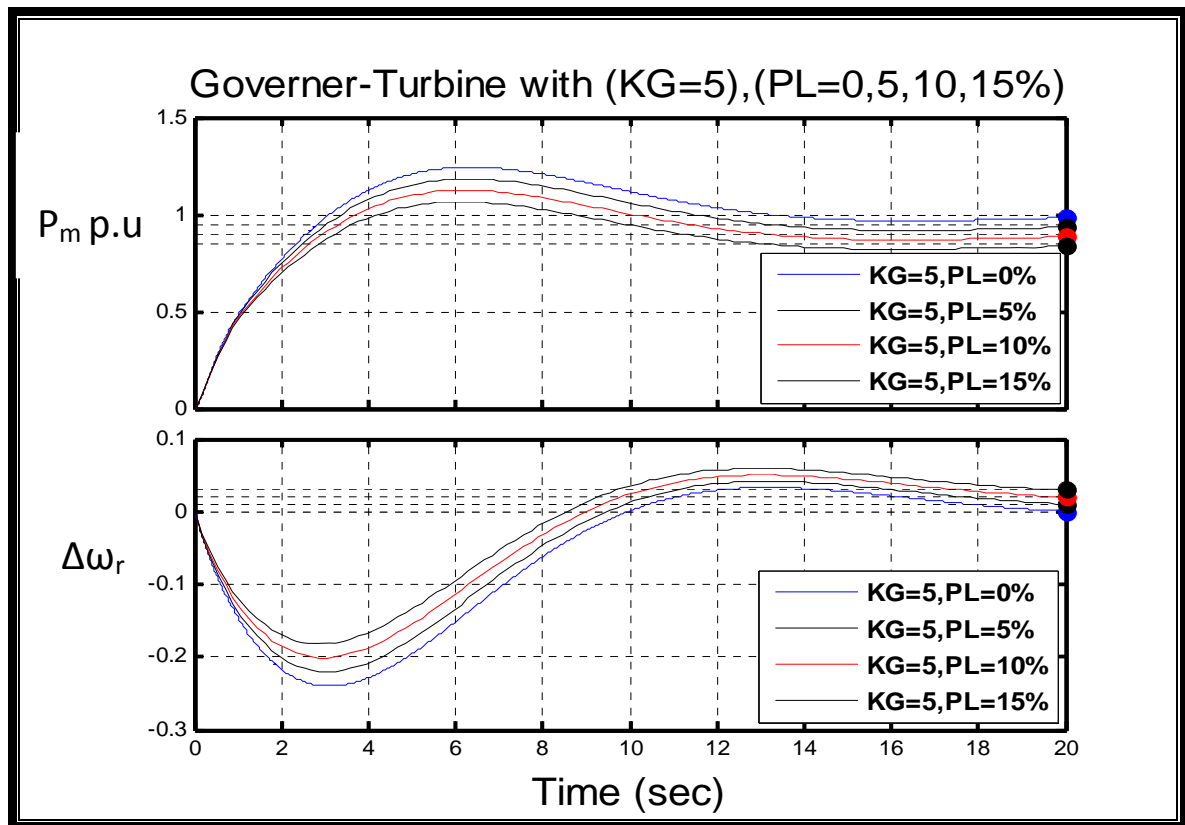
Figure (5.2b): Time Domain Performance For Turbine-Gov. test model
*$K_G = 5, \Delta P_L = (0, 5, 10, 15)$ %*

From the above test it is shown that the steady state values for P_m and $\Delta\omega_r$ are changed due to input disturbance. The second test is considered by changing the governor control K_G to show the effect of the overall governor gain control K_G in steady state and transient stability. Take the values (K_G = 5, 10, 15, 20) when ΔP_L = 15%. Table (5.2c), (5.2d) show the system eigen values and time domain performance indices for turbine governor control system and figure (5.2b) shows the time domain performance for step input control for P_m and $\Delta\omega_r$ for different K_G that are considered in this section.

Table (5.2c) System eigen values Turbine-Gov. test model

Case	K_G	System eign values (Turbine-Gov.)					
		$\lambda 1$	$\lambda 2$	$\lambda 3$	$\lambda 4$	$\lambda 5$	$\lambda 6$
1.	5	-99.9993	-0.1964 + 0.3116i	-0.1964 - 0.3116i	-5.8925	-3.6930 + 0.1721i	-3.6930 - 0.1721i
2.	10	-99.9986	-6.2878	-0.3724 + 0.4286i	-0.3724 - 0.4286i	-2.8306	-3.8087
3.	15	-99.9978	-6.5796	-0.6686 + 0.4782i	-0.6686 - 0.4782i	-1.9248	-3.8311
4.	20	-99.9971	-6.8186	-1.1659 + 1.0412i	-1.1659 - 1.0412i	-0.6833	-3.8397

Table (5.2d) System performance indices for Turbine-Gov. test model

case	K_G	(P_m) Time domain performance					($\Delta\omega_r$) Time domain performance				
		t_r	t_s	$P_{.amp}$	%M_P	P_m	t_r	t_s	$P_{.amp}$	%M_P	$\Delta\omega_r$
1.	5	2.14	19.4	1.06	25.3	0.85	0.95	18.6	-0.182	97.5	0.03
2.	10	1.35	8.38	0.11	23.7	0.9	0.532	12.4	-0.142	99	0.01
3.	15	1.01	6.63	1.18	24	0.95	0.544	6.18	-0.126	46.7	0.0033
4.	20	0.819	5.58	1.26	26.4	0.998	0	6.98	-0.182	∞	0
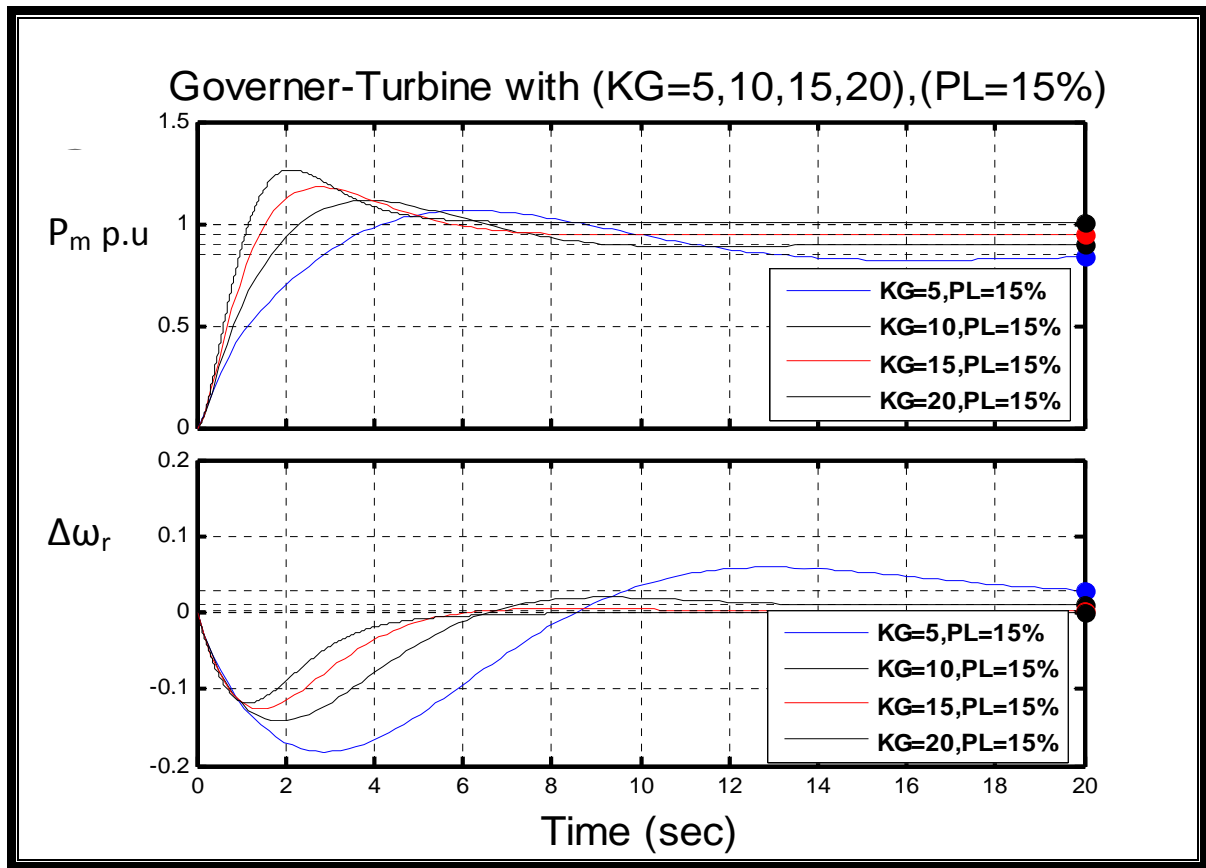
Figure (5.2a): Time Domain Performance For Turbine-Gov. test model,
$K_G = (5, 10, 15, 20), \Delta P_L = 15\%$

5.2.3   Performance and results of Combined Turbine-Gov. Generator test model

The state space mathematical model derived in chapter 3, equation (3.23) is programmed using MATLAB7 programming language where V_{ref}, P_{ref} are input control signals and E_t , $\Delta\omega_r$ equation (5.1) and (5.3) respectively are an output signals. The results in this case are evaluated when K_A =(40, 100, 150, 200, 400), K_G=20. Tables (5.3a), (5.3b) show the system eigen values, time domain performance indices respectively and Figure (5.3a) shows the time domain performance for the combined system when K_A=400, K_G=20.

Table (5.3a) System eigen values for Combined Turbine-Gov. - generator test model

Case	K_A	System eign values								
		λ1	λ 2	λ 3	λ 4	λ 5	λ 6	λ 7	λ 8	λ 9
1.	40	-99.9971	-0.1931+6.8056i	-0.1931-6.8056i	-6.2529	-3.7400+0.1705i	-3.7400-0.1705i	-0.2474+0.7817i	-0.2474-0.7817i	-0.1243
2.	100	-99.9971	-0.1941+6.7846i	-0.1941-6.7846i	-6.2499	-3.7442+0.1734i	-3.7442-0.1734i	-0.2437+1.2387i	-0.2437-1.2387i	-0.1243
3.	150	-99.9971	-0.1949+6.7664i	-0.1949-6.7664i	-6.2476	-3.7473+0.1755i	-3.7473-0.1755i	-0.2410+1.5200i	-0.2410-1.5200i	-0.1243
4.	200	-99.9971	-0.1958+6.7475i	-0.1958-6.7475i	-6.2453	-0.2385+1.7590i	-0.2385-1.7590i	-3.7501+0.1774i	-3.7501-0.1774i	-0.1243
5.	400	-99.9971	-0.1996+6.6636i	-0.1996-6.6636i	-6.2369	-0.2300+2.5142i	-0.2300-2.5142i	-3.7590+0.1831i	-3.7590-0.1831i	-0.1243

Table (5.3b) System performance indices for Combined Turbine-Gov. gen. test

case	K_A	Time domain performance for E_t					Time domain performance for $\Delta\omega_r$				
		t_r	t_s	$P_{.amp}$	%M_P	E_t	t_r	t_s	$P_{.amp}$	%M_P	$\Delta\omega_r$
1.	40	1.47	13.9	1.43	40.7	1.01	0	17.7	-0.00574	∞	0
2.	100	0.91	15.8	1.73	55.7	1.11	0	19	-0.00931	∞	0
3.	150	0.72	15.2	1.86	64.4	1.13	0	17.6	-0.0124	∞	0
4.	200	0.615	16.4	1.93	69	1.14	0	17.3	-0.0154	∞	0
5.	400	0.432	17.6	2.09	79.6	1.16	0	17.3	-0.0265	∞	0
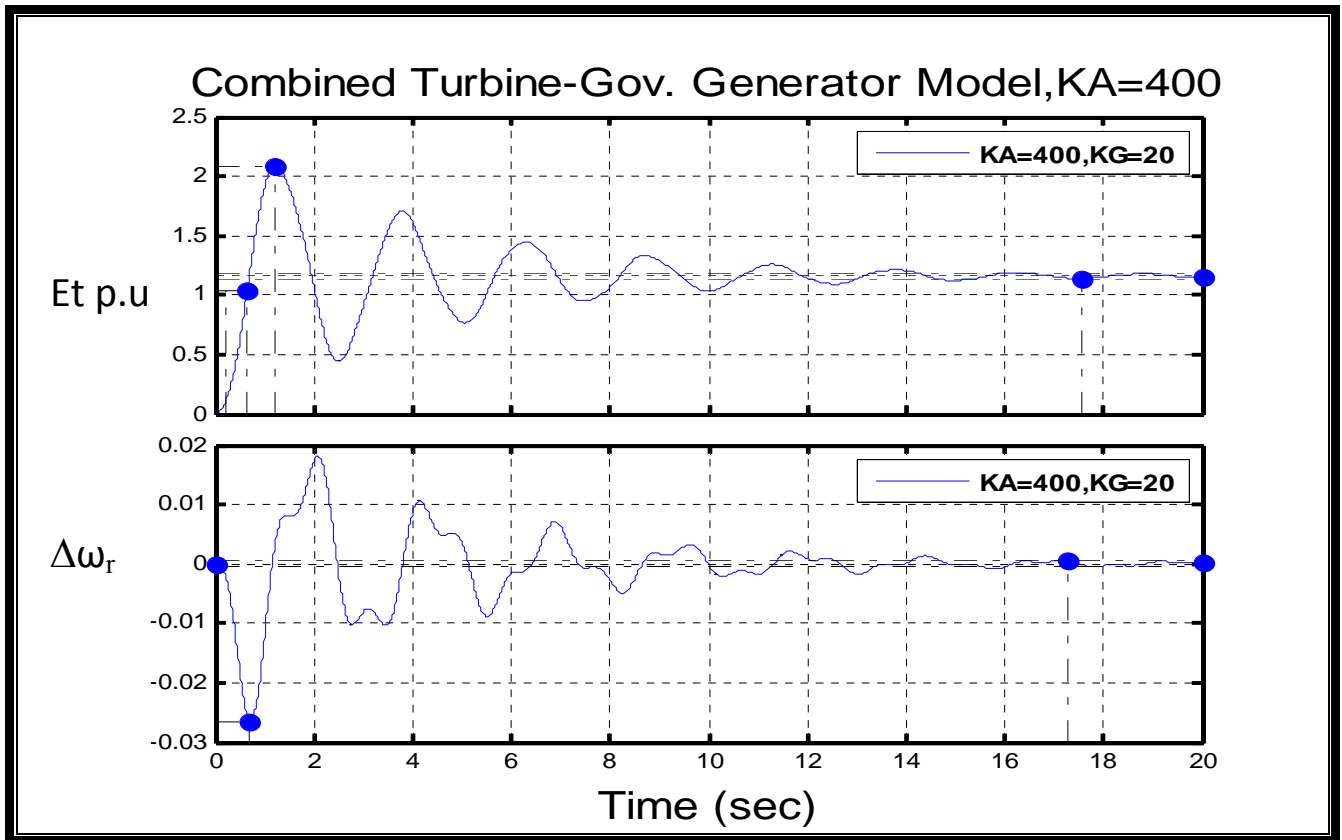
Figure (5.3a): Time Domain Performance for Combined Turbine-Gov. Generator test model $K_A = 400$, $K_G=20$

5.3 Results of Part Two (with LOC)

5.3.1 Performance and results of Exciter-voltage regulator (VR) using LOC test model

In the design of linear optimal control the system eigen values for the controlled system can be calculated from the co-state matrix $|(A-BKK)-\lambda I|=0$.

For the LOC design the weighted matrices Q,R can be selected by trial and error[5,13,14,29], in the case of exciter-voltage regulator test mode the choice of Q,R that give optimal control design that minimizes the performance index can be given bellow:

$$
Q = \begin{bmatrix} 5000 & 0 & 0 & 0 \\ 0 & 0.013 & 0 & 0 \\ 0 & 0 & 0 & 0 \\ 0 & 0 & 0 & 0 \end{bmatrix} \quad , \qquad R = \begin{bmatrix} 1 \end{bmatrix}
$$

Table (5.4a) show the closed loop eigen values and the full state feedback control gain KK. Table (5.4b) shows the time domain performance indices for the output terminal voltage in the case of VR using LOC controller when K_A is taken to be nominal value (K_A=400). Figure (5.4a) shows the time domain performance for VR using LOC by applying step input to the modified system state equation (5.10).

Table(5.4a)closed loop eigen values and feedback control gain KK for VRusing LOC

Case	K_A	Closed loop eigen values				Closed loop F.B gain KK			
		λ1	λ2	λ3	λ4	KK1	KK2	KK3	KK4
1.	400	-1.5614 + 7.0922i	-1.5614 - 7.0922i	-1.5838 + 1.6940i	-1.5866 - 1.6940i	4259.4	109.6	118.6	5.2

Table (5.4b) System performance indices for VR using LOC test model

Case	K_A	Damping of mechanical mode and Synchronizing torque					Time domain performance for E_t				
		K_{ST}	K_D	ω_n	ζ	ω_d	t_r	t_s	$P_{.amp}$	%M_P	E_t
1.	400	0.477	8.4541	5.367	0.1515	5.3051	0.689	2.65	1.06	5.62	1
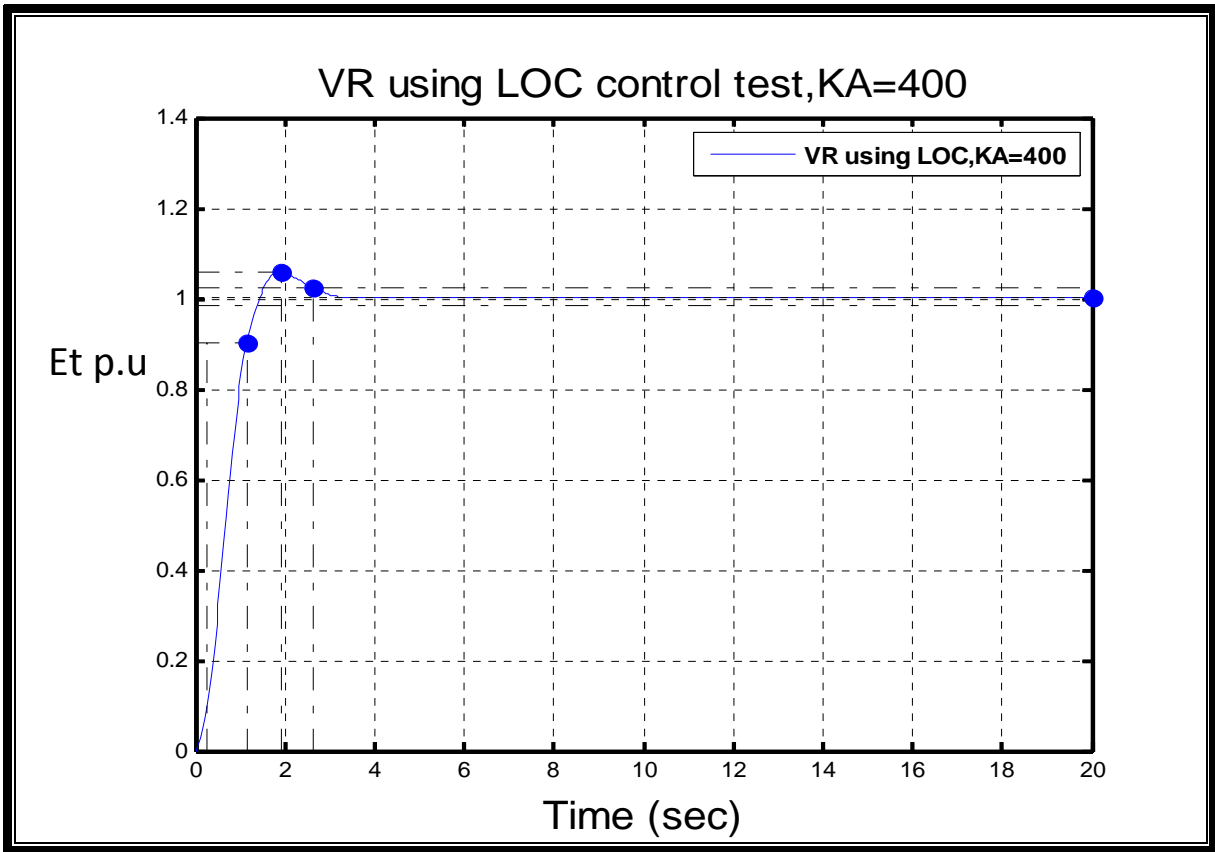
Figure (5.4a): Time Domain Performance for VR using LOC test model
, $K_A = 400$

5.3.2 Performance and results of a Governor-Turbine using LOC test model

In this section for turbine governor using LOC test mode the weighted matrices are selected as shown below:

$$Q = \begin{bmatrix} 325 & 0 & 0 & 0 & 0 & 0 \\ 0 & 0.001 & 0 & 0 & 0 & 0 \\ 0 & 0 & 0.001 & 0 & 0 & 0 \\ 0 & 0 & 0 & 0 & 0 & 0 \\ 0 & 0 & 0 & 0 & 0 & 0 \\ 0 & 0 & 0 & 0 & 0 & 0 \end{bmatrix} \quad , \qquad R = \begin{bmatrix} 10 \end{bmatrix}$$

The results of test considered in this section are tabulated in tables (5.5a),(5.5b) and (5.5c) which show the system eigen values, the closed loop feedback control gain KK and the time domain performance indices respectively. Figure (5.5a) shows the time domain performance by applying step input for P_{ref} to show the outputs P_m ,$\Delta\omega_r$ in time domain.

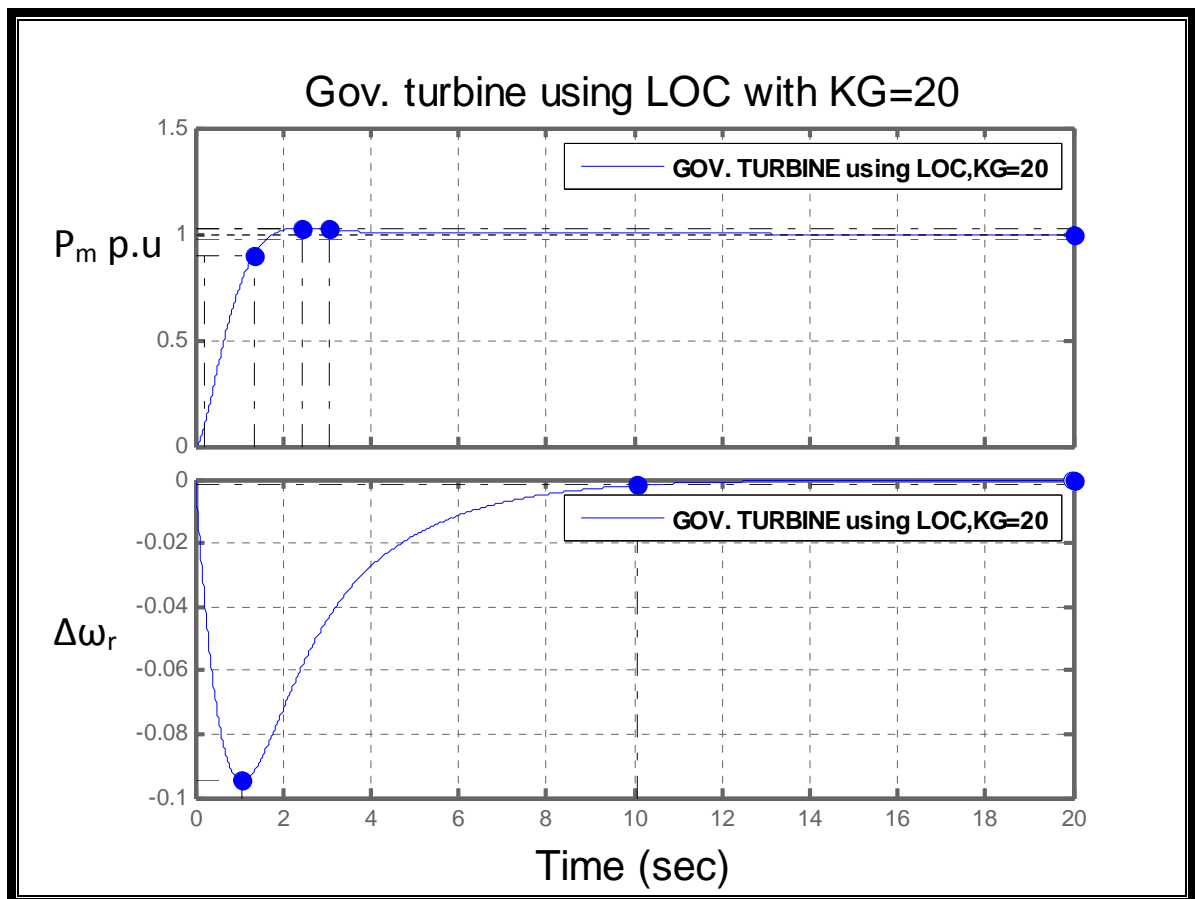*Table (5.5a): System eigen Values for Turbine-Gov. using LOC test model*

Case	K_G	System eign values (Turbine-Gov.)					
		λ1	λ 2	λ 3	λ 4	λ 5	λ 6
1.	20	-100	-6.8	-4.4	-3.5917 + 1.3499i	-3.5917 - 1.3499i	-3.84

Table (5.5b): Closed Loop F.B Control Gain KK for Turbine-Gov. using LOC test model

Case	K_G	Closed loop feedback control gain KK for (Turbine-Gov.)					
		KK1	KK2	KK 3	KK 4	KK 5	KK 6
1.	20	-312.1294	-0.0504	-1.2751	-2.2298	6.4439	-2.8786

Table (5.5c) System performance indices for Turbine-Gov. using LOC test model

case	K_G	(P_m) Time domain performance					($\Delta\omega_r$) Time domain performance				
		t_r	t_s	$P_{.amp}$	%M_P	P_m	t_r	t_s	$P_{.amp}$	%M_P	$\Delta\omega_r$
1.	20	1.13	3.07	1.03	2.81	1	0	10.1	-0.0947	∞	0

Figure (5.5a): Time Domain Performance for Turbine-Gov. using LOC test model, K_G = 20

5.3.3   Performance and results of a Combined Turbine-Gov. - Generator Using LOC test model

As seen in chapter four the number of the column for the rectangular matrix B depends on how many feedback control loops are used for the LOC design[18]. In this section we considered a combined turbine governor generator model that is derived in chapter three with two control input U_E , U_G and output signals E_t, P_m, with linear optimal control design using MATLAB7 programming language applied with Q , R chosen as shown below.

$$
Q = \begin{bmatrix}
30000 & 0 & 0 & 0 & 0 & 0 & 0 & 0 & 0 \\
0 & 0.001 & 0 & 0 & 0 & 0 & 0 & 0 & 0 \\
0 & 0 & 0 & 0 & 0 & 0 & 0 & 0 & 0 \\
0 & 0 & 0 & 0.01 & 0 & 0 & 0 & 0 & 0 \\
0 & 0 & 0 & 0 & 10000 & 0 & 0 & 0 & 0 \\
0 & 0 & 0 & 0 & 0 & 0 & 0 & 0 & 0 \\
0 & 0 & 0 & 0 & 0 & 0 & 0 & 0 & 0 \\
0 & 0 & 0 & 0 & 0 & 0 & 0 & 0 & 0 \\
0 & 0 & 0 & 0 & 0 & 0 & 0 & 0 & 0
\end{bmatrix}
\quad , \quad
R = \begin{bmatrix} 15 & 0 \\ 0 & 1 \end{bmatrix}
$$

Tables (5.6a) (5.6b) and (5.6c) show the system eigen values , the closed loop feedback control gain KK and time domain performance indices for the above selection. Also figure (5.6a) shows the time domain performance by applying a step input for V_{ref}, P_{ref} to show the output E_t and P_m in time domain.

*Table (5.6a): System eigen Values Combined Turbine-Gov. Generator using LOC test model, K_A=400, K_G=20*

Case	K_A	System eign values								
		λ1	λ2	λ3	λ4	λ5	λ6	λ7	λ8	λ9
1.	400	-101.46	-28.38+30.49i	-28.38-30.49i	-3.86+10.03i	-3.86-10.03i	-5.03+1.91i	-5.03-1.91i	-2.2	-4

Table (5.6b): Closed Loop Feedback Control Gain KK for Combined Turbine-Gov. Generator using LOC test model, K_A =400, K_G=20

Control input	Closed loop feedback gain KK due to U_E and U_G								
	KK1	KK2	KK3	KK4	KK5	KK6	KK7	KK8	KK9
U_E	2638.6	57.5	59.8	4.3	-1.2	-13.3	-2.3	-61.9	-5.2
U_G	-2028.5	-4.7	-6.3	-0.1	990.05	1.0	1.0	4.0	1.5

Table (5.3b) System performance indices for Combined Turbine-Gov. generator using LOC test model, K_A =400, K_G=20

case	K_A	Time domain performance for E_t					Time domain performance for $\Delta\omega_r$				
		t_r	t_s	$P_{.amp}$	$\%M_P$	E_t	t_r	t_s	$P_{.amp}$	$\%M_P$	$\Delta\omega_r$
1.	400	0.797	2.44	1.05	6.33	1	0	3.14	-0.0119	∞	0
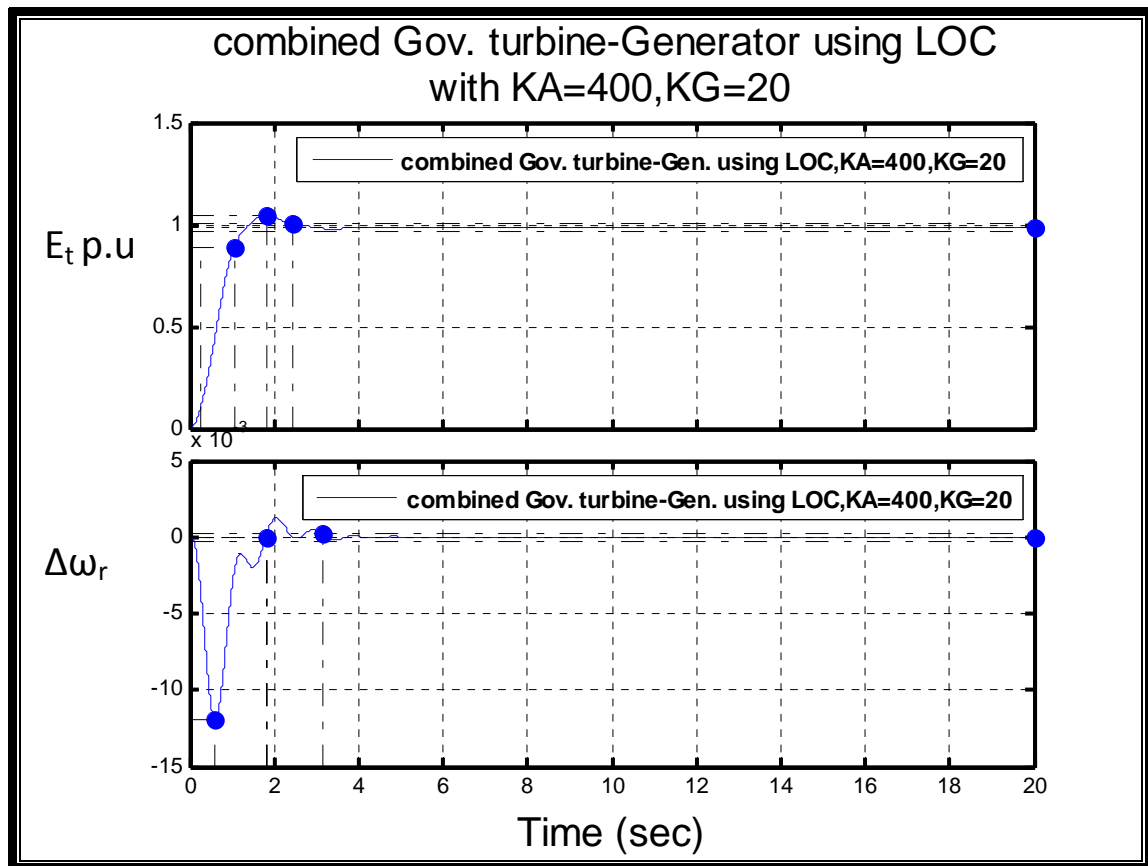
Figure (5.6a): Time Domain Performance for Combined Turbine-Gov. Generator using LOC test model, $K_A = 400$, $K_G = 20$

5.4   Summery of the results of control test modes

To simplify the above results for different test modes, summery of the results of control test modes are considered in this section taking into account the effect of LOC controller on improving the dynamic behavior of power system stability. Table (5.7) and figure (5.7) for exciter-voltage regulator, table (5.8) and figure (5.8) for turbine governor, table (5.9) and figure (5.9) for combined turbine governor generator test mode with and without LOC.

Table (5.7) System performance indices for VR with and without LOC

Case	Damping of mechanical mode and Synchronizing torque					Time domain performance for Et				
	K_{ST}	K_D	ω_n	ζ	ω_d	t_r	t_s	$P_{.amp}$	$\%M_P$	E_t
Without LOC	0.1081	0.4746	2.5544	0.179	2.554	0.416	16.3	1.85	80	1.04
With LOC	0.477	8.4541	5.367	0.1515	5.305	0.689	2.65	1.06	5.62	1
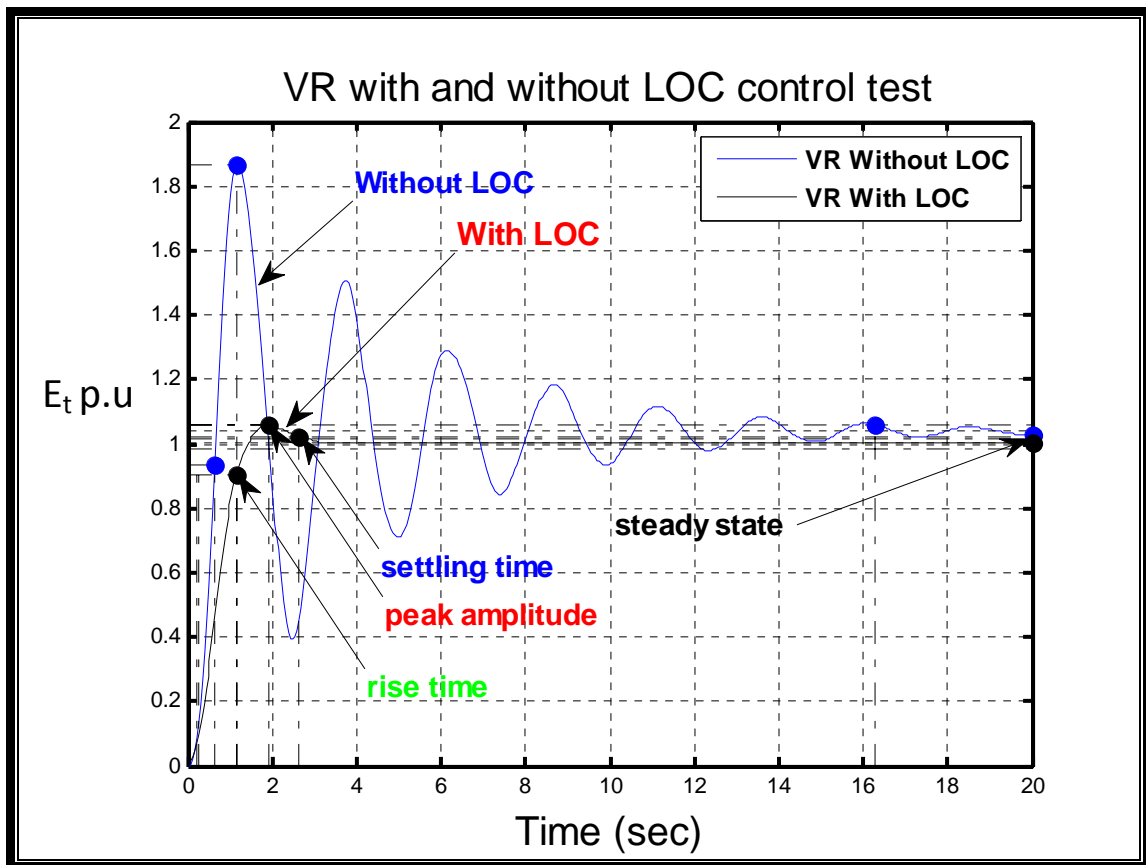
Figure (5.7): Time Domain Performance for VR with and without LOC

Table (5.8) System performance indices for Turbine-Gov. with and without LOC

case	(Pm) Time domain performance					(Δωr) Time domain performance				
	t_r	t_s	$P_{.amp}$	$\%M_P$	P_m	t_r	t_s	$P_{.amp}$	$\%M_P$	$\Delta\omega_r$
Without LOC	0.819	5.58	1.26	26.4	0.998	0	6.98	-0.182	∞	0
With LOC	1.13	3.07	1.03	2.81	1	0	10.1	-0.0947	∞	0
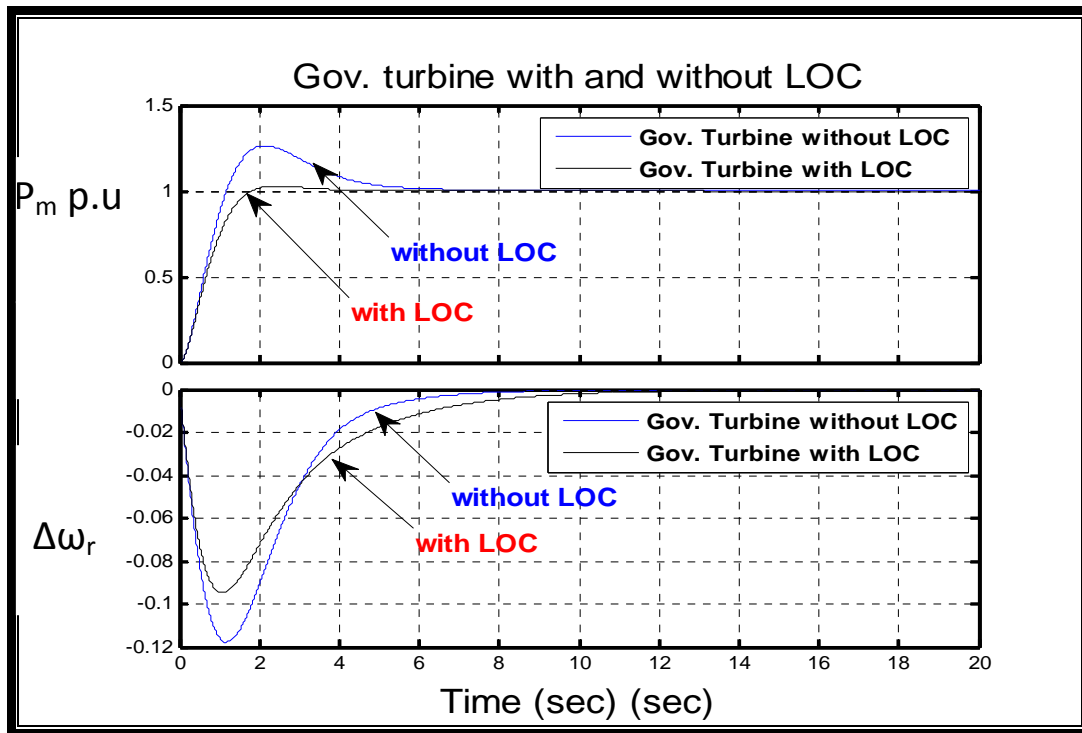
Figure (5.8): Time Domain Performance for Turbine-Gov. with and without LOC

*Table (5.9) System performance indices for a turbo-generator with and without LOC*

case	Time domain performance for E_t					Time domain performance for $\Delta\omega_r$				
	t_r	t_s	$P_{.amp}$	$\%M_P$	E_t	t_r	t_s	$P_{.amp}$	$\%M_P$	$\Delta\omega_r$
Without LOC	0.432	17.6	2.09	79.6	1.16	0	17.3	-0.0265	∞	0
With LOC	0.797	2.44	1.05	6.33	1	0	3.14	-0.0119	∞	0
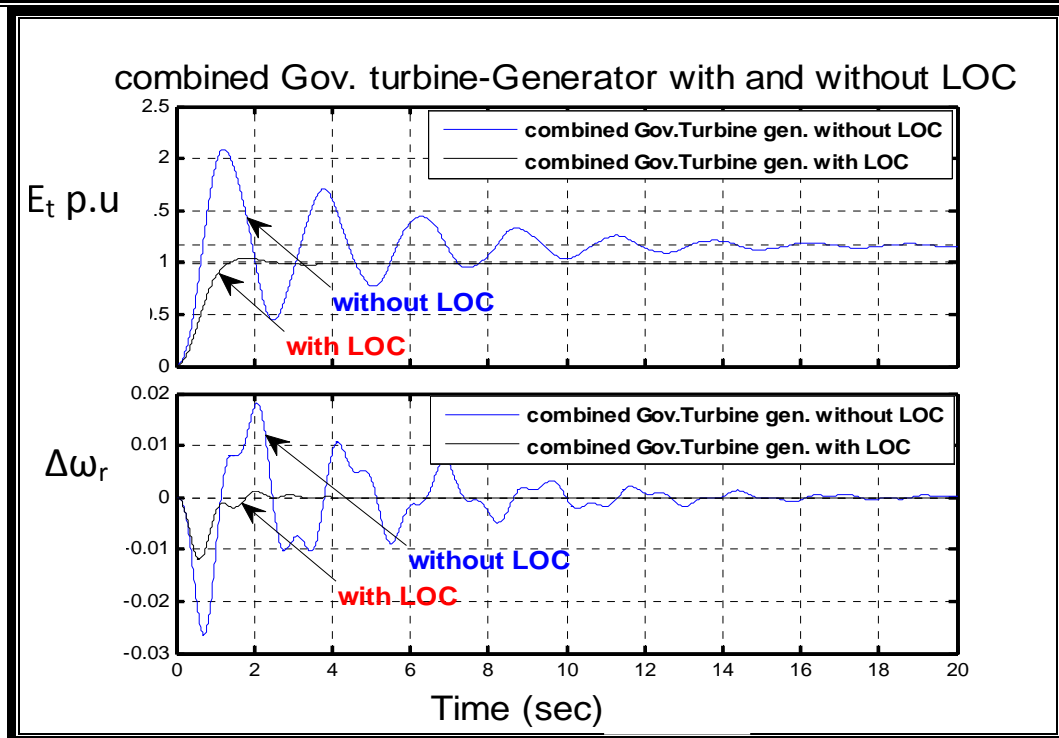
Figure(5.9):Time Domain Performance for a turbo-generator with and without LOC

Also the deviation in states (ΔE_t, ΔP_m, $\Delta \omega_r$) were taken to be as an example about the equilibrium points for the system state equation was considered to be in the form of ($\Delta \dot{X} = A_C \Delta X$), when ($\Delta P_{ref}=0$, $\Delta V_{ref}=0$, $\Delta P_L=0$, $\Delta V_L=0$). In time domain figure (5.10) below show the state deviation for previous cases (without and with LOC) for different test modes.
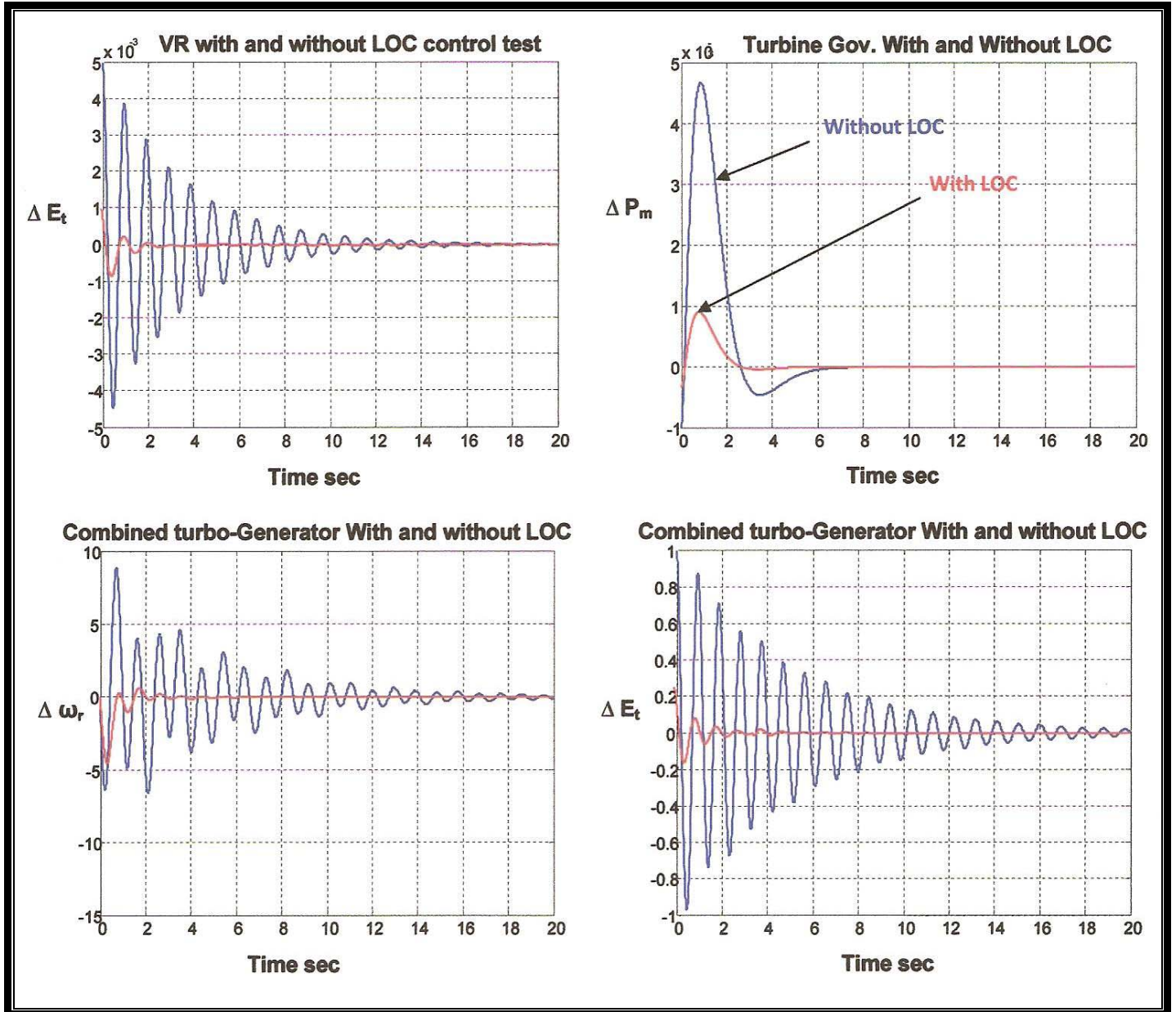
Figure(5.10):Time domain for states deviation (ΔE_t, ΔP_m, $\Delta \omega_r$)about equilibrium point for different test modes.

CHAPTER SIX
CONCLUSIONS AND SUGGESTIONS FOR FUTURE WORK

6.1 Conclusions

The aim of this thesis is to study a test model for a power stability control using LOC is given. The effectiveness of the LOC controller is applied in several test cases. Three test modes are considered in this work, these are exciter control, governor turbine control and the combined turbo generator control test modes. The models were selected starting from the two axis theorem and swing equation. These models were tested without linear optimal control LOC, and then with LOC. The controller is designed and tested using MATLAB 7 programming language. From the results obtained the following points can be concluded.

1. In the case of VR a problem occurred by increasing K_A from initial value 40 to the nominal 400 (this test was used to reject the effect of load influence as a disturbance acting continuously on a power system that cause reduction in the steady state terminal voltage), the damping of the mechanical mode reduced from **0.6538** to **0.4746**, with increase in the synchronizing torque due to increasing in the voltage regulator gain K_A from **0.0111** to **0.1081,** but these two values are insufficient, or in other word may cause instability of a power system due to lack of damping in the mechanical mode and synchronizing torque. Then the effect of using LOC can increase both damping of mechanical mode and synchronizing torque to **8.4541** and **0.477** respectively.

2. Using LOC can improve over all power system stability by minimizing over all performance indices (**t_r, t_s, $P_{amplitude}$** and **%M_p**) this is show briefly in tables and figures (5.7),(5.8) and (5.9) for different test modes. The steady state error (**e_{ss}**) was minimized to zero (with constant voltage and constant frequency).

3. It is shown in this test that the effect of using LOC is to increase the stability degree of a power system by shifting the eigen values to the left side of s-plain meaning that the real part of the complex roots become more negative than without using LOC this can be shown in tables (5.1c) and (5.4a).

4. In this test the weighted matrices Q and R were selected by trial and error in order to give the weight for both states (X) and control (U) in the LOC method design. It is shown that the two states rotor angle $\Delta\delta$, and the rotor speed $\Delta\omega_r$ are more affective than other states in the rotor angle stability problem. This happens because the electrical torque having a two components in phase with $\Delta\delta$ and $\Delta\omega_r$, ($\Delta T_e = K_S \Delta\delta + K_D \Delta\omega_r$). Also because of the property of Q as a diagonal semi positive definite matrix, meaning that its values ($q_{(i,i)} \geq 0$), then this can reduce the trial and error in the selection of Q by actuating the weight for $\Delta\delta$, $\Delta\omega_r$ in the case of VR test mode. This reduction can give optimum performance for different test modes. This is shown in tables and figures (5,7),(5.8) and (5.9), which make it easy to select the weighted matrices Q ,R. The reduction from 4 to 2 choices in the case of VR test mode and from 6 to 3 in the case of gov. turbine test mode and from 9 to 4 in the case of combined gov. turbine generator test models.

5. A simple MATLAB 7 program shown in flow chart (4.1) uses for the closed form solution of Riccati matrix equation also obtained in this work. This simplistic program can also be used with other applications of linear optimal control (LQR, LQG, H_2, $H_{\infty,...}$) .

6.2 Future Works

The following ideas are presented as suggestions for future works:

1. Applying the hardware of the LOC method in order to specify the controller performance practically.

2. Applying the LOC method on a multi machine power system to show and check the effectiveness of this controller on electrical power system stability.

3. Using this method with other types of generators (hydro, gas, ...) by taking other data base.

4. Applying the flow chart (4.1) with other applications of a linear optimal control (LQR, LQG, H_2, $H_{\infty,....}$) that were dependent on solution of a Riccati matrix equation.

5. Applying the flow chart (4.1) with other high level languages than MATLAB 7 programming language, as a part of mane program needs for solution Riccati matrix equation.

REFERENCES

1. V. Venikov,: transient phenomena in electrical power system, Mir publishers, Moscow (English translation from the Russian), 1977.

2. P. Kundor: power system stability and control, Mc Graw Hill, Inc, 1994.

3. Anderson P. M. and Fouad A: power system control and stability, John Wiley and Sons Inc 2003.

4. Katsuhikoogata: modern control engineering; fourth edition, Prentice-Hall. Inc, 2002.

5. Hamdy A. M Moussa and Yao-nanyu "optimal power system stabilization through excitation and/ or governor control" paper 71 TP 581- PWR, IEEE International symposium on high power testing, Portland, Ore., July 18-23, 1971.

6. B. S. Habibullah "optimal governor control of a synchronous machine", IEEE transactions on automatic control, Vol. AC-26. No. 2. April 1981.

7. G. orelind, Lwozniak, J. Medanic and T. Whittemore "optimal PID gain schedule for hydrogenerators-design and application "IEEE transactions on energy conversion, Vol. 4, No. 3. September 1989.

8. Youssef A Smaili and Ali T. Alouani "An H∞ governor/ exiter controller design for a power system" paper,IEEE, 1992.

9. H. Bourles, F. Colledani and M. P. Houry "Robust continuous speed governor control for small-signal and transint stability" IEEE transaction on power system, Vol. 12, No. 1, February 1997.

10. Hiroaki Nakanishi, Takehisa Kohda and Koichi Inoue "a design method of optimal control system by use of neural network" IEEE 1997.

11. H. Yang, E. C. Tan and K. K. Wang "a neural optimal voltage regulator" IEEE international conference on intelligent processing system, October 28-31, 1997.

12. M. L. Kothari, A. Sharma, R. Segal, J. Nanda and A shish Kumar Batwara "optimum power system stabilizer parameters as affected by the a mortissurs of the synchronous generator" IEEE, 1998.

13. young-Hyun Moon, Heon-Su Ryu, Baik Kim, and Kyoung-Bin Song" optimal tracking approach to load frequency control in power system", IEEE, 2000.

14. Firas Mohammed To'aima "optimal control of governor and exciter for turbo generator using LQG", Ph.D. thesis, university of Baghdad, college of electrical engineering, November 2006.

15. K. Ohtsuka, T. Taniguchi, T. Sato, S. Yoko Kawa and Y. ueki "AH∞ optimal theory based generator control system", IEEE transactions on energy conversion, Vol. 7, No. 1, March 1992.

16. Bok Eng Law, "simulation of the transient response of synchronous machines", B.SC. thesis, University of Queens Land, October 2001.

17. Chee Munong: Dynamic simulation of electric machinery using MATLAB; prentice hall, 1998.

18. Yao-nan Yu: electrical power system dynamics; Academic press, A subsidiary of Harcourt brace Jovanovich, publishers, copyright 1983.

19. J. A. Momoh and M. E. EL – Hawary, electric systems, Dynamics and stability with artificial Intelligence Applications, Marcel Dekker Inc., New York, 2000.

20. J. Faiz ,"closed – loop control stability for permanent magnet synchronous motor", International journal of electrical power and energy systems, vol. Issue 5, pp 331 – 337, June 1997.

21. P. C. Krause ," Analysis of electric machinery", IEEE press, 1995.

22. F. P demello and C. Concordia, "concepts of synchronous machine stability as affected by excitation control", IEEE Trans. , vol. PAS – 88, PP. 316 – 329, April 1969.

23. IEEE committee report, "Excitation system models for power system stability studies", IEE Trans. Vol. PAS – 100, PP. 494 – 509 February 1981.

24. IEEE Recommended practice for excitation system models for power system stability studies, IEEE standard 421.5 – 1992.

25. Computer representation of excitation system; IEEE Committee report; IEEE Trans. on PAS-87, No.6, june 1968.

26. Peter W. Sauer and M. A. Pai: power system dynamics and stability, prentice Hall. Inc. 1998.

27. Goram Andersson: dynamics and control of electric power system, book ETH Zurich, March 2004.

28. IEEE Committee, "Dynamic models for steam and hydro turbines in power system studies", IEEE Trans. Pas., PP 1904 – 1915 December 1973

29. F. L. Lewis: control System Design Project; Lecture 11, 1999.

30. Dr.Mohammad K.Hadi Al-Alawi and Ibrahim I. Hamad," Design of prespecified root controller for asynchronous generator";A scientific Refereed journal published by, college of engineering-university of Baghdad. Vol.7, No.2, June 2004.

31. IEEE Guide for Identification, testing and evaluation of the Dynamic performance of excitation control systems, IEEE standard 421.2 – 1990 (revision to IEEE standard 421 A – 1978).

APPENDIX A

## Typical Data test system for a Fossil Steam Unit [3]

Generator	
S (apparent power)	384 MVA
P (active power)	0.9 p.u
Q (reactive power)	0.3 p.u
E_t (terminal voltage)	24 kv
Frequency	50 HZ
E_B (infinite bus voltage)	1 p.u
Connection	Y
H	2.6 MW. s/ MVA
D	2 p.u
X_d	1.798 p.u
X_d'	0.3 p.u
X_q	1.778 p.u
X_ℓ	0.193 p.u
R_a	0.0014 p.u
T_{do}'	5.21s
K_1	0.7323 p.u
K_2	0.8742 p.u
K_3	0.2728 p.u
K_4	1.2829 p.u
K_5	- 0.1387 p.u
K_6	0.3565 p.u
T_3	2.3244s

| Exciter Regulator	
K_A	400
T_R	0s
K_E	1
T_E	0.812s
Turbine Governor	
K_G	20MW/Hz
F_{HP}	0.2
F_{IP}	0.4
F_{LP}	0.4
T_{SR}	0.1s
T_{SM}	0.22s
T_{RH}	8s
T_{CH}	0.2s
T_{CO}	0.25s
Transmission Line	
Transformer reactance	0.15 p. u.
First line reactance	0.5 p. u.
Second line reactance	0.93 p. u.

APPENDIX B

The object of the figure (B. 1) below which represent a thermal generator of 384 MVA 24 KV, 50 Hz when **short circuit fault** occur in transmission line T.L.2, is to determine synchronizing torque for single machine connected to infinite bus when ($E_t = 1.05\angle36^o$ p. u).
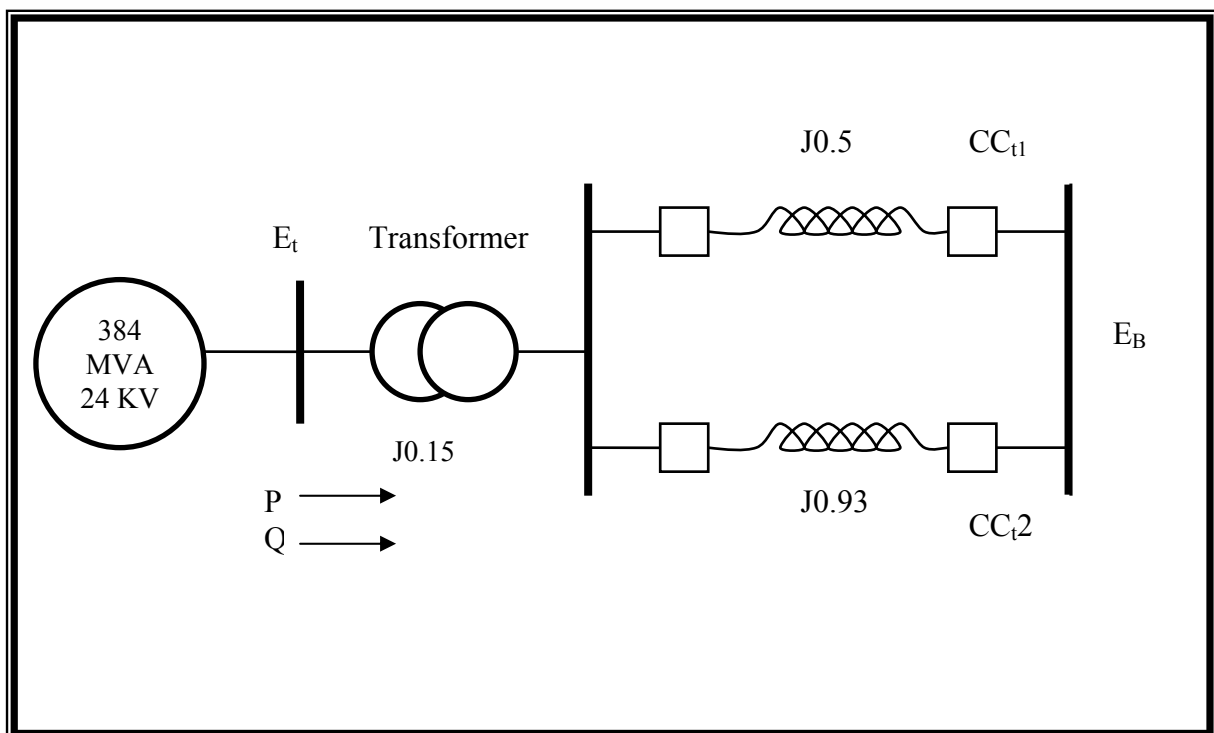
Figure (B.1)[2]

Figure (B.2) below show the circuit model representing the post fault steady state operating condition with all parameters expressed in per unit.

C
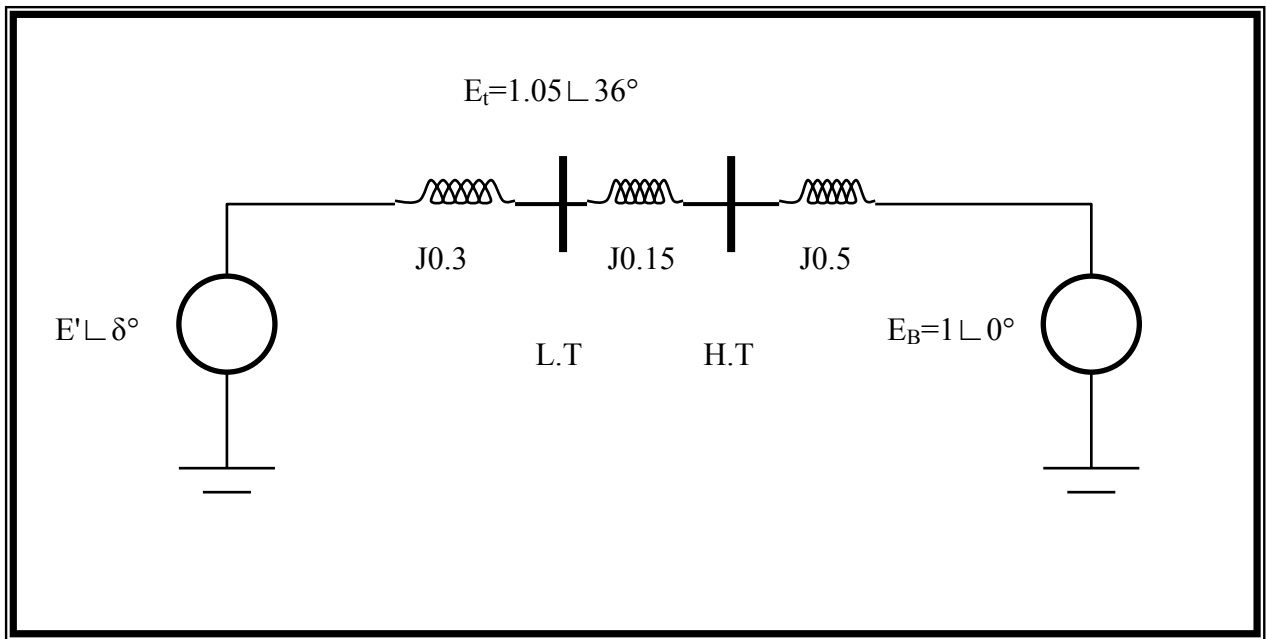
Figure (B. 2)[2]

With E_t as reference phasor, the generator stator current is given by:

$$I_t = \frac{(p + jQ)^*}{E_t^*} = \frac{0.9 - j0.3}{1.05} = 0.86 - j0.29$$

The voltage behind transient reactance is:

$$E' = E_t + jX'd\ I_t$$
$$= 1.05 + j0.3(0.86 - j0.29)$$
$$= 1.137 + j0.258 = 1.166\angle 12.8$$

The angle by which E′ lead E_B is:

$$\delta_0 = 12.8 + 36 = 48.8°$$

The total system reactance is:

$$X_T = 0.3 + 0.15 + 0.5 = 0.95 \text{ p. u}$$

The corresponding synchronizing torque, from equation (2. 44) is:

$$K_S = \frac{E'E_B}{X_T}\cos\delta_O$$
$$= \frac{1.166 \times 1}{0.95}\cos 48.8°$$
$$= 0.81 \text{ p.u torque/ rad}$$

D

APPENDIX C

As an example were taken in this APPENDIX, From figure (2.10) shown in chapter two (K_S, K_{ST}, K_D, ω_n, ξ, ω_d) can be calculated as shown below with details in[2,3,18]. Then these derivations were extended for generator-exciter model in the case of without and with LOC.

where:

K_S: synchronizing torque due to demagnetizing effect of the armature reaction ($K_S = K_1 \Delta\delta$).

K_{ST}: total synchronizing torque coefficient.

K_D: damping torque coefficient.

ω_n: undamped natural frequency in rad/ sec.

ξ: damping ratio.

ω_d: damping frequency in rad/ sec.

From equation (2. 69) the electrical torque:

$$\Delta T_e = K_1 \, \Delta\delta + K_2 \, \Delta\psi_{fd} \quad\text{...(C. 1)}$$

From the block diagram (2. 10) can derive ΔT_e due to $\Delta\psi_{fd}$:

$$\left.\frac{\Delta T_e}{\Delta\delta}\right|_{\text{due to }\Delta\psi_{fd}} = \frac{-K_2 K_3 K_4 (1 - ST_3)}{1 - S^2 T_3^2} \quad\text{..(C. 3)}$$

Therefore ΔT_e due to $\Delta\psi_{fd}$ after simplification.

$$\left.\Delta T_e\right|_{\text{dueto }\Delta\psi_{fd}} = \frac{-K_2 K_3 K_4}{1 + S^2 T_3^2}\Delta\delta + \frac{K_2 K_3 K_4 T_3}{1 - S^2 T_3^2}S\Delta\delta \quad\text{...........................(C. 4)}$$

E

But

$$S\Delta\delta = \Delta\omega_r * \omega_0 \quad\text{...}\text{(C. 5)}$$

Then:

$$\Delta T_e\big|_{\Delta\Psi_{fd}} = K_S(\Psi_{fd})\Delta\delta + K_D(\Delta\Psi_{fd})\Delta\omega_r\omega_o \quad\text{...}\text{(C. 6)}$$

From equations (C. 4) and (C. 6):

$$K_S = -\frac{K_2 K_3 K_4}{1 + S^2 T_3^2} \quad\text{..}\text{(C. 7)}$$

From equation (C. 1):

$$K_{ST} = K_1 \Delta\delta + K_2 \Delta\psi_{fd} \quad\text{...}\text{(C. 8)}$$

From equations (C. 4) and (C. 6):

$$K_D = \frac{K_2 K_3 K_4 T_3}{1 - S^2 T_3^2}\omega_0 \quad\text{...}\text{(C. 9)}$$

let the general form of the second order characteristic equation is:

$$|SI - A| = 0 \Rightarrow S^2 + 2\zeta\omega_n S + \omega_n^2 = 0 \quad\text{...}\text{(C. 10)}$$

The characteristic equation can calculated from equation (2.44):

$$|SI - A| = 0 \Rightarrow S^2 + \frac{K_D}{2H}S + \frac{K_{ST}\omega_O}{2H} = 0 \quad\text{..}\text{(C. 11)}$$

From (C.11) ω_n, ξ, ω_d can calculate as shown:

$$\omega_n = \sqrt{K_{ST}\frac{\omega_0}{2H}} \text{ rad/sec} \quad\text{..}\text{(C. 12)}$$

$$\zeta = \frac{1}{2}\frac{K_D}{\sqrt{K_{ST}2H\omega_0}} \quad\text{...}\text{(C. 13)}$$

$$\omega_d = \omega_n\sqrt{1-\zeta^2} \quad\text{..}\text{(C. 14)}$$

In this work the field flux variation $\Delta\psi_{fd}$ can be derived from the figures (3.5a) and (C.1) for a generator-exciter model without and with LOC respectively shown in equations (C.15) and (C.16) below:
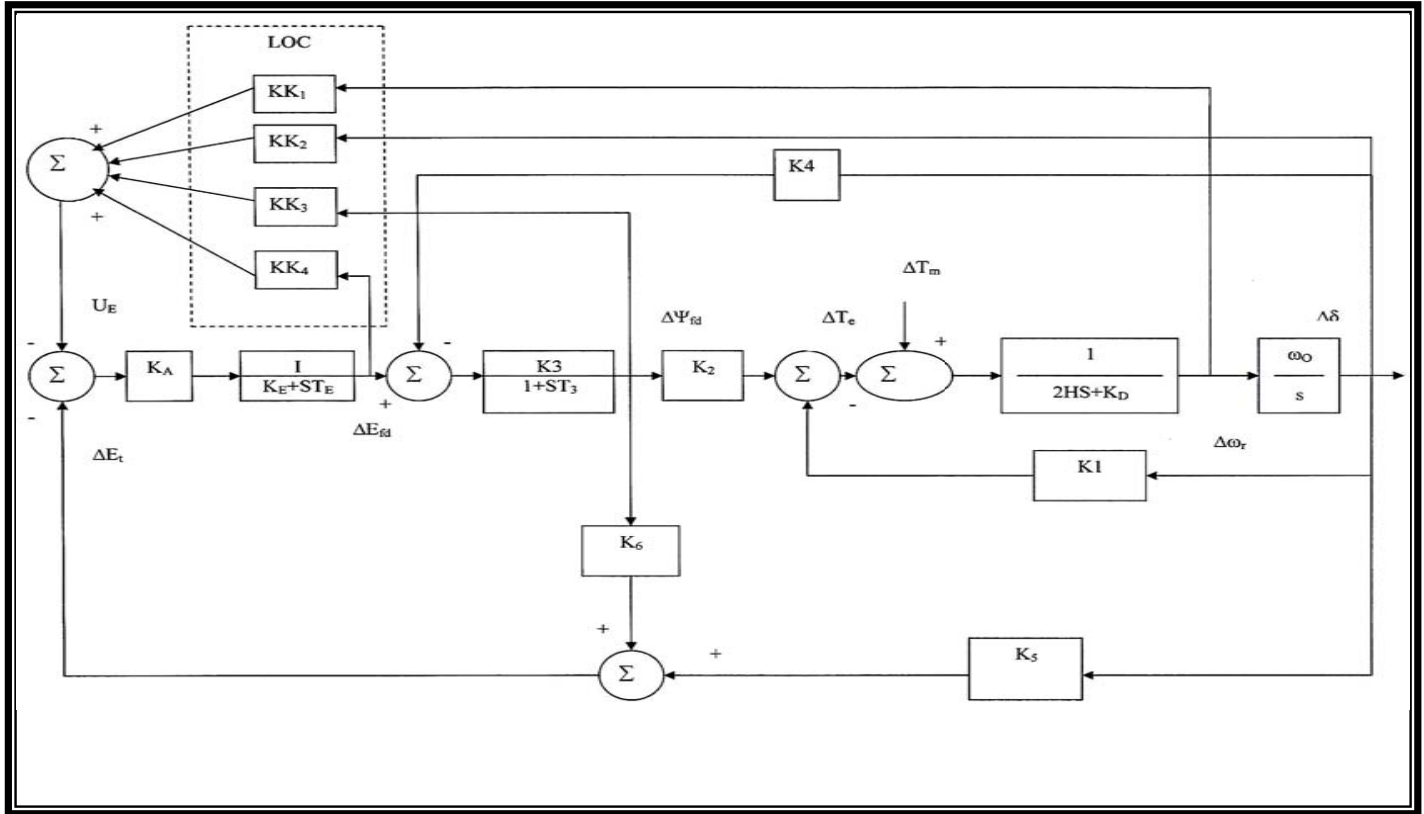
Figure (C.1) block diagram representation for generator-exciter with LOC

1. Without LOC The final formula of $\Delta\psi_{fd}$ is:

$$\Delta\psi_{fd} = \frac{\left(-K_5 K_3 K_A - K_4 K_3 K_E - K_4 K_3 T_E S\right)}{\left(K_E + T_3 K_E S + T_E S + T_3 T_E S^2 + K_3 K_6 K_A\right)}\Delta\delta \dots\dots\dots\dots\dots\dots\dots\dots\dots\dots(C.15)$$

2. With LOC The final formula of $\Delta\psi_{fd}$ is:

$$\Delta\psi_{fd} = \frac{\left(-\omega_o K_4 K_3 K_E - \omega_o K_4 K_3 T_E S - \omega_o K_4 K_3 KK_4 K_A - \omega_o K_3 K_5 K_A - \omega_o KK_2 K_3 K_A - K_3 K_A KK_1 S\right)}{\omega_o\left(K_E + T_E S + KK_4 K_A + T_3 K_E S + T_3 T_E S^2 + T_3 KK_4 K_A S + K_3 K_6 K_A + KK_3 K_A K_3\right)}\Delta\delta\dots.(C.16)$$

For calculation (K_S, K_{ST}, K_D, ω_n, ξ, ω_d), substitute equations (C.15), and (C.16) in the case of without and with LOC respectively, in equation (C.1) to find the complex ΔT_e by replacing λ instead of S.

G

APPENDIX D

In many practical cases, the desired performance characteristics of control systems can be given in terms of transient-response characteristics. Frequently, such performance characteristics are specified in terms of the transient response to a unit step input, since it is easy to generate and is sufficiently drastic[4]. The transient response of a practical control system often exhibits damped oscillations before reaching steady state. In specifying the transient response characteristics of a control system to a unit step input, it is common to name the; delay time, t_d; rise time t_r; peak time t_p; maximum overshoot, mp and settling time, t_s. These specifications are defined in what follows and are graphically shown in figure (D. 1).
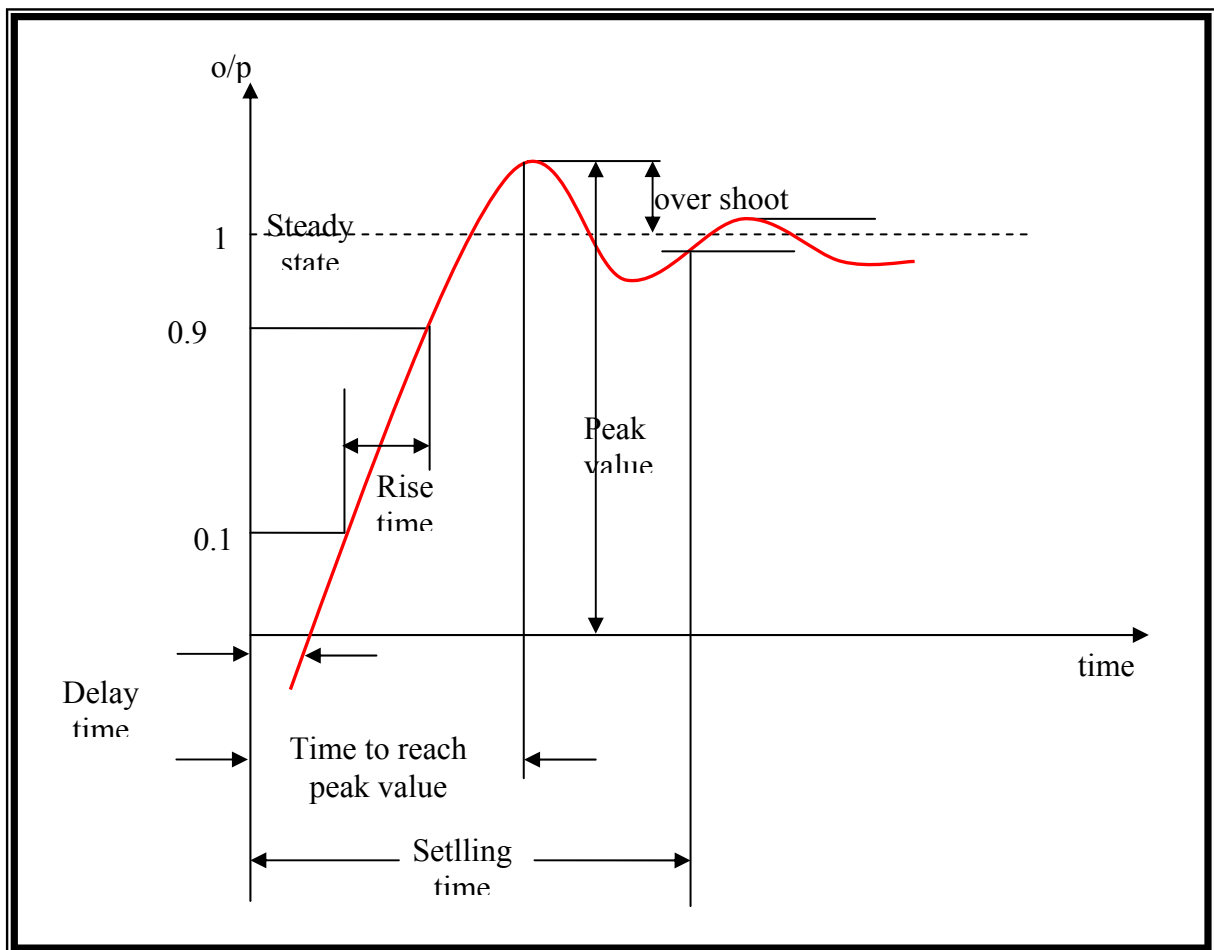
Figure (D. 1): Typical Time Response to Step Input [(C)] IEEE 1990[31]

H

- Delay time. The delay time t_d is the time needed for the response to reach half the final value.

- Rise time. The rise time t_r is the time required for the response to rise from 10% to 90%, or 5% to 95% or 0% to 100% of its final value.

- Peak time t_p is the time required for the response to reach the first peak of the over shoot.

- Max (percent over shoot). The maximum over shoot m_p is the maximum peak value of the response curve [C (t) versus t] measured from unity. If the final steady state value of the response drift from unity, then it is common practice to use the maximum percent overshoot:

Maximum percent overshoot $= \dfrac{C(t_p) - C(\infty)}{C(\infty)} *100\%$

  The amount of the maximum (percent) overshoot directly indicates the relative stability of the system.

- Settling time. The settling time t_s is the time required for the response curve to reach and stay within 2% of the final value. (Note that in some cases 5% instead of 2% is used as the percentage of the final value. The settling time is related to the largest time constant of the system[4].

الخلاصة

هذا البحث يتناول تحقيق الأستقرارية لمولد متزامن (turbo-generator) نتيجة التغيرات الحاصلة بالحمل. أن معادلات الحالة (state equations) لنظام السيطرة الخطي يجب أن تشتق. وبالتالي فإن نظرية السيطرة الحديثة (modern control theory) تستخدم مع معادلات الحالة قبل تطبيق تقنية الأمثلية. لإيجاد السيطرة المثالية التي تحقق الحد الأدنى لدالة الثمن (cost function) لكل من انحرافات الحالة (state deviation) وجهد السيطرة (control effort).

إبتداء" الدراسة كرست لإختيار النموذج المناسب لماكنة متزامنة و عمود لانهائي (SMIB) مبتدئين من نظرية المحورين (two axis theorem) ومعادلة التأرجح (swing equation) ، والتوسع بالنموذج بإضافة المؤثر-المولد (generator-exciter) و الحاكم-التوربين -turbine) governo).

إن طريقة الأمثلية والتي تدعى السيطرة المثالية الخطية (linear optimal control LOC) إستخدمت لتحسين الإستقرارية الكاملة لمنظومة القدرة الكهربائية. إن هذه الطريقة (LOC) تم إختبارها بإستخدام عدة إختبارات درست بتطبيقها لتحسين اداء منظم الفولتية ، الحاكم-التوربين وكذلك تطبيقه على منظومة السيطرة مجتمعتا" .

إن نتائج إختبار السيطرة المثالية الخطية (LOC) اظهرت تحسين الإستقرارية الكاملة العابرة (transient) والثابتة (steady state) لمنظومة القدرة الكهربائية من خلال زيادة عزم التخميد الميكانيكي (mechanical damping torque) والتزامني (synchronizing torque) والذي يظهر في إختبار منظم الفولتيةِ لنظام السيطرة. إستطاع زيادة درجة إستقرارية نظام القدرة بواسطة تزحيف الاقطاب للإتجاه السالب لمستوي-س (S-Plane). الحصول على أفضل جودة لنظام السيطرة من خلال التحسين الظاهر في جميع خواص الأداء لمجال الزمن (time domain performance indices). إن الخطاء والصواب (trial and error) في إختيار (Q and R) مصفوفات الوزن لدالة الثمن أيضا تم تقليلها في هذا الإختبار.

وأخيرا فإن الصيغة المغلقة (closed form) لحل معادلة مصفوفة الريكاتي (Riccati matrix equation) قد تم حلها باستخدام برنامج بسيط بلغة البرمجة مات لاب السابع 7 MATLAB) programming language).

المسيطر الأمثل لمولد متزامن يحتوي على منظم فولتية وسيطرة التوربين

رسالة

مقدمة الى كلية الهندسة ـ جامعة بغداد

كجزء من متطلبات نيل شهادة الماجستير

في

الهندسة الكهربائية

من قبل

آلاء عبود عبد الرسول حسين

بكالوريوس علوم في الهندسة الكهربائية ـ جامعة بغداد

بأشراف

الدكتور محمد خضر هادي العلوي

كانون الأول ٢٠٠٨